Simulation of Ground-Water Flow and Contributing Recharge Areas in the Missouri River Alluvial Aquifer at Kansas City, Missouri and Kansas

By Brian P. Kelly

U.S. GEOLOGICAL SURVEY

Water-Resources Investigations Report 96–4250

Prepared in cooperation with the
MID-AMERICA REGIONAL COUNCIL

Rolla, Missouri
1996

U.S. DEPARTMENT OF THE INTERIOR
BRUCE BABBITT, Secretary

U.S. GEOLOGICAL SURVEY
Gordon P. Eaton, Director

For addtional information write to:

District Chief
U.S. Geological Survey
1400 Independence Road
Mail Stop 100
Rolla, MO 65401

Copies of this report can be purchased from:

U.S. Geological Survey
Branch of Information Services
Box 25286
Denver, CO 80225-0286

CONTENTS

PLATES

[Plates are at the back of this report]

FIGURES

TABLES

Simulation of Ground-Water Flow and Contributing Recharge Areas in the Missouri River Alluvial Aquifer at Kansas City, Missouri and Kansas

By Brian P. Kelly

ABSTRACT

The Missouri River alluvial aquifer in the Kansas City metropolitan area supplies all or part of the drinking water for more than 900,000 people and is the only aquifer in the area that can supply large quantities of ground water for public and industrial use. Hydrogeologic data collected and compiled for more than 1,400 locations in the study area were entered into a geographical information system and interfaced with the U.S. Geological Survey ground-water flow model MODFLOWARC, a modified version of MODFLOW, and the U.S. Geological Survey particle tracking program MODPATH to determine the contributing recharge areas for public-water-supply well fields. The model has a uniform grid size of 150 by 150 meters and contains 310,400 cells in 4 layers, 160 rows, and 485 columns. The number of active cells in the model is 67,362. The model was calibrated to both quasi-steady state and transient hydraulic head data. Sensitivity analysis indicates that the model is most sensitive to increases and decreases in calibrated hydraulic conductivity values and least sensitive to decreases in vertical conductance between layers 1 and 2 and increases in riverbed conductance. Ground-water flow was simulated for the range of conditions expected to occur with the following well-pumping-rate/river-stage scenarios: (1) low pumping rates and low river stage; (2) low pumping rates and high river stage; (3) quasi-steady state conditions; (4) high pumping rates and low river stage; and (5) high pumping rates and high river stage.

Ground-water-flow and particle tracking results indicate that (1) the capture of ground water by pumped wells as it moved downgradient toward the Missouri River caused the long upvalley extent of some contributing recharge areas; (2) well fields located near alluvial valley walls have total contributing recharge areas that extend a long distance from the walls because little water is available from this boundary; (3) induced recharge caused by proximity to a major river decreases the size of the contributing recharge area when compared to the contributing recharge areas of other wells or well fields with similar pumping rates located farther from a major river; (4) induced recharge from a river causes the contributing recharge area to be skewed toward the river; (5) the distribution of vertical anisotropy of hydraulic conductivity in the aquifer affects ground-water travel times within the contributing recharge area of each well or well field; (6) high river stage may decrease the regional ground-water gradient in the vicinity of a well field and may actually increase the contributing recharge area of those well fields; and (7) movement of ground water beneath rivers because of well pumping occurs in several locations in the study area.

The effect of well pumping and river stage on the total contributing recharge area of each well field in the study area is different because of

the unique qualities of each well field with respect to the orientation of the well field to the geometry of the aquifer, the alluvial valley walls, the rivers, and other pumped wells; the magnitude and spatial distribution of the hydraulic properties of the aquifer in the vicinity of each well field; and the rate of pumping from each well field.

INTRODUCTION

The Missouri River alluvial aquifer in the Kansas City metropolitan area (fig. 1; pl. 1) supplies all or part of the drinking water for more than 900,000 people in 90 municipalities and public-water-supply districts (Missouri Department of Natural Resources, 1991). In 1995, 11 public well fields were supplied by the aquifer, a new well field was planned, and 1 well field was being expanded. The Missouri River alluvial aquifer, and to a much lesser extent, the adjoining alluvial aquifers of the Kansas, Blue, and Little Blue Rivers are the only aquifers in the area that can supply large quantities of ground water for public and industrial use.

The Mid-America Regional Council (MARC), a planning association of city and county governments in the Kansas City metropolitan area, currently (1996) is developing a comprehensive ground-water protection plan for the Missouri River alluvial aquifer near Kansas City. In 1991, the U.S. Geological Survey (USGS) in cooperation with MARC began a study to provide hydrogeologic data for the Missouri River alluvial aquifer. In 1993, a ground-water flow model was used to evaluate the response of ground-water levels, ground-water travel times, contributing recharge areas (CRAs) of well fields, and directions of ground-water flow to changes in pumping and river stage. Knowledge of ground-water flow directions between potential sources of ground-water contamination and public-water-supply well fields is needed to understand the potential effects of present and planned development on ground-water quality in the aquifer and provide a better understanding of flow systems in developed alluvial aquifers.

Purpose and Scope

The purpose of this report is to describe the development, calibration, and application of a ground-water flow model of the Missouri River alluvial aquifer in the Kansas City metropolitan area. In particular, the simulated results of five different scenarios of pumping rates and river stage that represent the range of conditions expected to occur are presented: (1) low pumping rates and low river stage, (2) low pumping rates and high river stage, (3) quasi-steady state conditions of January 1993, (4) high pumping rates and low river stage, and (5) high pumping rates and high river stage. The CRA for each public-water-supply well field and related ground-water travel times at various distances from each public-water-supply well field are presented for each of the five scenarios.

Much of the data used in the model were collected during a previous study of the Missouri River alluvial aquifer (Kelly and Blevins, 1995). Data collected during the present study were two synoptic water-level measurements of 123 wells in October 1993 and 98 wells in February 1994. Data indicating rates of ground-water pumpage from public-water-supply well fields and industrial water-supply wells located in the study area, daily rainfall amounts, and river stages for the Missouri, Kansas, Blue, and Little Blue Rivers also were collected.

Description of Study Area

The study area extends from approximately 8 km (kilometers) north of the Leavenworth County-Wyandotte County line in Kansas to approximately 4 km east of the Jackson County-Lafayette County line in Missouri and is bounded by the Missouri River alluvial valley walls on the north and south. Parts of the alluvial valleys of the Kansas, Blue, Little Blue, and Fishing Rivers (pl. 1) are included. Parts of Clay, Jackson, Lafayette, Platte, and Ray Counties in Missouri and Leavenworth and Wyandotte Counties in Kansas are within the study area.

About two-thirds of the land use in the study area is row-crop agriculture, and about one-third is industrial. Land use in the remainder of the study area consists of single- and multiple-family dwellings, commercial establishments, undeveloped land, and publicly owned land, including airports, sewage and water treatment plants, and parks (Kelly and Blevins, 1995).

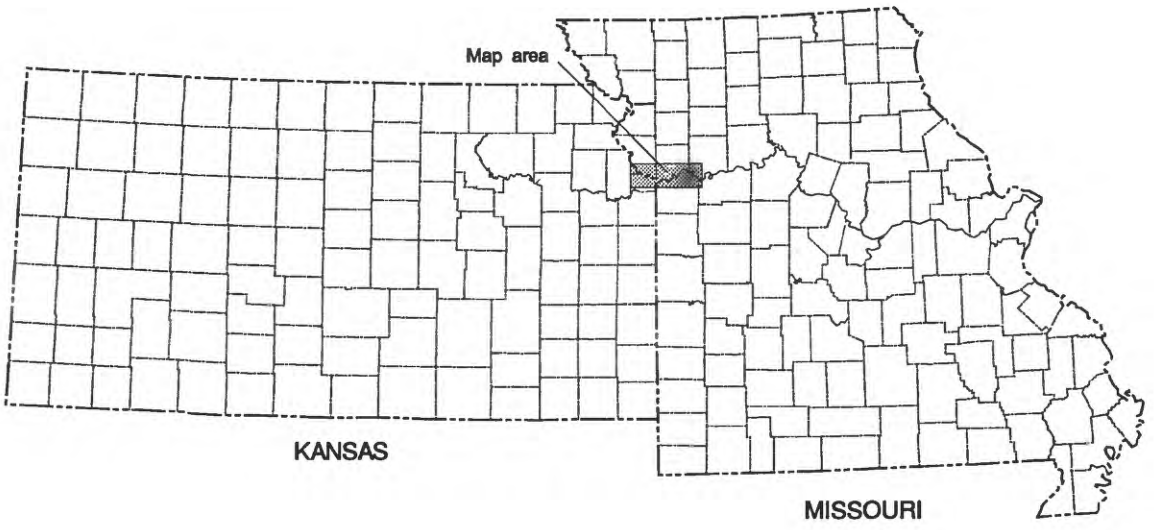

Figure 1. Location of the study area near Kansas City, Missouri and Kansas.

Acknowledgments

The author thanks the many residents, landowners, and businesses in the study area for their cooperation during the collection of water-level data. The assistance provided by personnel from Missouri Cities Water Company; Gladstone, Missouri; Kansas City, Missouri; North Kansas City, Missouri; Sugar Creek, Missouri; Independence, Missouri; Liberty, Missouri; Excelsior Springs, Missouri; Lake City Army Ammunition Plant; Ray County Public Water Supply District Number 2; Community Water Company; and Tri-County Water Company also is appreciated.

HYDROGEOLOGIC FRAMEWORK

Data from numerous sources provide the basis for the following discussion of the hydrogeologic framework of the Missouri River alluvial aquifer. Hydrogeologic data from numerous geologic and hydrologic investigations within the study area were also compiled (McCourt and others, 1917; K.E. Anderson and F.C. Greene, Missouri Division of Geology and Land Survey, written commun., 1948; Fischel, 1948; Fischel and others, 1953; Emmett and Jeffery, 1969, 1970; Gann and others, 1973; Crabtree and Older, 1985; Hasan and others, 1988). Water-level data for the Missouri River alluvial aquifer were collected from 187 wells in August 1992 and 155 wells in January 1993 (Kelly and Blevins, 1995).

Physiography and Drainage

The Missouri River alluvial valley is relatively flat within the study area. However, highway embankments, levees, and some construction activities have raised the surface of the alluvial valley in developed areas. Total relief within the study area is approximately 25 m (meters) with the highest altitudes between 235 and 240 m above sea level in the northwest and along the valley walls and the lowest altitudes between 210 and 215 m above sea level in the southeast and near the Missouri River.

Major tributaries to the Missouri River within the study area include the Kansas, Blue, Little Blue, and Fishing Rivers (pl. 1). Numerous smaller streams and constructed agricultural drains and ditches also drain into the Missouri River. Low-lying areas collect surface runoff during wet periods, and standing water may remain for some time where soils are poorly drained.

The Missouri River is too small to have eroded the valley in which it flows (Grannemann and Sharp, 1979). Changes in discharge, sediment load, and base level during glacial and interglacial stages have caused the width, meander wavelength, and meander length of the Missouri River valley to be larger than that which can be produced by the present day Missouri River. Consequently, the Missouri River and its major tributaries are underfit streams.

Climate

The humid continental climate of the study area is characterized by large variations and sudden changes in temperature and precipitation. The average high temperature in July, the hottest month of the year, is 26.7 °C (degrees Celsius), and the average high temperature in January, the coldest month, is 2.3 °C (Hasan and others, 1988). Average annual precipitation ranges from about 86 cm (centimeters) in the northwest to about 91 cm in the eastern part of the study area. About 70 percent of precipitation is during the growing season from April to October (Bevans and others, 1984).

Geology

The floodplains of the Missouri, Kansas, Blue, Little Blue, and Fishing Rivers are underlain by alluvial deposits of Quaternary age consisting of clay, silt, sand, gravel, cobbles, and boulders (Kelly and Blevins, 1995). These deposits overlie shale, limestone, and sandstone bedrock and form the alluvial aquifer that is the focus of this investigation. The nature and extent of the alluvial deposits have been greatly affected by glacial processes that caused numerous changes in discharge, sediment load, and course of these rivers. The present course of the Missouri River approximates the southernmost limit of continental glaciation.

Several abandoned alluvial channels are hydraulically connected to the Missouri River alluvial aquifer and exist as a result of changes in the course of the Missouri River and its tributaries during glacial and interglacial periods. The largest abandoned channel is located in the eastern part of the study area near the Lake City Army Ammunition Plant and is now occu-

pied by the Little Blue River and Fire Prairie Creek (pl. 1). This abandoned channel is connected to a buried alluvial channel that extends north from Buckner, then divides with one arm extending northeast to the Missouri River alluvial aquifer near Sibley and the other arm extending northwest to the Missouri River alluvial aquifer near the Little Blue River (McCourt and others, 1917; K.E. Anderson and F.C. Greene, written commun., 1948).

Bedrock

The alluvial deposits lie atop interbedded thin units of shale, limestone, sandstone, siltstone, conglomerate, coal, and clay of Pennsylvanian age. These units form the base and walls of the alluvial aquifer (Gentile and others, 1994). The altitude of the bedrock surface below the alluvial aquifer (fig. 2), as determined from existing borehole and well data (Kelly and Blevins, 1995), is bowl shaped in cross section with steeply sloping sides, a relatively flat bottom, and several deeply incised narrow channels. The incised channels probably were formed by erosion of the relatively soft bedrock clay and shale when glacial ice dams melted and released large quantities of water (McCourt and others, 1917; Fischel, 1948; Hasan and others, 1988).

Alluvial Deposits

The uppermost finer-grained clay, silty clay, and clayey silt are recent (Holocene) alluvial deposits and the lower coarser-grained sand, gravel, cobbles, and boulders are thought to be Wisconsinian-age alluvial deposits of glacial origin (Hasan and others, 1988). Although grain size typically increases with depth, grain-size distribution in locally heterogeneous deposits can be reversed. Lithologic sections for 12 locations in the study area (pl. 1) were developed from existing drill-cutting descriptions and borehole log data to illustrate the shape of the alluvial aquifer and the extent and lithology of the alluvial deposits.

The alluvial deposits of the Missouri River have a typical grain-size distribution that includes several meters of fine-grained clays and silts at shallow depths, a thick layer of sand and gravelly sand in the middle depths, and a thin layer of sandy gravel, gravel, and boulders in the deepest parts of the aquifer (figs. 3–8). The depth and shape of deeply incised bedrock channels are shown in figures 5 and 6.

The alluvial deposits of the Kansas River are similar to those of the Missouri River (figs. 9, 10). However, lithologic section C-C' (fig. 9) illustrates a heterogeneous grain-size distribution containing more silt and silty sand than the Missouri River alluvium and shows the presence of a deep bedrock channel at the mouth of the Kansas River. A grain-size distribution and bowl-shaped bedrock surface more like that of the Missouri River alluvium is shown in lithologic section D-D' (fig. 10).

The alluvial deposits of the Little Blue River and an abandoned channel near Lake City Army Ammunition Plant are shown in figures 11 through 14. The grain-size distribution is similar to that of the Missouri and Kansas River deposits except that thicker clay and silty clay deposits are present at shallow depths and fewer sandy gravels and gravels are present at depth.

Hydrology and Conceptual Model

Ground-water flow in the Missouri River alluvial aquifer is affected by the hydraulic properties of the aquifer material, the areal extent and thickness of the aquifer, the stage of the Missouri River and its major tributaries, and processes that control ground-water flow across the boundaries of the aquifer. The following descriptions and quantification of aquifer properties and ground-water flow processes, including the internal and external boundaries of the ground-water flow system, the inflow and outflow of water at each of these boundaries, and the effect each boundary has on ground-water flow in the aquifer, define the conceptual model used to construct a numerical ground-water flow model.

Hydraulic Properties of the Aquifer

Ground water exists in the small openings between the particles of sand, silt, clay, and gravel that constitute the alluvial deposits of the aquifer. The percentage of the total volume of the aquifer occupied by these openings or pores is called the porosity. Typical porosity values for alluvial deposits are 40 to 70 percent for clay, 35 to 50 percent for silt, 25 to 50 percent for sand, and 25 to 40 percent for gravel (Freeze and Cherry, 1979). The total volume of ground water in the saturated part of the aquifer at any one time can be estimated by multiplying the saturated volume of the aquifer by the porosity. Assuming an average porosity

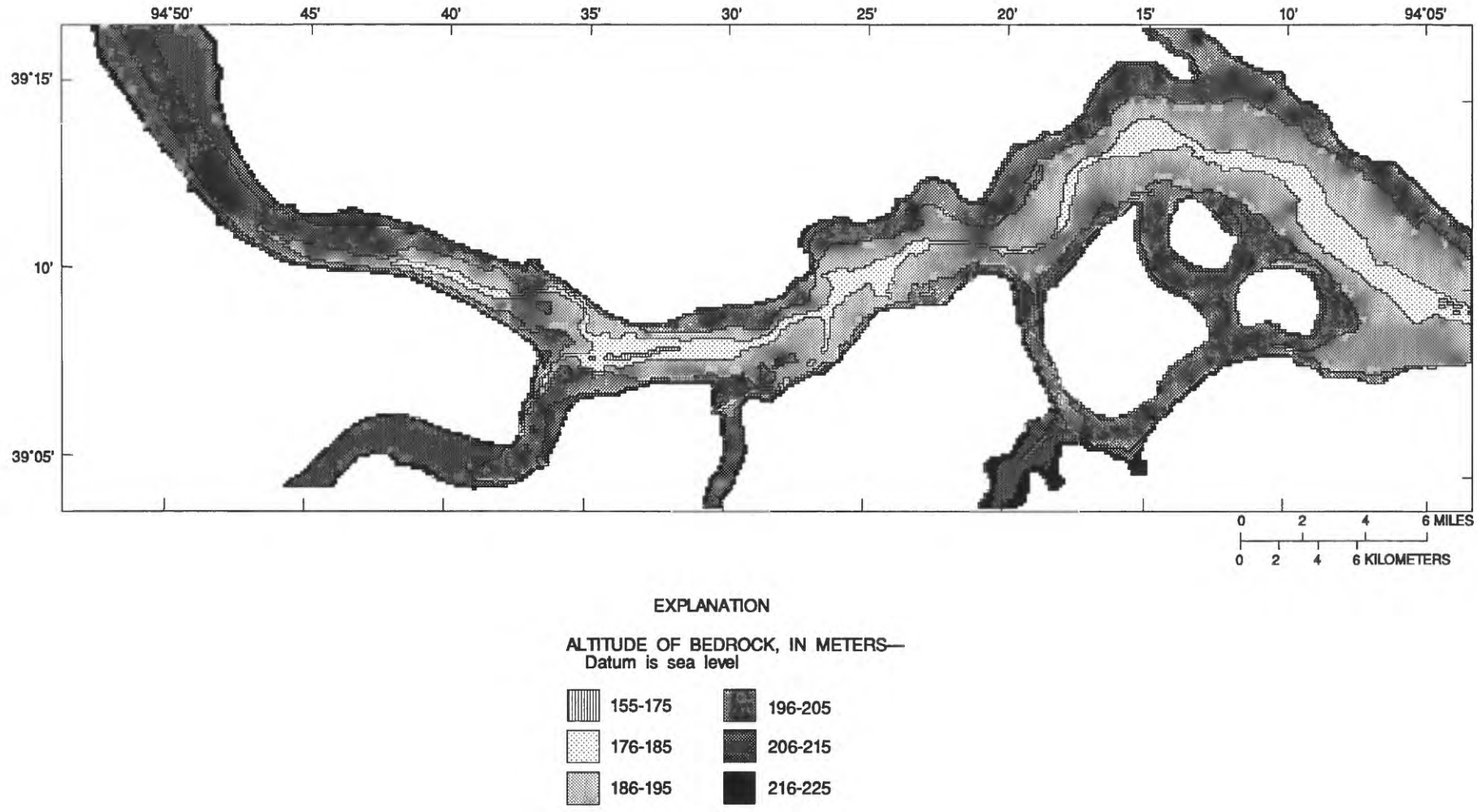

Figure 2. Altitude of bedrock underlying the Missouri River alluvial aquifer.

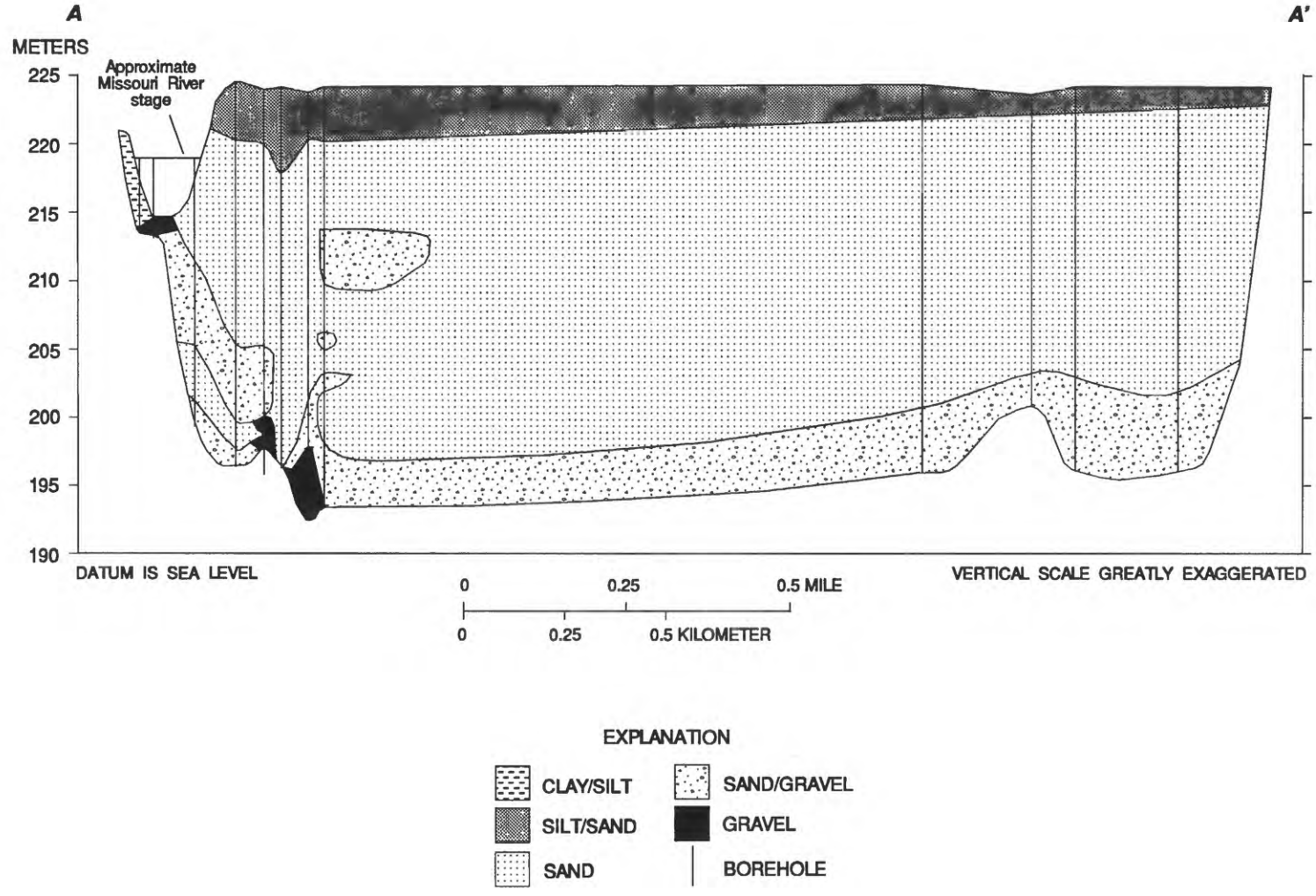

Figure 3. Lithologic section *A-A'*.

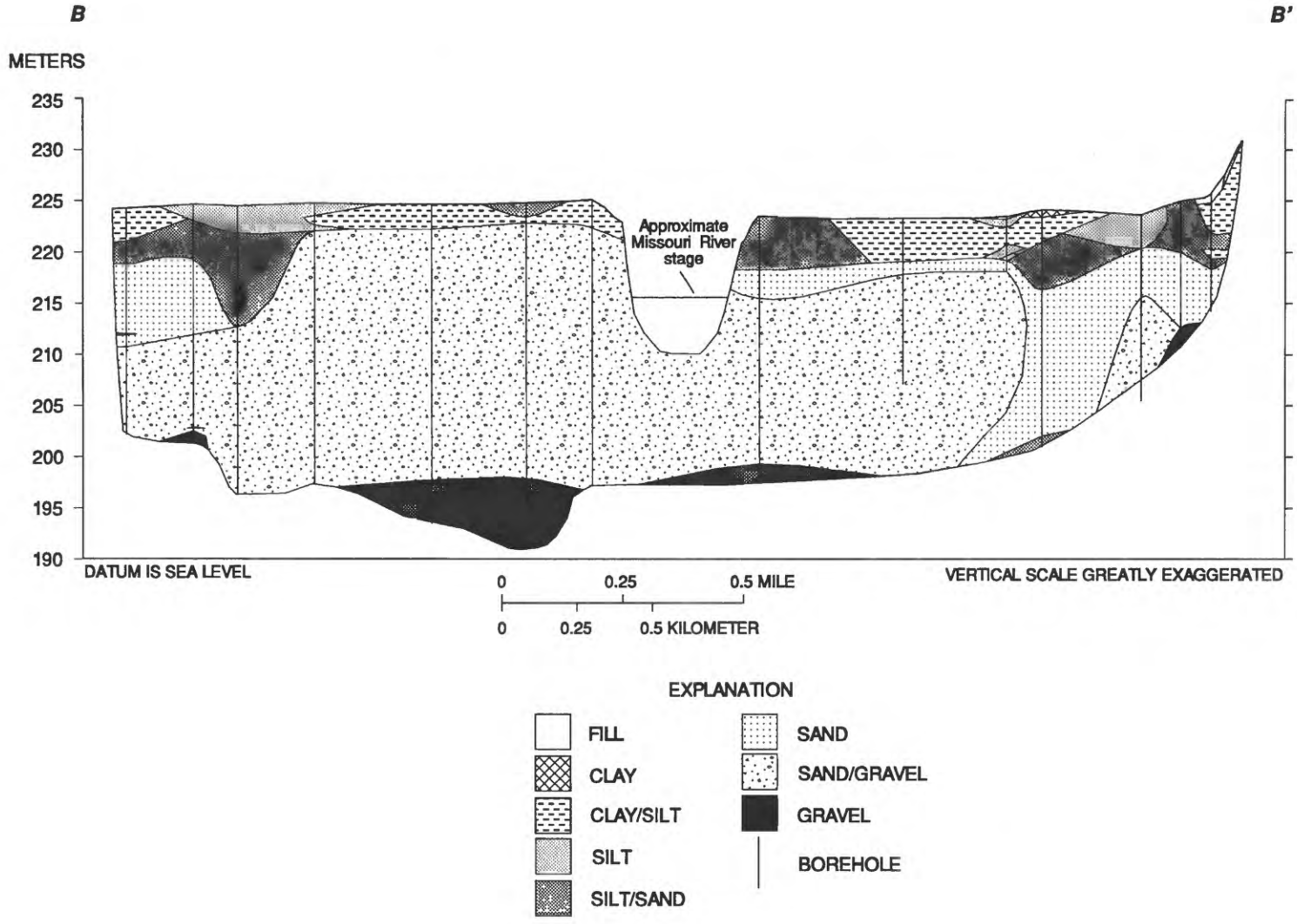

Figure 4. Lithologic section *B-B'*.

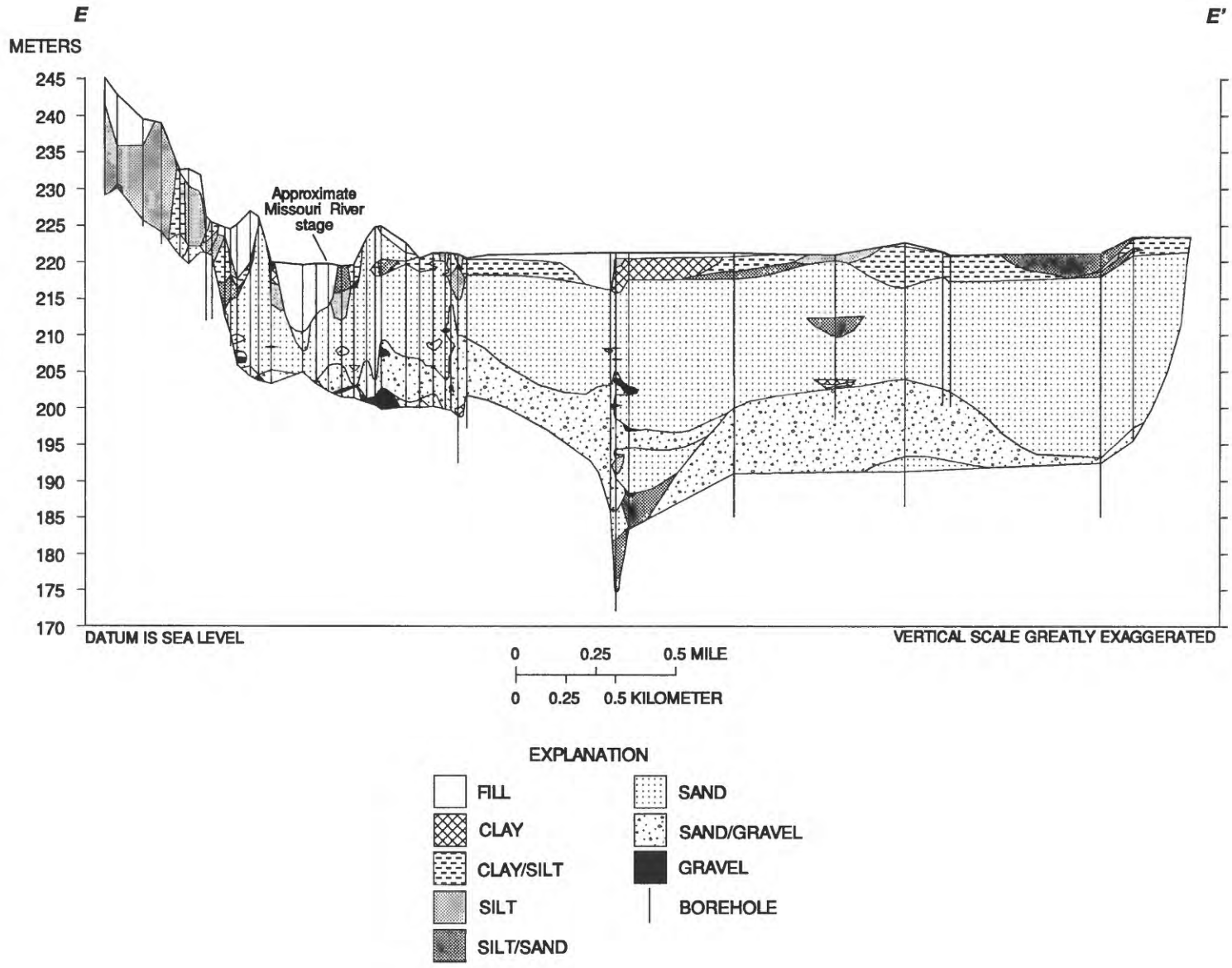

Figure 5. Lithologic section *E-E'*.

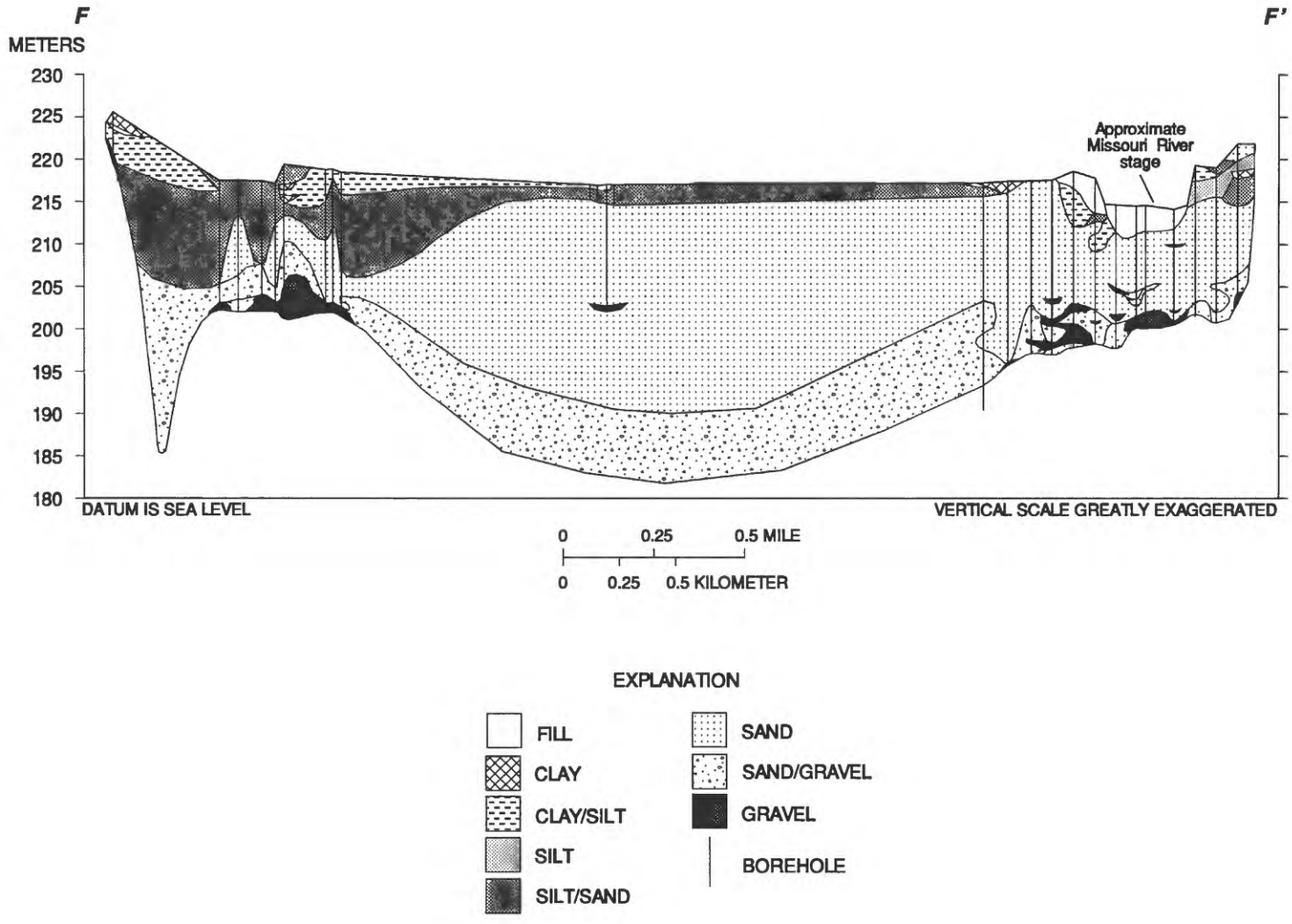

Figure 6. Lithologic section *F-F'*.

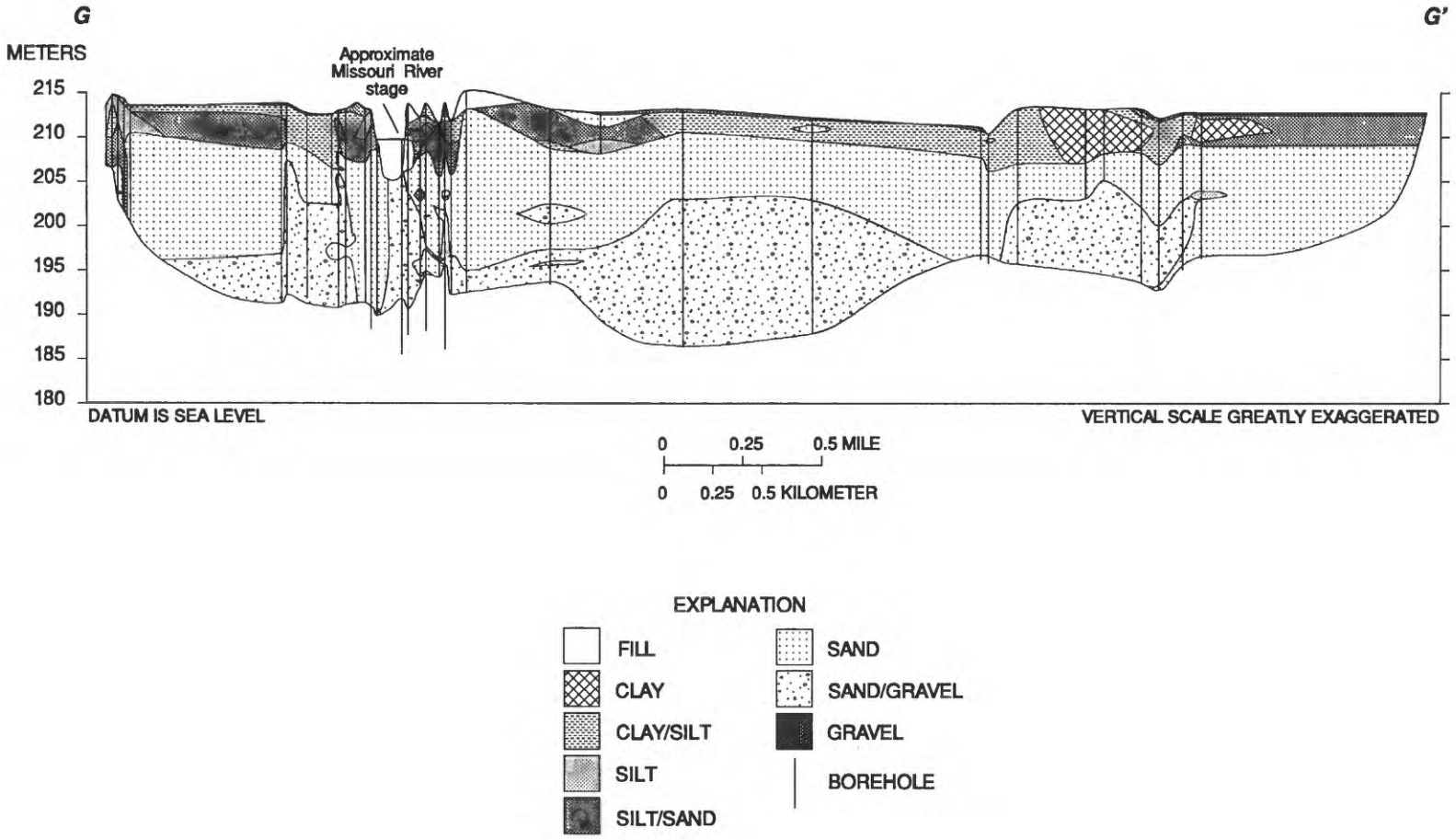

Figure 7. Lithologic section *G-G'*.

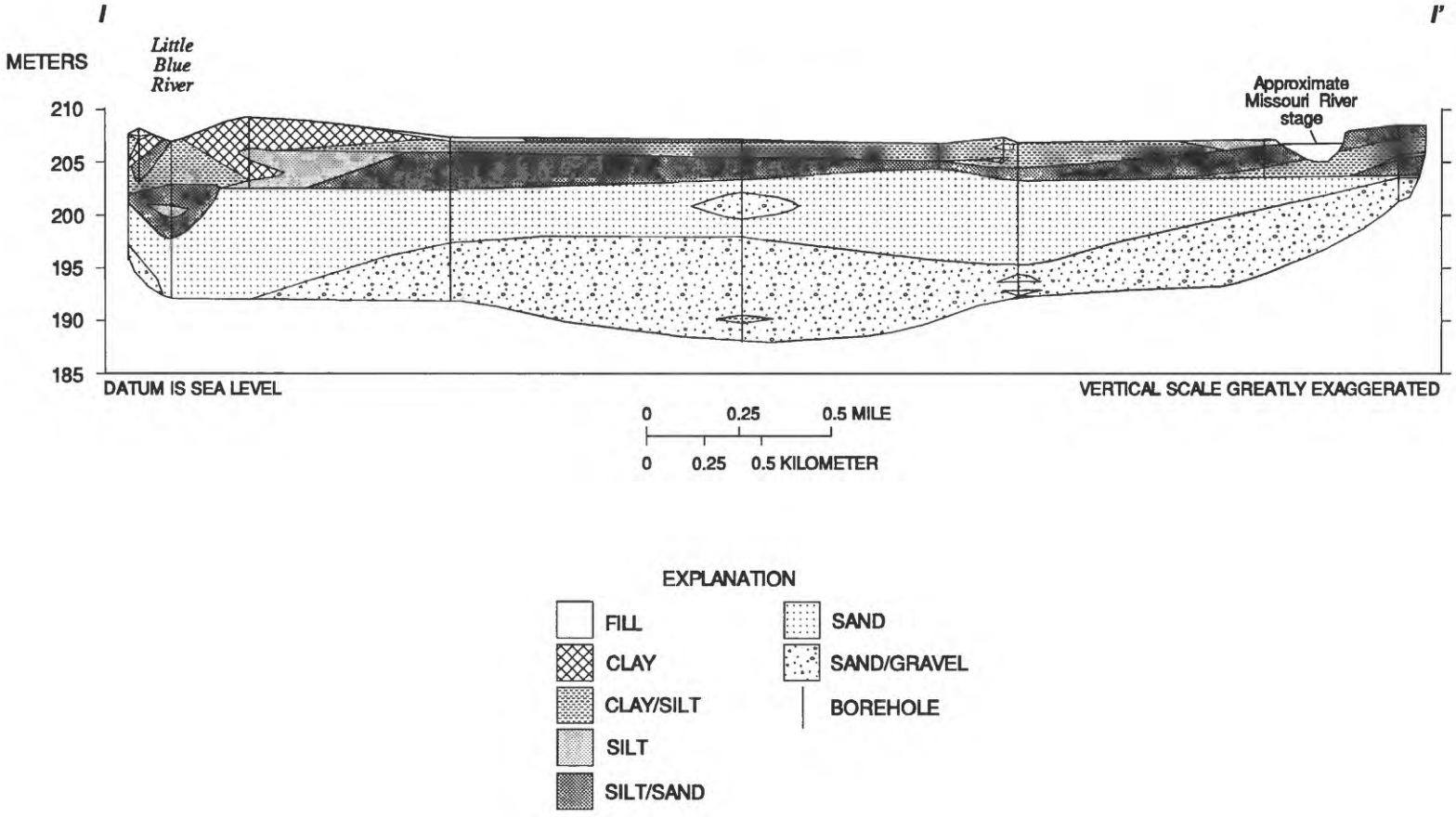

Figure 8. Lithologic section *I-I'*.

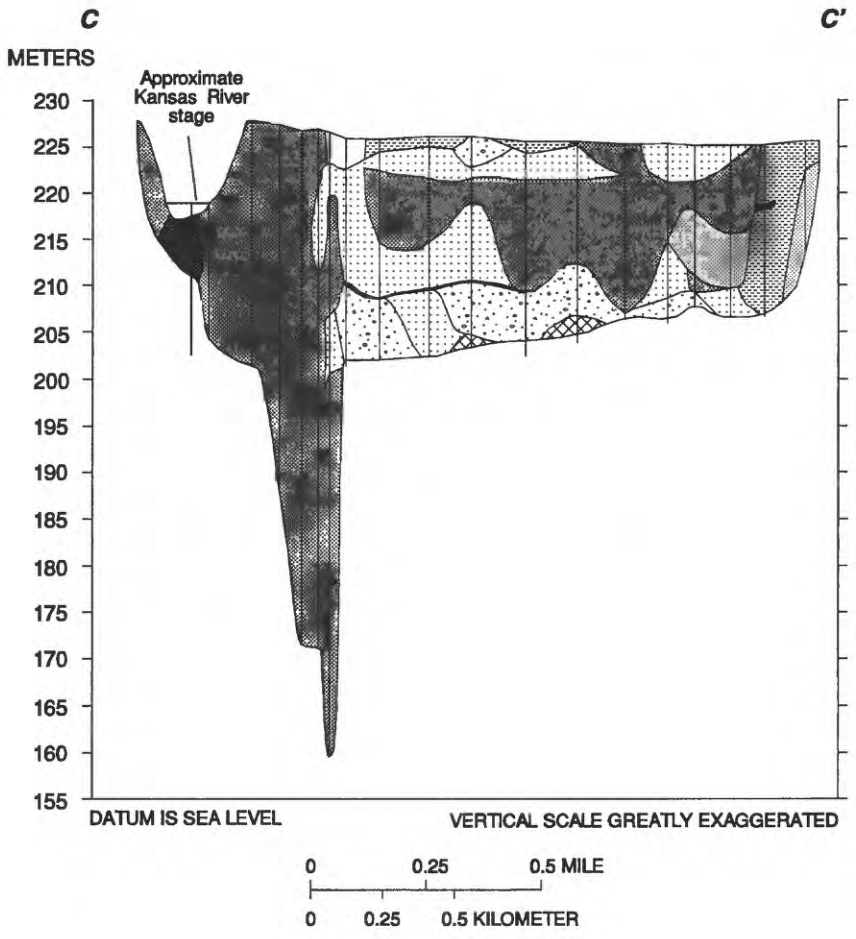

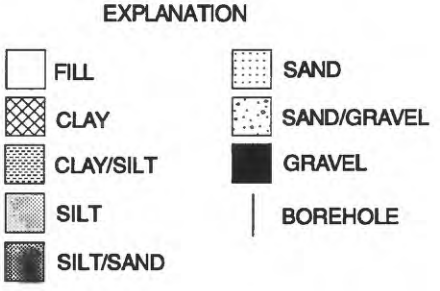

Figure 9. Lithologic section *C-C'*.

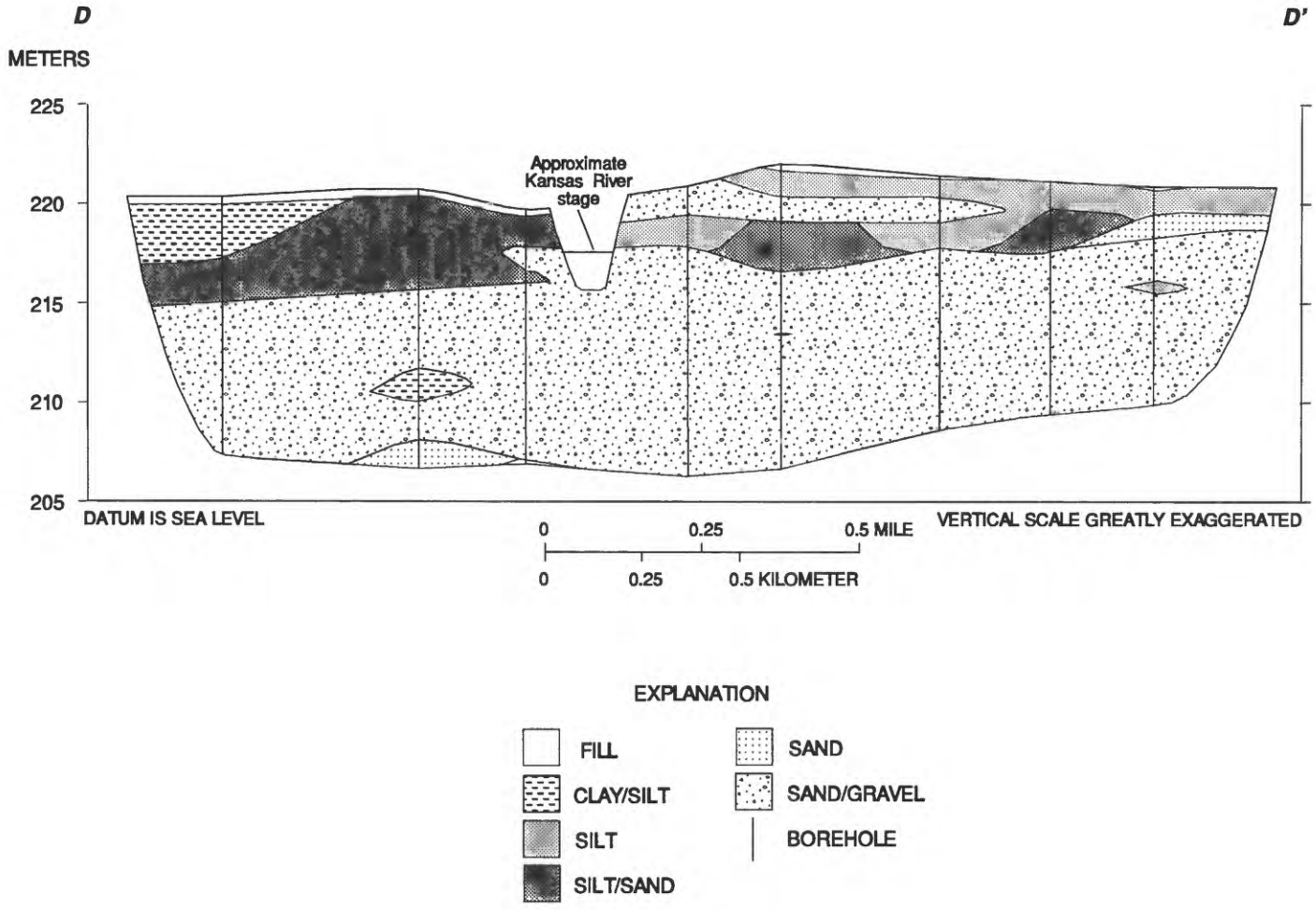

Figure 10. Lithologic section *D-D'*.

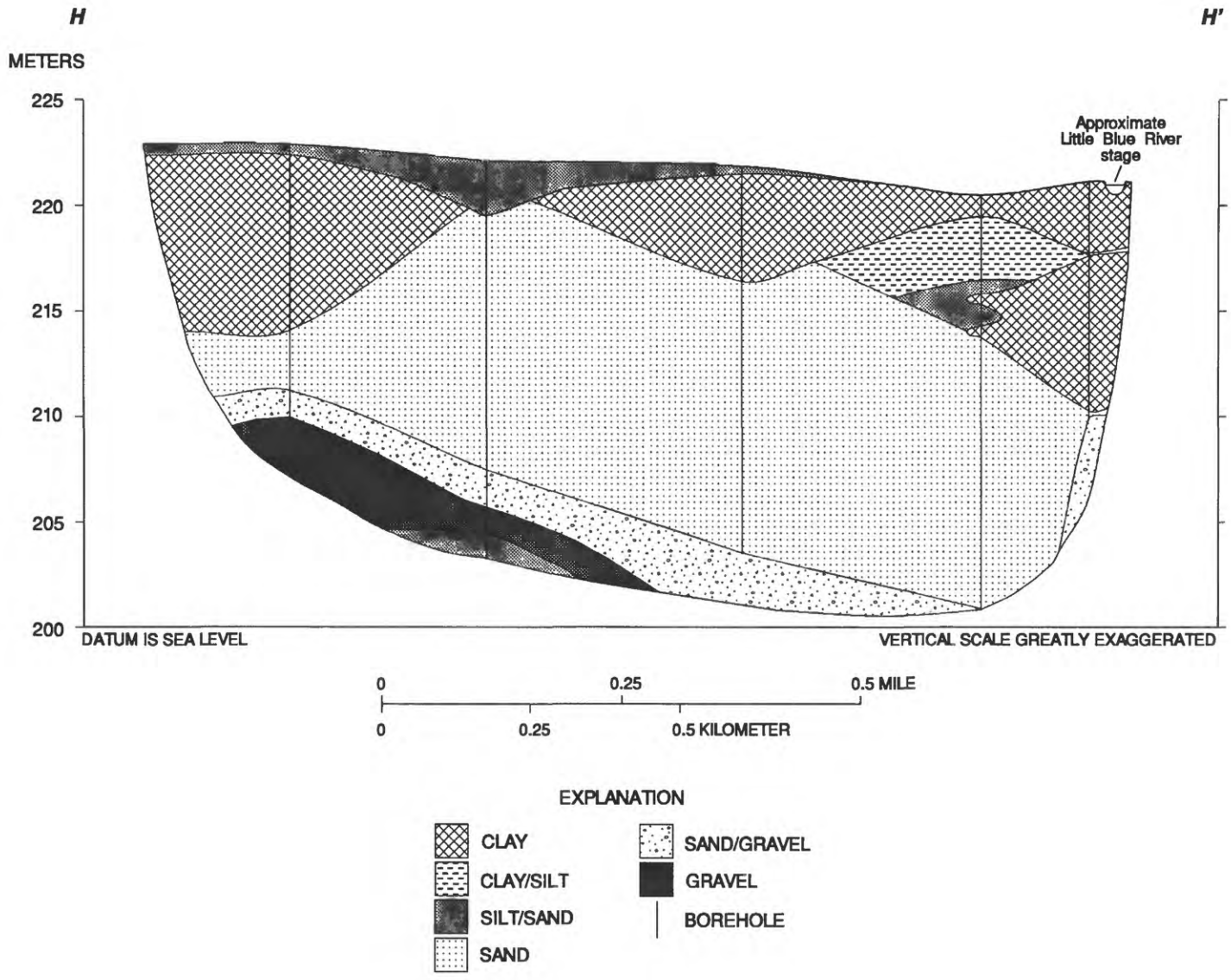

Figure 11. Lithologic section *H-H'*.

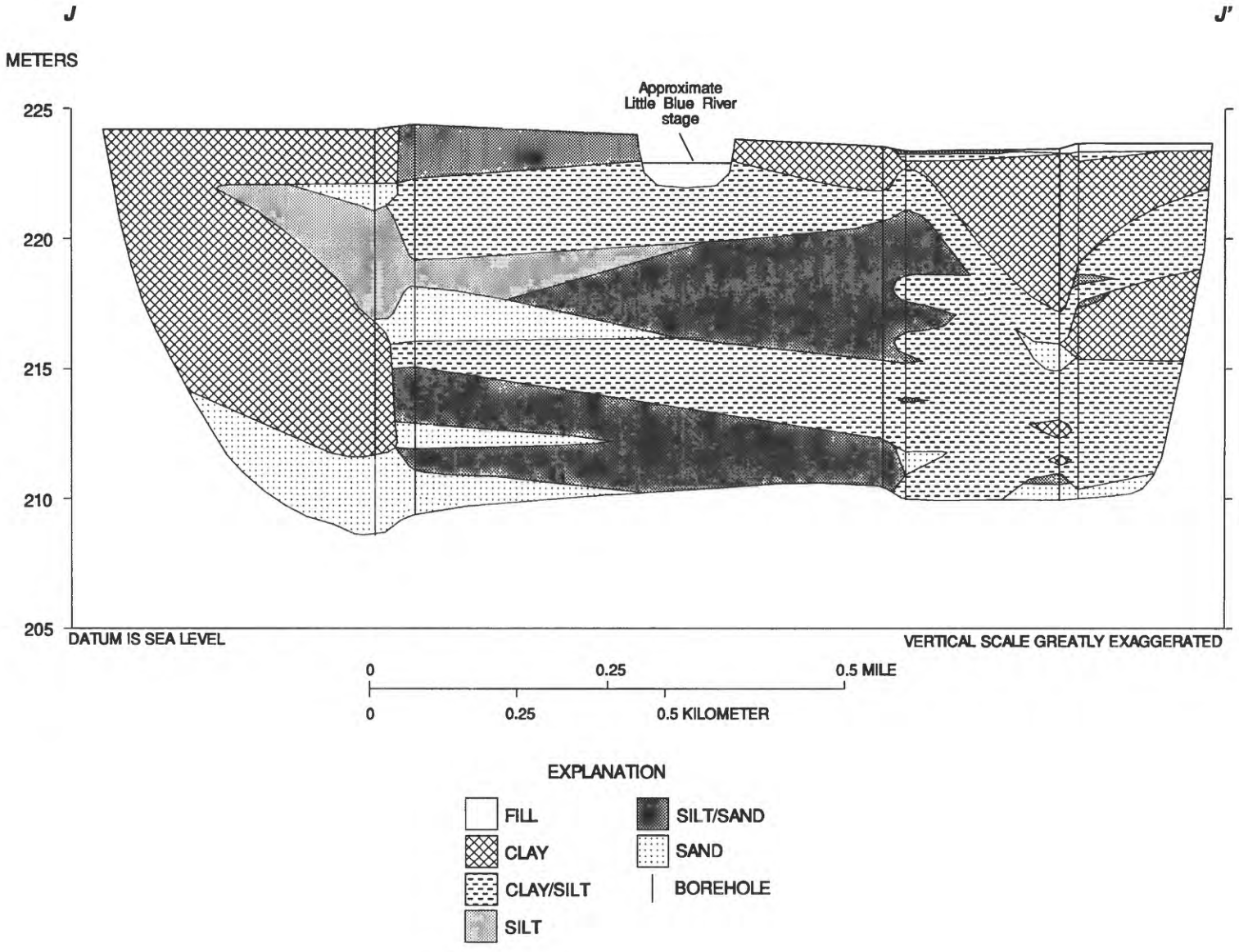

Figure 12. Lithologic section *J-J'*.

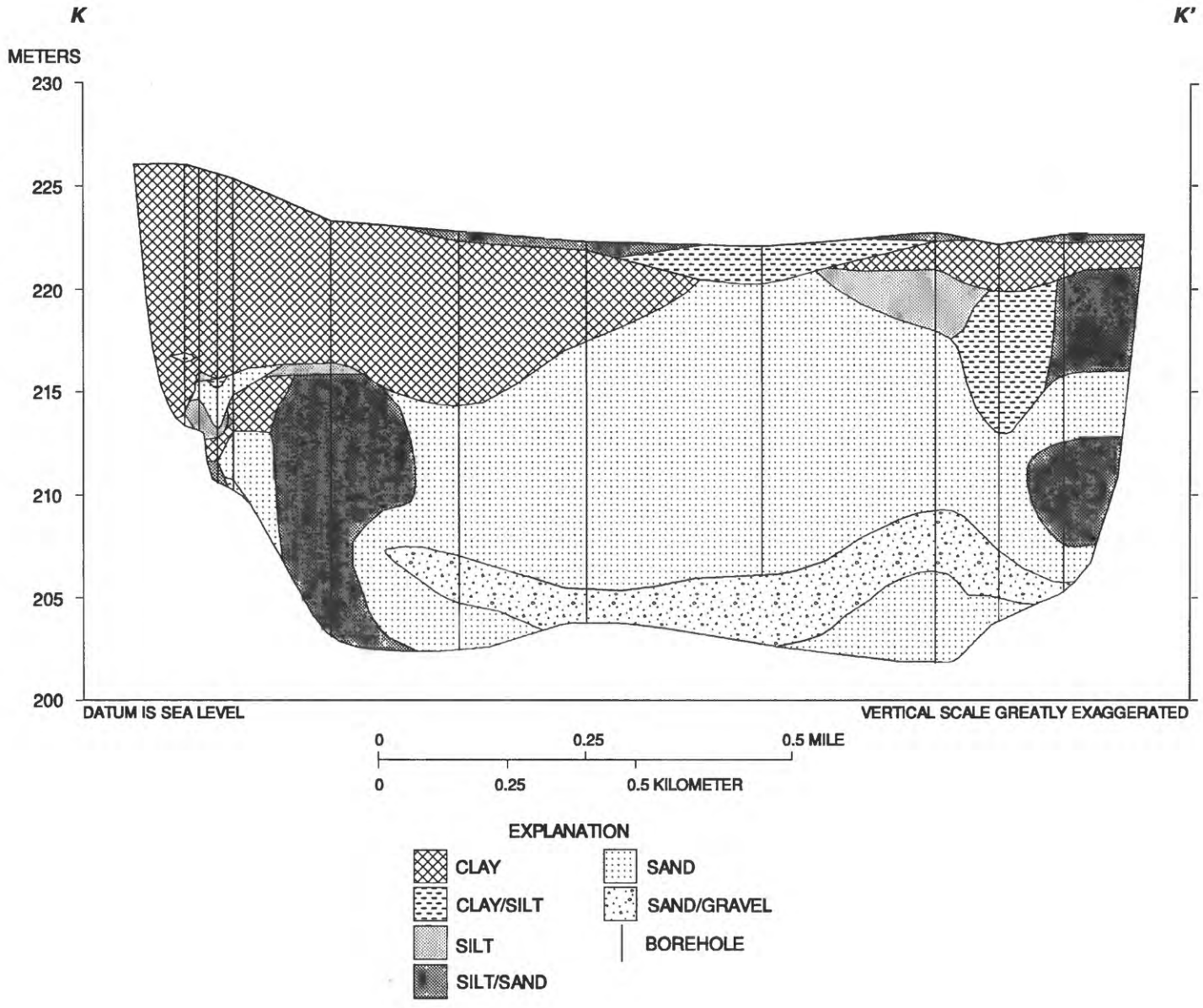

Figure 13. Lithologic section *K-K'*.

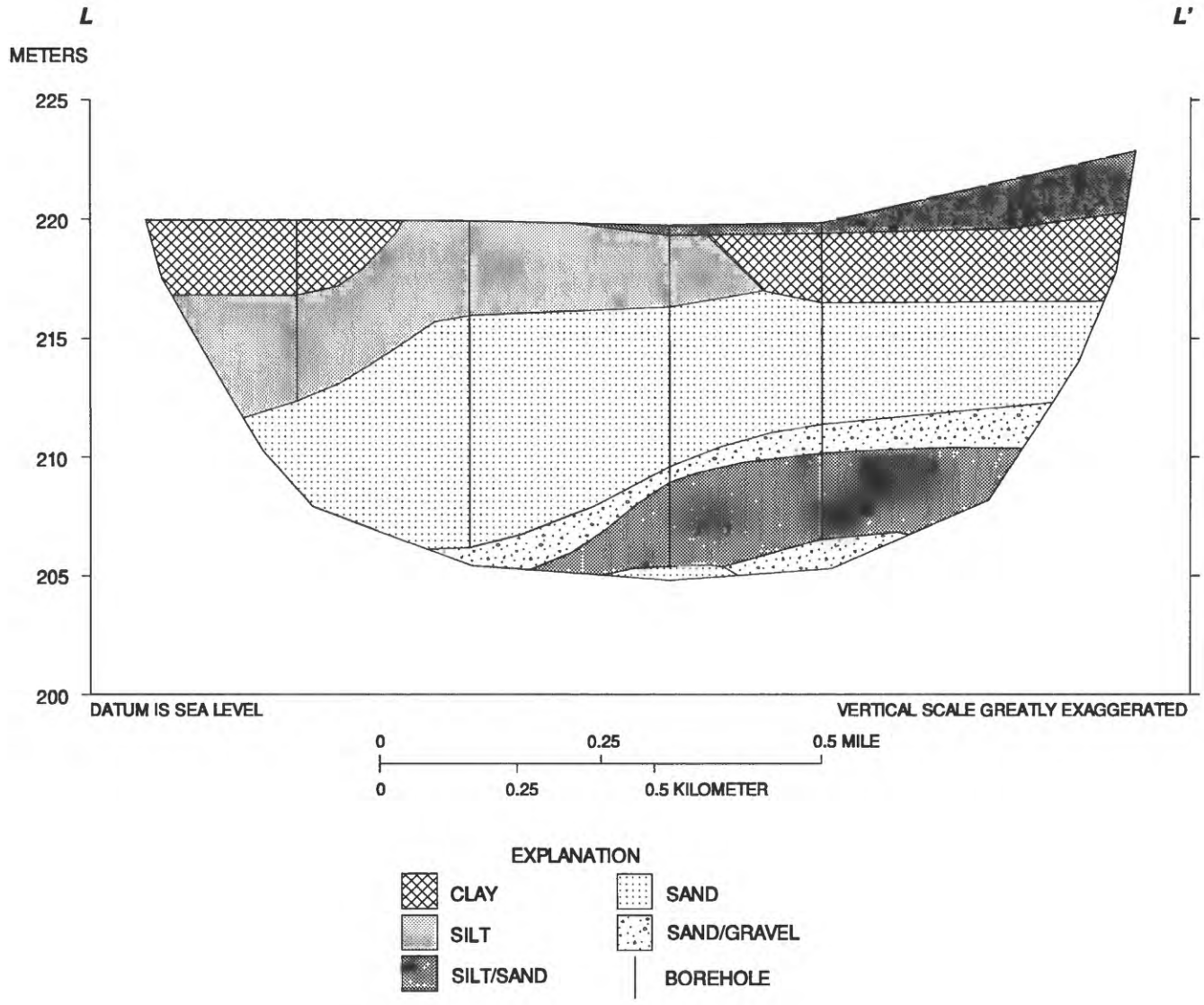

Figure 14. Lithologic section *L-L'*.

of 30 percent in the saturated aquifer volume of 1.25 x 10^{10} m^3 (cubic meters), the volume of water in the aquifer is approximately 3.75 x 10^9 m^3.

The porosity determines the total volume of water the aquifer can hold, but does not determine how much water can be obtained from the aquifer for use. The specific yield is a measure of the ratio of the volume of water that will drain under the effect of gravity to the total volume of saturated aquifer. For the alluvial aquifer in the study area, the specific yield is commonly between 0.15 and 0.2 (Emmett and Jeffery, 1969, 1970). Specific yield applies to unconfined aquifers where the upper surface of the saturated zone, the water table, is within the aquifer and is free to move up or down. The volume of water that can be obtained from an unconfined aquifer is estimated by multiplying the saturated volume by the specific yield of the aquifer. Using a specific yield of 0.2, the volume of water available from the alluvial aquifer is approximately 2.5 x 10^9 m^3. The aquifer is confined by a clay layer during high-water-table conditions in small isolated areas, and the upper surface of the saturated zone is restrained from upward movement. In these confined areas, the volume of water available until the aquifer becomes unconfined is determined by the storage coefficient. The storage coefficient is about 0.001 for the aquifer under confined conditions (Emmett and Jeffery, 1969, 1970).

The hydraulic conductivity is the capacity of the aquifer to transmit water and is the volume of water at the existing kinematic viscosity that will move in unit time under a unit hydraulic gradient through a unit area measured at right angles to the direction of flow. Hydraulic conductivity or transmissivity data are available for 94 locations within the study area. Locations for which lithologic data are known are more numerous and have the widest distribution within the study area. Aquifer tests conducted during previous investigations to determine hydraulic conductivity or transmissivity typically were performed at wells where the lithology and altitude of the screened interval were known. Other reported values of hydraulic conductivity were derived in a laboratory on samples of aquifer material. Reported hydraulic conductivity values for the aquifer are between 0.1 m/d (meter per day) for clay and silty clay and 1,400 m/d for sandy gravel and gravel (Kelly and Blevins, 1995). Transmissivity is the rate at which water of the prevailing kinematic viscosity is transmitted through a unit width of an aquifer under a unit hydraulic gradient and equals the hydraulic conductivity multiplied by the saturated thickness of the aquifer. Reported transmissivity values are between 5 and 7,400 m^2/d (meters squared per day; Fischel, 1948; Emmett and Jeffery, 1969, 1970; Layne-Western Co., written commun., 1981; W.C. Walton, Geraghty and Miller, written commun., 1982; Crabtree and Older, 1985).

The thickness of the alluvium and extent of the aquifer in the study area are shown in figure 15. The greatest alluvium thickness is about 59 m. The average thickness is about 25 m. The water table typically is 4.5 to 7.6 m below land surface.

Aquifer Boundaries

The alluvial aquifer is bounded at the top by the water table and laterally and at the base by bedrock. Arbitrary study area boundaries were established at the upstream and downstream edges of the aquifer. The Missouri River, its major tributaries, lakes and ponds, and pumped wells are boundaries internal to the alluvial aquifer where water flows into or out of the aquifer. The potentiometric surface of the aquifer is defined by the levels to which water will rise in tightly cased wells from a reference level. In an unconfined aquifer, the potentiometric surface is the water table and is the boundary where recharge from precipitation enters the aquifer.

Rivers and Lakes

The fluctuation of river stage in the Missouri and Kansas Rivers, and to a lesser extent, the Blue, Little Blue, and Fishing Rivers has the largest effect on ground-water levels in the study area. Cooley Lake and other smaller lakes and ponds also are present in the study area (pl. 1), but do not substantially affect ground-water levels. The degree of influence a river or lake has on ground-water flow depends on the size of the river or lake with respect to the aquifer, the river or lake stage, the hydraulic conductivity of the river or lake bed material, and the altitude of the river or lake bottom with respect to the potentiometric surface.

An increase in river stage with respect to the altitude of the potentiometric surface causes water to flow from the river into the aquifer and the altitude of the potentiometric surface to increase. A decrease in river stage with respect to the potentiometric surface causes water to flow from the aquifer into the river and the altitude of the potentiometric surface to decrease. The magnitude of the change in the potentiometric

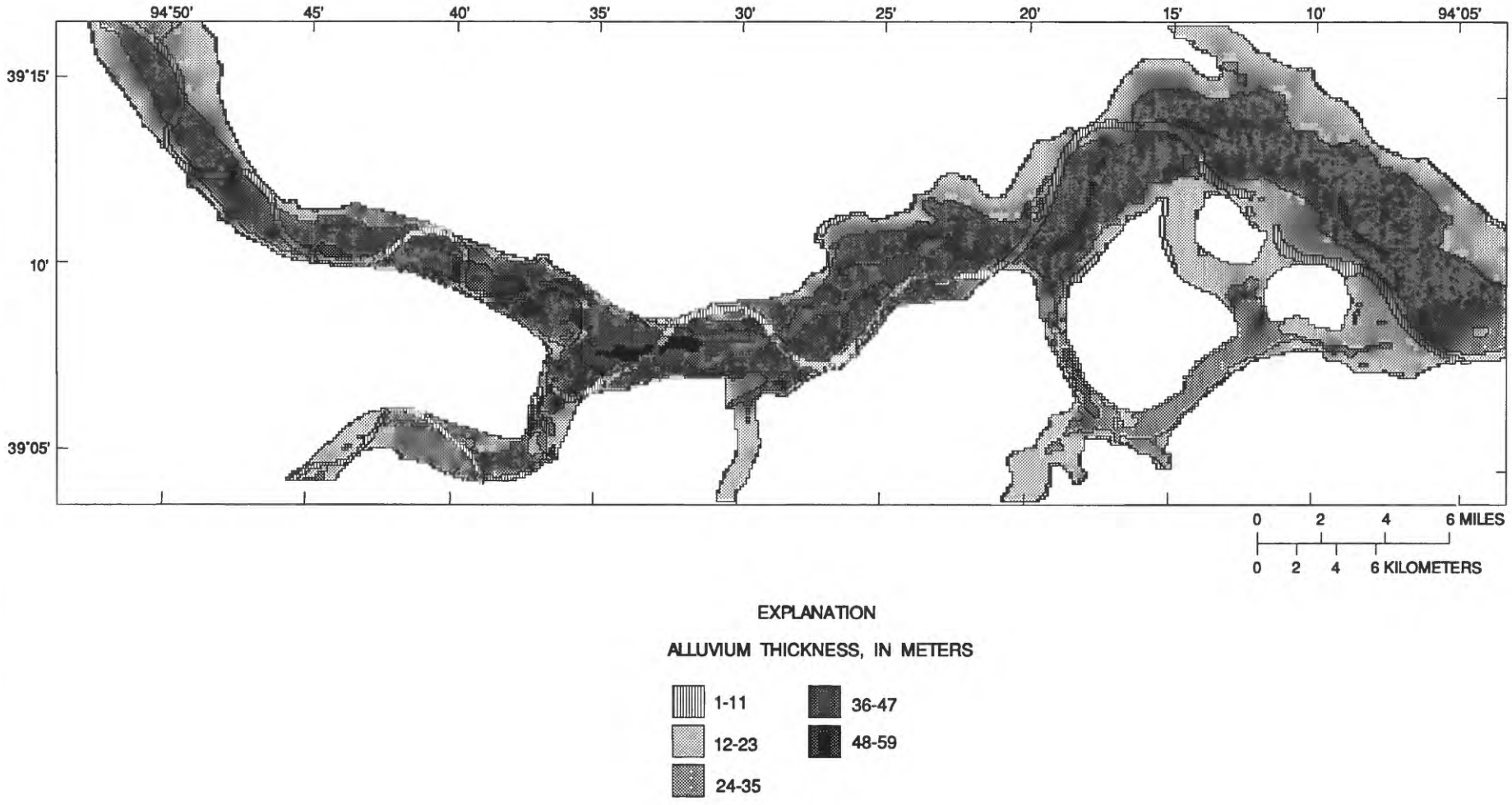

Figure 15. Thickness of the Missouri River alluvium.

surface altitude in response to fluctuations in river stage depends on the magnitude of the change in river stage with respect to previous river stage, the length of time the river remains at the current river stage, the hydraulic properties of the aquifer material, and the distance from the river to the point of interest (Grannemann and Sharp, 1979). The change in the potentiometric surface altitude in response to a change in river stage is more rapid in areas closer to the river than in areas farther from the river because of the time required for the change to propagate into and through the aquifer. Therefore, the area of the aquifer that is affected by a change in river stage depends on the length of time that the river stage remains at the new altitude. Changes in the altitude of the potentiometric surface at some distance from the river are the result of long-term river stage changes typically caused by seasonal high and low flows or long-term management of river stage.

The largest rivers in the study area, the Missouri and Kansas Rivers, have the greatest effect on ground-water flow. The riverbeds of these rivers have a large hydraulic conductivity and the bottom of the river channels are below the top of the potentiometric surface. The riverbed deposits of the Missouri and Kansas Rivers typically are composed of sand and gravel, and the bottoms of the channels intersect the sand and gravel in the middle depths of the aquifer (figs. 3–10). Thus, both the Missouri and Kansas Rivers are well connected hydraulically to the underlying alluvial aquifer.

The Blue, Little Blue, and Fishing Rivers have less effect on ground-water flow than the larger Missouri and Kansas Rivers. The hydraulic conductivity of the riverbeds for these rivers is smaller, and in some places, the bottoms of the river channels are above the top of the potentiometric surface. Riverbed deposits of the Blue, Little Blue, and Fishing Rivers typically are composed of finer grained clay, silt, and sand, and the bottoms of the channels intersect the finer grained alluvial deposits located at shallower depths (figs. 11–14). Thus, these rivers are less well connected to the underlying alluvial aquifer, but can have some effect on ground-water flow.

Numerous smaller streams and drainage ditches are present in the study area. During most of the year, the bottoms of these streams are above the top of the potentiometric surface, and the streams have less effect on ground-water flow than larger streams like the Little Blue and Fishing Rivers. These smaller streams and ditches have low and sometimes intermittent discharges and supply small amounts of recharge to the aquifer during the year. However, these small streams may affect ground-water flow locally during floods when they supply recharge to the aquifer or during periods when the potentiometric surface rises above the water level in the streams and water from the aquifer discharges into the streams.

The water level of Cooley Lake, an oxbow lake, is maintained at a constant level as part of a wildlife management plan (Missouri Department of Conservation, oral commun., 1992). Lake bottom deposits of oxbow lakes typically are composed of clay and silt of low hydraulic conductivity. Cooley Lake recharges the aquifer when the potentiometric surface is below the managed lake level and drains the aquifer when the potentiometric surface is above the managed lake level. This recharge rate is low, however, because of the low hydraulic conductivity of the lake bottom deposits.

Water levels in other small lakes are not maintained at constant levels, but these lakes may be areas of increased recharge because they collect surface runoff. Water levels in these lakes are affected by increases or decreases in the altitude of the potentiometric surface that cause a corresponding increase or decrease in lake water levels.

Potentiometric Surface

The potentiometric surface is free to move up or down in the unconfined Missouri River alluvial aquifer, and it is the boundary across which recharge from infiltrated precipitation flows into the aquifer. Areally distributed recharge occurs when the rate of infiltrated precipitation or snowmelt exceeds the rate of evapotranspiration from the soil. However, because the water table typically is deeper than 4.5 m from land surface, evapotranspiration is not a large source of discharge from the aquifer. During periods of high recharge rates, the altitude of the potentiometric surface increases because the aquifer is gaining water faster than losing water. When recharge rates are low or zero, the altitude of the potentiometric surface decreases because the discharge rate exceeds recharge rate.

Recharge to alluvial aquifers in this area has been estimated in several previous studies to be between 2 and 25 percent of precipitation (K.E. Anderson and F.C. Greene, written commun., 1948; Fischel and others, 1953; Layne-Western Co., written

commun., 1979; Hedman and Jorgensen, 1990). Recharge to the aquifer from precipitation is about 7.6 x 10^7 m^3 per year, assuming about 15 cm of recharge per year (16 percent of precipitation).

Because the study area has low local relief, topography has little effect on the areal distribution of recharge. Rather, the vertical hydraulic conductivity of soils directly controls the rate of infiltration. Aquifer recharge is greater beneath a soil with a larger vertical hydraulic conductivity than beneath a soil with a smaller vertical hydraulic conductivity. Therefore, soil variability affects the areal distribution of recharge to the aquifer, and a vertical hydraulic conductivity map of soils (Kelly and Blevins, 1995) indicates areas of larger or smaller aquifer recharge.

Bedrock

Ground-water flow between the alluvial aquifer and the bedrock has not been quantified. However, the bedrock has an estimated hydraulic conductivity between 0.003 and 3 m/d and an extremely slow rate of water flow (Gann and others, 1974). This range of hydraulic conductivity is between 10 and 10,000 times lower than the range for the alluvial aquifer. Hedman and Jorgensen (1990) attempted to calculate gains and losses in discharge at the Missouri River because of ground-water flow from and to the bedrock. However, the uncertainty in the estimates was greater than the estimated gains and losses. Flow between the aquifer and bedrock is thought to be small in comparison to the total flow of ground water in the aquifer.

Upstream and Downstream Aquifer Boundaries

The Missouri River alluvial aquifer extends the length of the Missouri River. The alluvial aquifers of the Kansas, Blue, Little Blue, and Fishing Rivers also extend beyond the study area. The upstream and downstream aquifer boundaries used in this study are not physical hydraulic boundaries, but were chosen based on the study objectives and area of interest. Ground water flows into the system through the upstream boundaries of the study area and flows out of the system through the downstream boundary of the study area. The ground-water flow rate across the boundary depends on the angle of the direction of ground-water flow with respect to the boundary, the hydraulic conductivity of the material at the boundary, the gradient of the potentiometric surface at the boundary, and the saturated thickness of the aquifer at the boundary. When the direction of ground-water flow is parallel to the boundary, no ground water crosses the boundary. These boundaries were chosen to be parallel or sub-parallel to the direction of ground-water flow to minimize the flow rate across the boundaries.

Well Pumping

In 1995, 12 public-water-supply well fields, numerous industrial well fields, irrigation wells, and domestic wells were in operation in the study area. The total volume of water withdrawn from the aquifer by pumping of public-water-supply wells was recorded monthly for most well fields and was obtained from each water supplier when available. Pumping rates for industrial wells were obtained from owners' records. The total annual volume of water removed from the aquifer by other wells in the study area, including industrial wells, irrigation wells, and small public-water suppliers, was obtained from the Missouri Department of Natural Resources (1991). Pumping rates for wells with no records were estimated based on type of use and pump rating. Water pumped from the alluvial aquifer in the study area by public-water-supply well fields (pl. 1) in 1990 totalled 109,740 m^3/d (cubic meters per day) or 10.58 billion gallons per year (Kelly and Blevins, 1995). Recharge from precipitation supplies about 7.6 x 10^7 m^3 (20 billion gallons) of water per year to the aquifer, and the volume of stored water available for use at any one time is about 2.5 x 10^9 m^3. Therefore, about 50 percent of annual recharge supplied to ground water from precipitation and about 1.6 percent of the ground water stored in the aquifer was withdrawn in 1990 by public-water-supply well fields. However, the volume of water available to wells close to the Missouri River is much greater because they can obtain a large part of their water from recharge induced from the river because of drawdown near pumped wells. For example, about 50 percent of the water pumped at the city of Independence well field in 1975 was from induced recharge from the Missouri River (C.E. Nuzman, Layne-Western Co., written commun., 1975).

Withdrawal of water from the aquifer by pumped wells creates cones of depression around each well or well field and causes ground water to flow toward the wells. A cone of depression generally has the shape of an inverted cone with the lowest part centered at the pumped well. Extensive pumping within the study has resulted in numerous cones of depression. The source area for water that discharges from a

pumping well is the CRA for that well. Most water recharging the Missouri River alluvial aquifer comes from surface recharge.

Ground-Water Movement

In the absence of pumping, ground-water flow within the alluvial aquifer typically is away from the valley walls, toward the Missouri River, and down the river valley (Emmett and Jeffery, 1969, 1970; Kelly and Blevins, 1995). A rapid increase in river stage can temporarily reverse the direction of ground-water flow. Flooding, irrigation, pumped wells, and dewatering during construction also can alter ground-water flow directions. Two potentiometric surface maps based on synoptic water-level measurements conducted in August 1992 and January 1993, during a previous study (Kelly and Blevins, 1995), illustrate both the general flow of ground water down the river valley and toward the Missouri River and the effects of local recharge and pumped wells on ground-water movement.

Ground-water flow in the aquifer in October 1993 and February 1994 is illustrated with two potentiometric surface maps (figs. 16, 17) based on synoptic water-level measurements and river-stage data obtained during this study. These synoptic water-level measurements of 123 wells between October 18 and 22, 1993, and of 98 wells between February 14 and 18, 1994, were obtained following the July-August flood of 1993. The number of wells available for the synoptic water-level measurement during this study was less than in the previous study (Kelly and Blevins, 1995) because the flood of 1993 destroyed many wells. However, water-level measurements were available for most parts of the study area. River-stage data were obtained from six gages on the Missouri River and one gage each on the Kansas, Blue, and Little Blue Rivers.

The flood of 1993 caused large amounts of water to flow into the aquifer from the rivers and saturated nearly all of the alluvium. Beginning in August 1993, as river stage decreased to normal levels, water from the aquifer began to drain into the rivers. Drainage continued as river stage declined until ground-water flow in the aquifer returned to a more typical pattern by the end of February 1994. Thus the October 1993 and the February 1994 potentiometric surface maps represent two "snapshots" of ground-water levels in the aquifer during a prolonged period of drainage after the flood.

SIMULATION OF GROUND-WATER FLOW

Ground-water flow was simulated for the Missouri River alluvial aquifer using the three-dimensional finite-difference ground-water flow model MODFLOWARC (Orzol and McGrath, 1992). MODFLOWARC is a modified version of MODFLOW (McDonald and Harbaugh, 1988) that reads and writes files using a geographic information system (GIS). The equation used in the computer model to describe ground-water flow is:

$$\frac{\partial}{\partial x}\left(Kxx\frac{\partial h}{\partial x}\right)+\frac{\partial}{\partial z}\left(Kyy\frac{\partial h}{\partial y}\right)+\frac{\partial}{\partial z}\left(Kzz\frac{\partial h}{\partial z}\right)-W=S_s\frac{\partial h}{\partial t},$$

where

Kx, Ky, and Kz are the values of hydraulic conductivity along the x, y, and z coordinate axes and are assumed to be parallel to the major axes of hydraulic conductivity, in meters per day;

h is the potentiometric head, in meters;

W is a volumetric flux per unit volume and represents sources or sinks, or both, of water, such as well discharge, leakage through confining units, riverbed leakage, recharge, and water removed from the aquifer by drains, per day;

S_s is the specific storage of the porous material, per meter; and

t is time, in days.

The flow equation was solved by the strongly implicit procedure (SIP; McDonald and Harbaugh, 1988, p. 12–1), a method for solving a large number of simultaneous linear equations by iteration.

Three-dimensional simulation of ground-water flow in the alluvial aquifer was necessary to accurately determine the hydraulic head distribution beneath the main rivers and near the many well fields in the study area. Discharge from the aquifer to rivers may vary according to river size or depth of incision. Ground-water flow may be divided into smaller flow subsystems because of the degree of interaction between ground water and the large and small rivers in the study area. Three-dimensional simulation also was necessary to analyze ground-water travel times and determine the CRA around each pumped well field because vertical flow of ground water was induced by

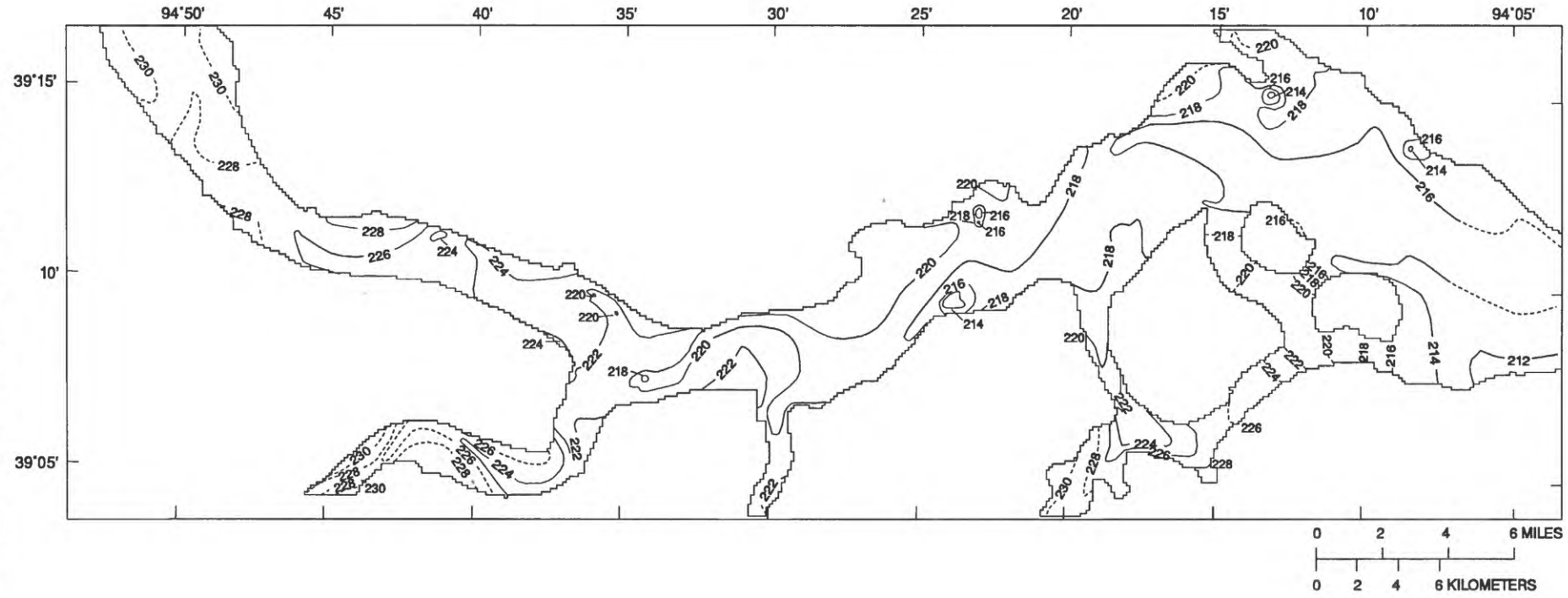

Figure 16. Potentiometric surface of the Missouri River alluvial aquifer, October 1993.

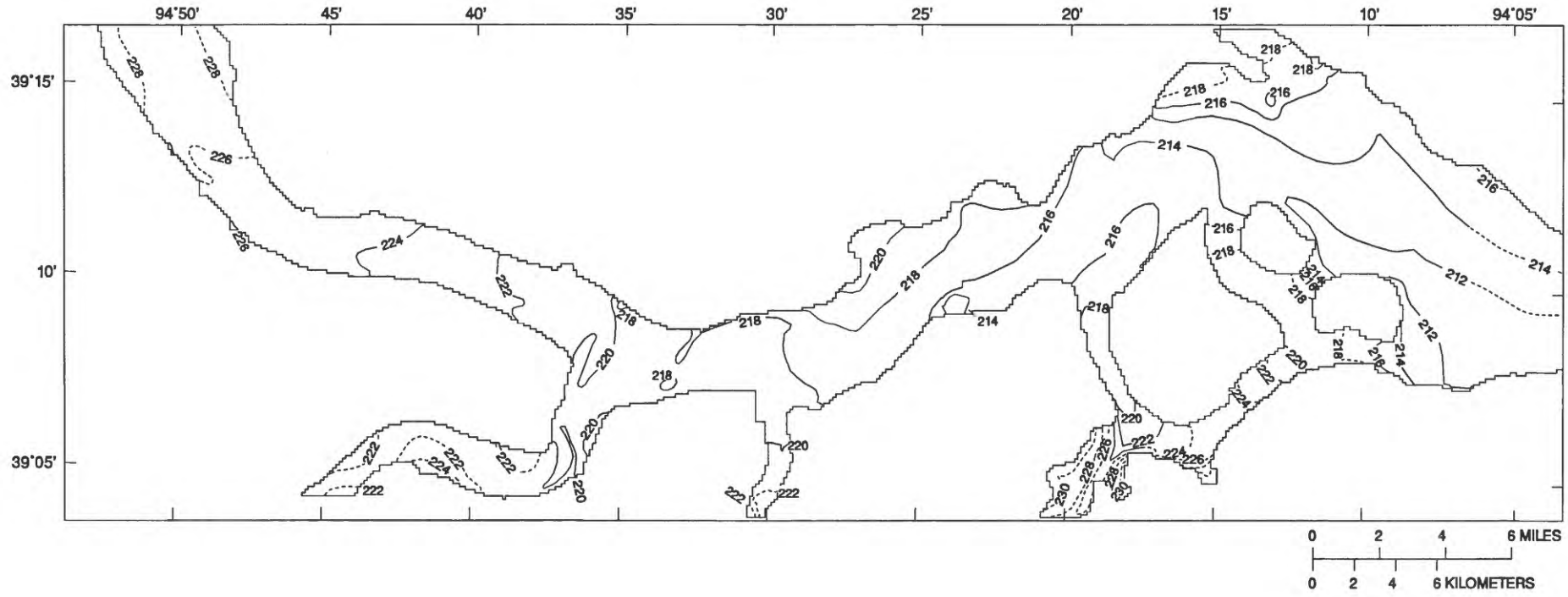

EXPLANATION

— 220 --- POTENTIOMETRIC CONTOUR—Altitude to which water in a tightly cased well would have risen from hydrostatic pressure in aquifer. Dashed where approximately located. Contour interval 2 meters. Datum is sea level

Figure 17. Potentiometric surface of the Missouri River alluvial aquifer, February 1994.

well pumping. Also, pumping from the well fields located near the Missouri River can induce recharge from the river and cause ground-water flow beneath the river.

Model Description

The modeled area is 73 by 24 km and is shown on plate 1. The model uses a uniform grid size of 150 by 150 m and contains 310,400 cells in 4 layers, 160 rows, and 485 columns. The irregular shape of the study area resulted in 67,362 active cells in the model, with 20,835 active cells in layer 1; 22,198 active cells in layer 2; 17,978 active cells in layer 3; and 6,351 active cells in layer 4. The uniform grid facilitated data input from the GIS and analysis of model output by the GIS, and the grid size minimized errors in flow-path analysis that would be caused by a larger grid size (Pollock, 1994; Zheng, 1994).

The model represents the alluvial aquifer using four layers, numbered 1 to 4, of variable thickness (figs. 18–21) with no intervening confining layers. Layer 1 corresponds to the upper part of the aquifer where clay, silt, and fine-grained sand are dominant. The thickness of layer 1 is large enough to account for the anticipated range of water-level variation within the aquifer during ground-water flow simulation and was modeled using unconfined aquifer hydraulic properties. Layers 2 and 3 correspond to the middle part of the aquifer where sand and gravelly sand predominate. These layers were not anticipated to dewater during the simulations and were modeled using confined aquifer hydraulic properties. Layer 4 corresponds to the deep parts of the aquifer where gravel and sandy gravel are present and also was modeled using confined aquifer hydraulic properties.

Hydrogeologic data from more than 1,400 locations within the study area were used in the model. Values for hydrogeologic parameters were assigned to each model cell by interpolation from the GIS. Lithologic descriptions recorded during the installation of wells and boreholes are the most numerous and have the greatest areal extent of all data types in the GIS. The distribution of clay, silt, sand, and gravel within the aquifer was used to distribute the hydraulic conductivity and storage coefficients among model cells, and the depth to bedrock was used to determine the geometry represented by the model.

Boundary and Initial Conditions

The conceptual model described ground-water flow and identified boundaries needed for computer simulation of ground-water flow. These boundaries include rivers and lakes, the water table, bedrock, other edges of the study area, and pumped wells. The ground-water flow model simulates each of these boundaries as a specified-head boundary, a specified-flow boundary, a head-dependent flow boundary, or a free-surface boundary (Franke and others, 1984). A specified-head boundary maintains the hydraulic head at a specified value as a function of time and position, and ground-water flow across the boundary varies with respect to the difference in hydraulic head between the boundary and the aquifer. For a specified-flow boundary, the volume of water that flows across the boundary is a function of time and position, and hydraulic head varies as a function of flow. The volume of flow across a head-dependent flow boundary varies as a function of hydraulic head at the boundary. The position of a free-surface boundary is not fixed but varies with time.

The Missouri, Kansas, Blue, Little Blue, and Fishing Rivers and Cooley Lake are represented in the model as a head-dependent flow boundary. The altitude of the river or lake stage must be known at each model cell that simulates the effect of a river or lake. Flow into or out of the aquifer at these cells is a function of the river or lake stage with respect to the altitude of the potentiometric surface, the hydraulic conductivity of the riverbed or lakebed material, the cross-sectional area of flow between the river or lake bed and the aquifer, and the altitude of the potentiometric surface with respect to the altitude of the riverbed or lakebed (McDonald and Harbaugh, 1988, p. 6–5).

River stage in the Missouri, Kansas, Blue, and Little Blue Rivers was recorded at gaging stations (pl. 1) hourly. The altitude of the river surface used in each simulation was assigned to each model cell by interpolation along the midline of each river of the specified river surface altitude between gaging stations. Altitude of the river surface between tributary gaging stations or between tributary gaging stations and the altitude of the Missouri River surface at the tributary mouth were interpolated along the midline of each tributary. Altitude of the river surface in the ungaged Fishing River was estimated using the Missouri River stage at the mouth of Fishing River and the slope of the land sur-

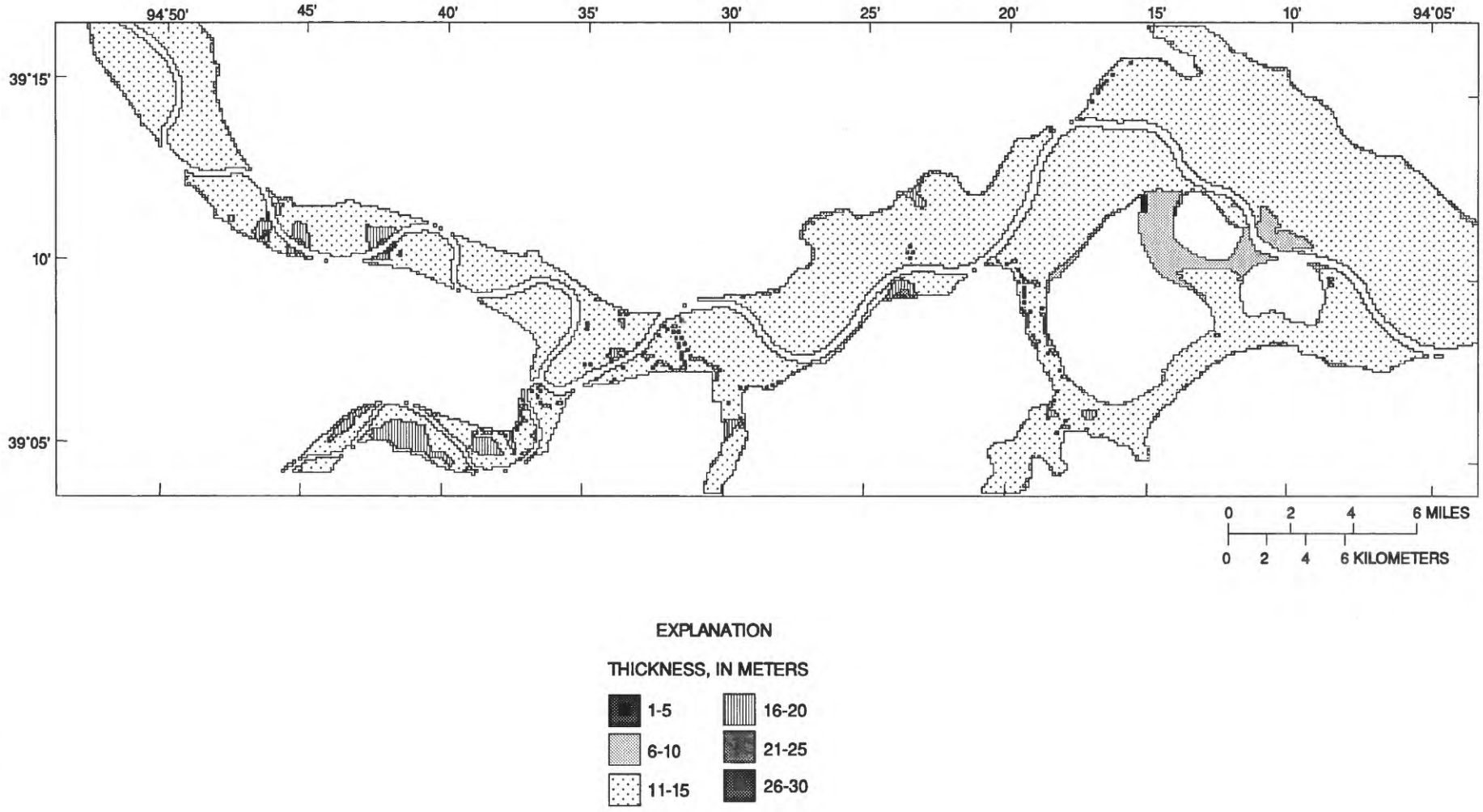

Figure 18. Thickness represented in model layer 1.

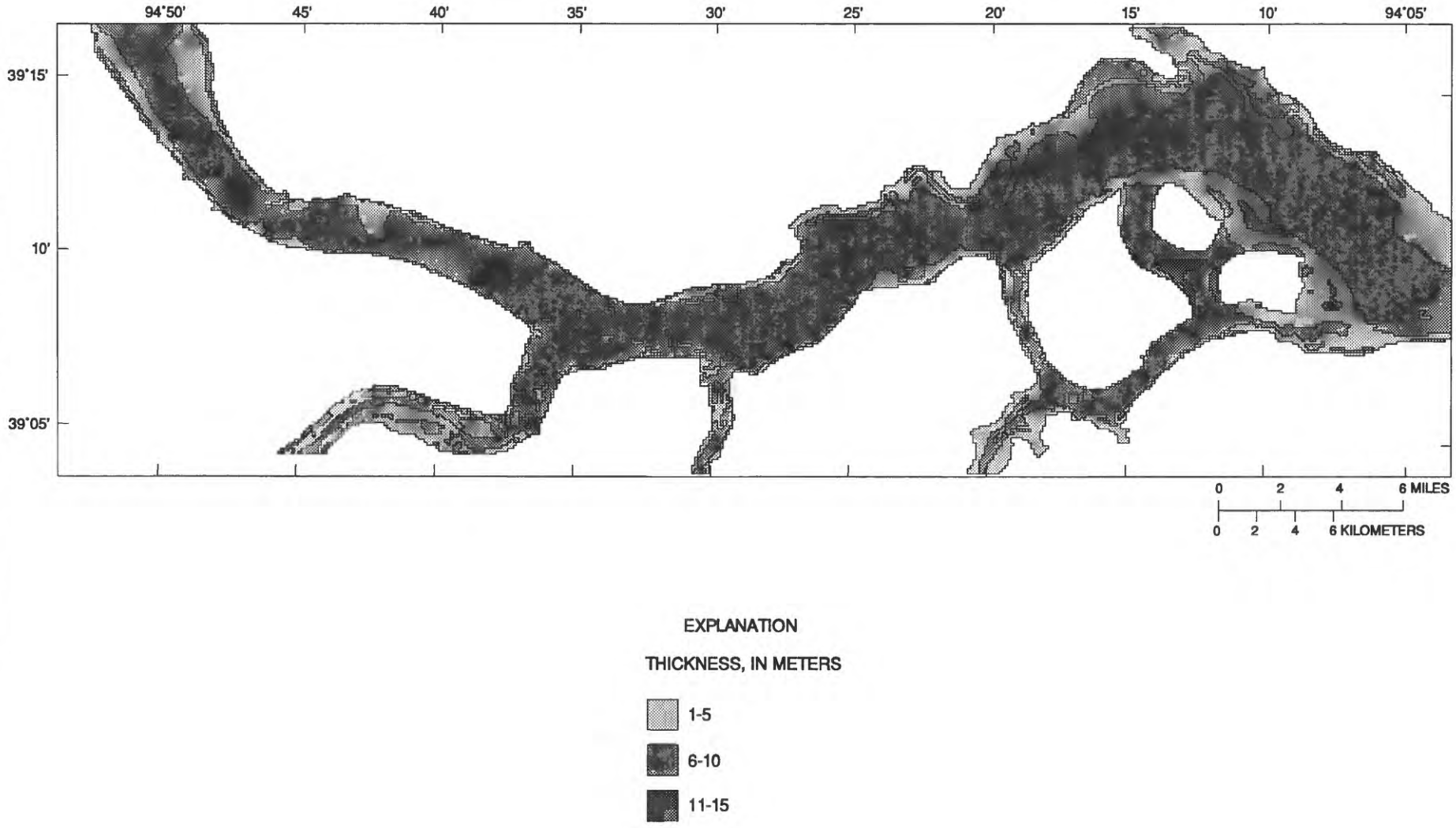

Figure 19. Thickness represented in model layer 2.

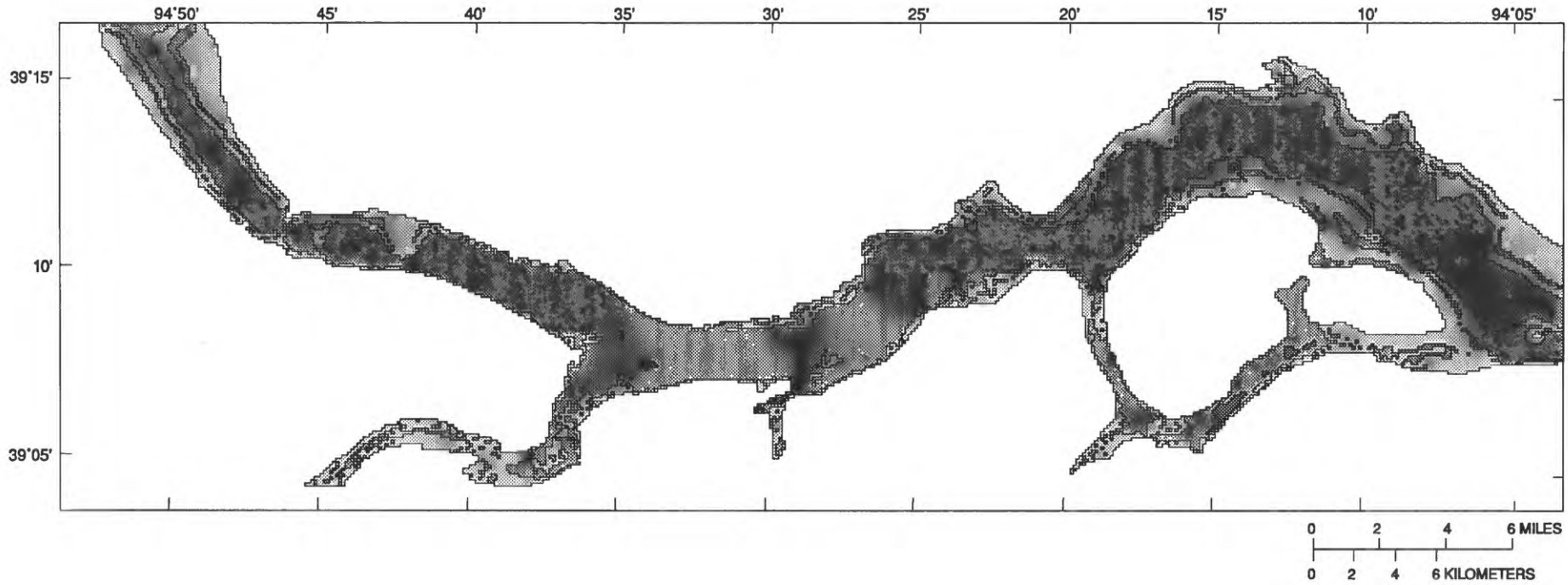

Figure 20. Thickness represented in model layer 3.

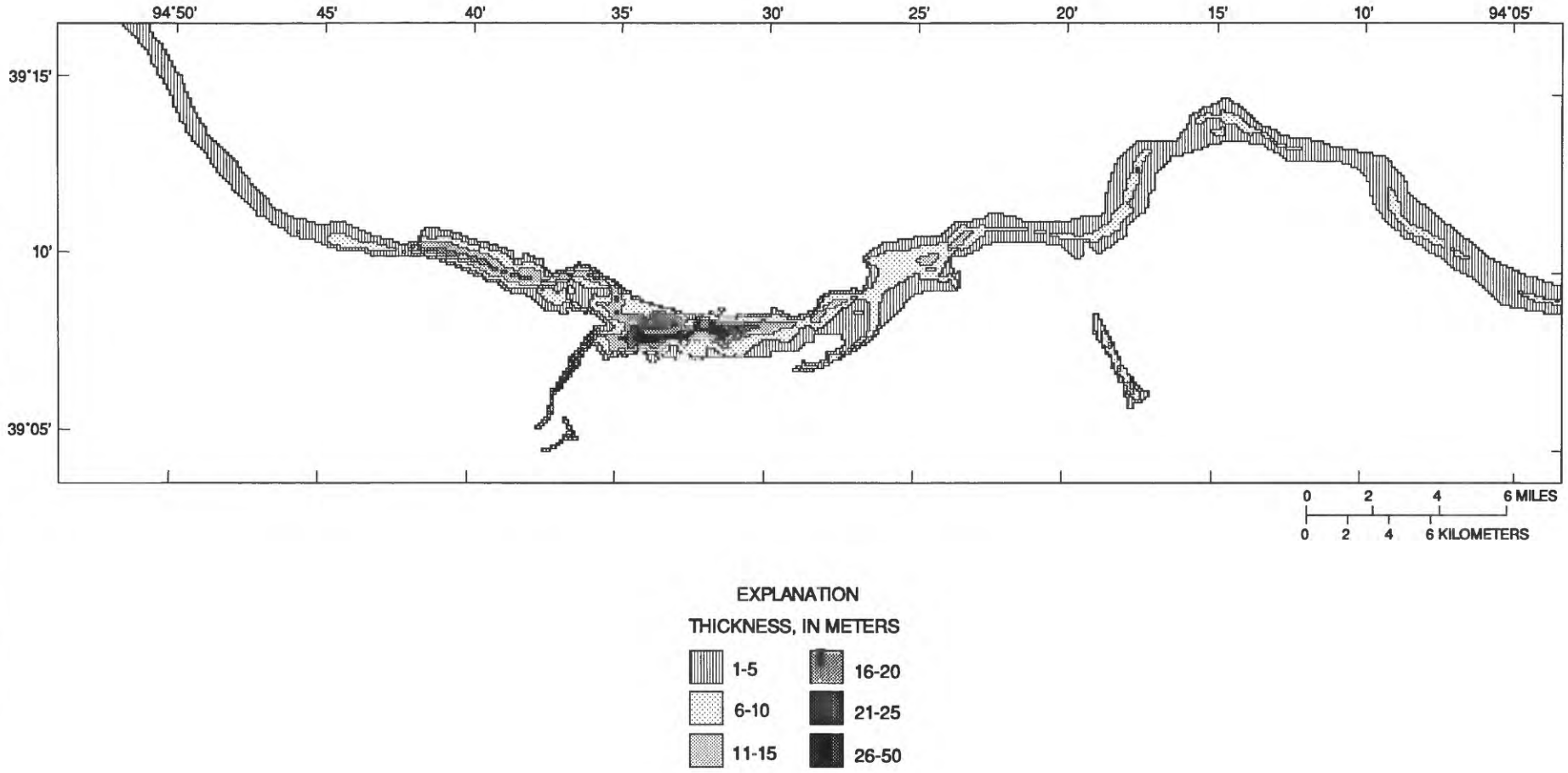

Figure 21. Thickness represented in model layer 4.

face and interpolated along the midline of Fishing River to the edge of the study area.

The channel bottoms of the Missouri and Kansas Rivers intersect the sand and gravel in the part of the aquifer that corresponds to model layer 2. Therefore, the bottoms of these rivers were placed in layer 2. The channel bottoms of the smaller Blue, Little Blue, and Fishing Rivers are within model layer 1 because they are shallower than the bottoms of the Missouri and Kansas Rivers and intersect the shallower clay and silt in the upper part of the aquifer. The effect on ground-water flow of the artificially maintained lake stage in Cooley Lake is similar to the effect of a river on ground-water flow and is simulated in the model with the same equation used for the rivers. The lake bottom of Cooley Lake intersects the clay and silt of the upper part of the aquifer, and the lake bottom is within model layer 1.

Riverbed conductance was calculated by multiplying the vertical hydraulic conductivity assigned to the model cell within which the river reach was located by the area of the river within the cell and the thickness of the riverbed. For all rivers and streams represented in the model, riverbed thickness was assumed to be 1 m. This value was adjusted for each river during model calibration. The factors used to adjust riverbed conductance for each river are shown in table 1.

Table 1. Adjustment factors for riverbed conductance

River or lake	Adjustment factor
Missouri River	0.4, or 0.1 if the horizontal hydraulic conductivity assigned to the cell is less than or equal to 50 meters per day
Kansas River	0.4, or 0.1 if the horizontal hydraulic conductivity assigned to the cell is less than or equal to 50 meters per day
Blue River	0.1
Little Blue River	0.3, or 0.15 if the river mile is greater than 12
Fishing River	0.1
Cooley Lake	0.05

Numerous small streams and drainage ditches in the study area were simulated in the model as drains. Drains are head-dependent flow boundaries, but, unlike the simulated rivers, do not supply water to the aquifer. Water was removed from the aquifer by the drains at a rate proportional to the difference between the hydraulic head in the aquifer and the altitude of the bottom of the drain and the hydraulic conductivity of the bottom material of the drain (McDonald and Harbaugh, 1988, p. 9–3). Drains were ranked in three classes according to their size. Drain conductances were calculated in the same manner as the riverbed conductances and then adjusted based on their relative size. The factors used to adjust drain conductances are shown in table 2 for each class of drain. All drain bottoms are within layer 1 of the model. The altitude of the drain bottom within layer 1 was assigned using a constant altitude of 1 m less than the land surface altitude for agricultural ditches (class 1) or 2 m less than the land surface altitude for small streams (class 2) and larger streams (class 3).

Table 2. Adjustment factors for drain conductance

Drain size class	Adjustment factor
1	0.01
2	.04
3	.3

The water table, the upper boundary of the alluvial aquifer, was simulated in the model as a free-surface boundary across which areally distributed recharge entered the aquifer. Recharge to the model was applied to the topmost active cell in each vertical column and was varied areally and temporally as a function of precipitation and the average vertical hydraulic conductivity of the class of soils in each model cell (Kelly and Blevins, 1995). Recharge was calculated as a percent of precipitation that was recorded daily at the Kansas City Municipal Airport, between August 1 and October 31, 1993, and at Independence, Missouri, between November 1, 1993, and March 27, 1994. Both locations are near the middle of the study area. The calibrated recharge rates used for each soil vertical hydraulic conductivity class are shown in table 3. Urbanized parts of the study area with unknown vertical hydraulic conductivity of soils were assigned a recharge rate considered intermediate for the study area.

Bedrock was simulated in the model as a no-flow boundary. The rate of water flow between the alluvial aquifer and the bedrock has not been quantified. However, the range of hydraulic conductivities of the bedrock is several orders of magnitude less than hydraulic conductivities in the alluvial aquifer. Therefore, simulating the bedrock as a no-flow boundary is

reasonable because the amount of flow across the boundary is a negligible percentage of the total flow.

Table 3. Recharge as a percentage of precipitation for each soil vertical hydraulic conductivity class

[<, less than; >, greater than]

Soil vertical hydraulic conductivity class	Vertical hydraulic conductivity range, in meter per hour	Recharge as a percentage of precipitation
1	<0.015	0.04
2	0.015 to 0.023	.15
3	0.023 to 0.043	.22
4	0.043 to 0.152	.40
5	>0.152	.50
6	Unknown	.15

Several boundaries of the model do not represent actual physical or ground-water flow boundaries of the alluvial aquifer, but are located where the alluvial aquifers of the Missouri, Kansas, Blue, Little Blue, and Fishing Rivers intersect the model boundary. These boundaries were placed as far as practical from areas of pumped wells to limit the effect of the boundary on model results within the anticipated CRA. Also, the orientation of each boundary was set parallel or sub-parallel to the estimated direction of ground-water flow at the boundary. This orientation further limits the effects of these boundaries on model results. These boundaries were simulated in the model as general-head boundaries, a form of the head-dependent flow boundary that allows flow to enter or exit proportional to the difference between the water level represented in the model and the water level assigned to the boundary multiplied by a conductance term that limits the rate of flow (McDonald and Harbaugh, 1988, p. 11–1). Water levels assigned to each general-head boundary cell were determined by linear interpolation of hydraulic head between the river and the alluvial walls. The conductance term was assigned according to the value of hydraulic conductivity assigned to each cell at the boundary.

Pumped wells are internal boundaries where water is removed at a specified rate equal to the discharge of each well. The depth of each pumped well represented in the model was based on the altitude of the screened interval when known, or assumed to be the bottommost layer when the altitude of the screened interval was unknown. The layer, row, and column of each pumping well are presented later in this report.

Hydraulic Properties

Hydraulic data collected during previous investigations and described earlier in this report were entered into the GIS (Kelly and Blevins, 1995) and used to associate a hydraulic conductivity value with a specific lithology. Typical ranges of the hydraulic conductivities of clay, silt, sand, and gravel (Freeze and Cherry, 1979; Driscoll, 1986; table 4) were initially used where hydraulic conductivity data were unavailable for a specific lithology. After the relation between hydraulic conductivity and lithology was established during model calibration, hydraulic conductivity was assigned to cells in each model layer based on the lateral and vertical distribution of lithology (figs. 22–25).

Table 4. Typical hydraulic conductivity ranges for clay, silt, sand, and gravel

Lithology	Hydraulic conductivity range, in meters per day[1]
Clay	10^{-7} to 10^{-4}
Silt	10^{-4} to 1
Sand	10^{-2} to 10^{3}
Gravel	10^{2} to 10^{5}

[1]Freeze and Cherry, 1979; Driscoll, 1986.

The simulated flow of water between adjacent model layers is controlled by the vertical conductance term. The vertical conductance terms between cells of adjacent layers were calculated from the vertical hydraulic conductivity, assumed to equal horizontal hydraulic conductivity, of each model cell using the method presented in McDonald and Harbaugh (1988, p. 5–11) and then multiplied by a factor to simulate the presence of vertical anisotropy in clay, silt, and fine sand deposits. The vertical anisotropy was assumed to decrease with depth because of the increase in particle grain size with depth and the higher probability that fine-grained layered depositional features, such as overbank and channel fill deposits, have been reworked or removed by erosional and depositional processes of the Missouri River. Therefore, the vertical conductance terms between adjacent cells of layers 1 and 2 were multiplied by a factor of 0.1 and between layers 2 and 3 by a factor of 0.5. The vertical conductance between layers 3 and 4 was not reduced.

The specific yield is the unconfined storage coefficient for layer 1. Typical specific yield values (Driscoll, 1986; table 5) were distributed among model cells in layer 1 based on the distribution of

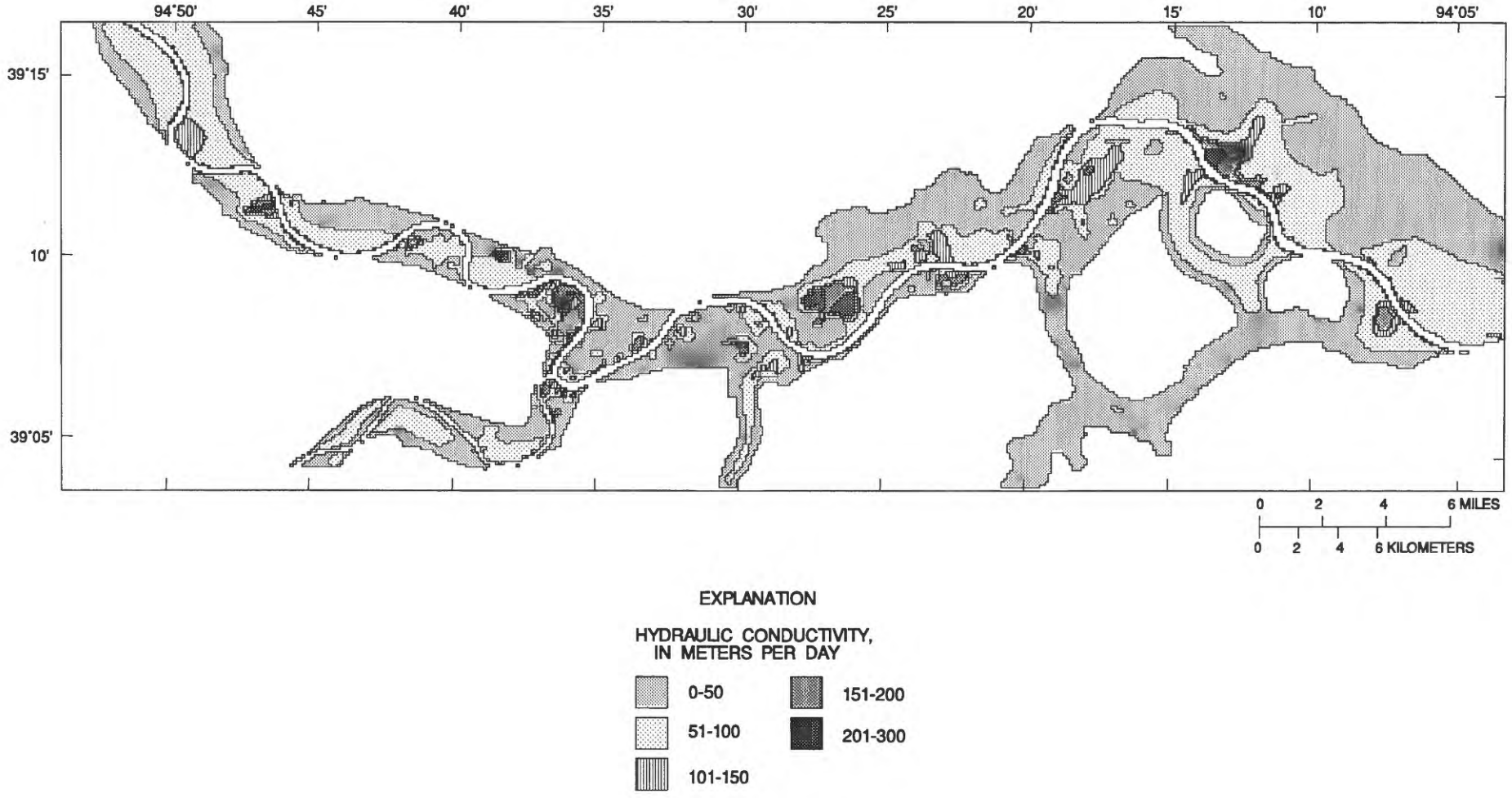

Figure 22. Hydraulic conductivity represented in model layer 1.

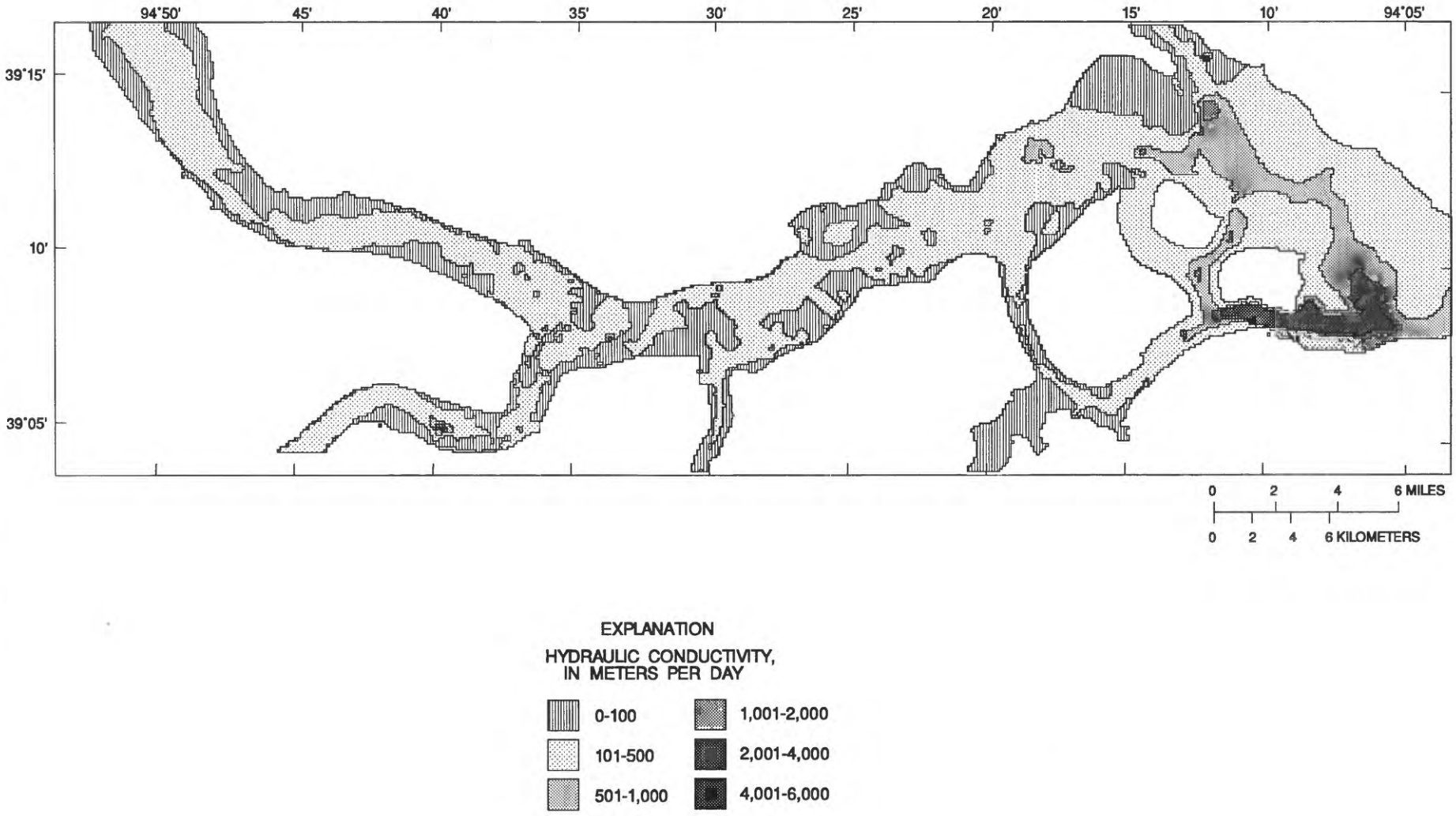

Figure 23. Hydraulic conductivity represented in model layer 2.

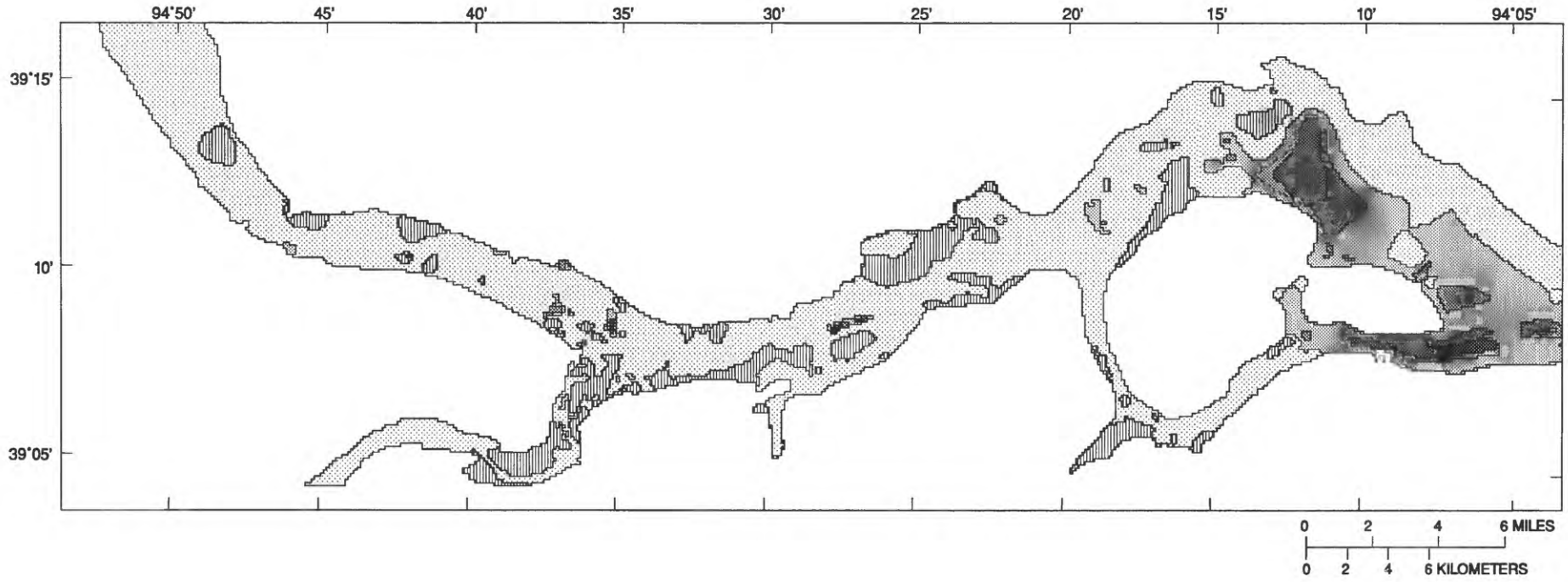

Figure 24. Hydraulic conductivity represented in model layer 3.

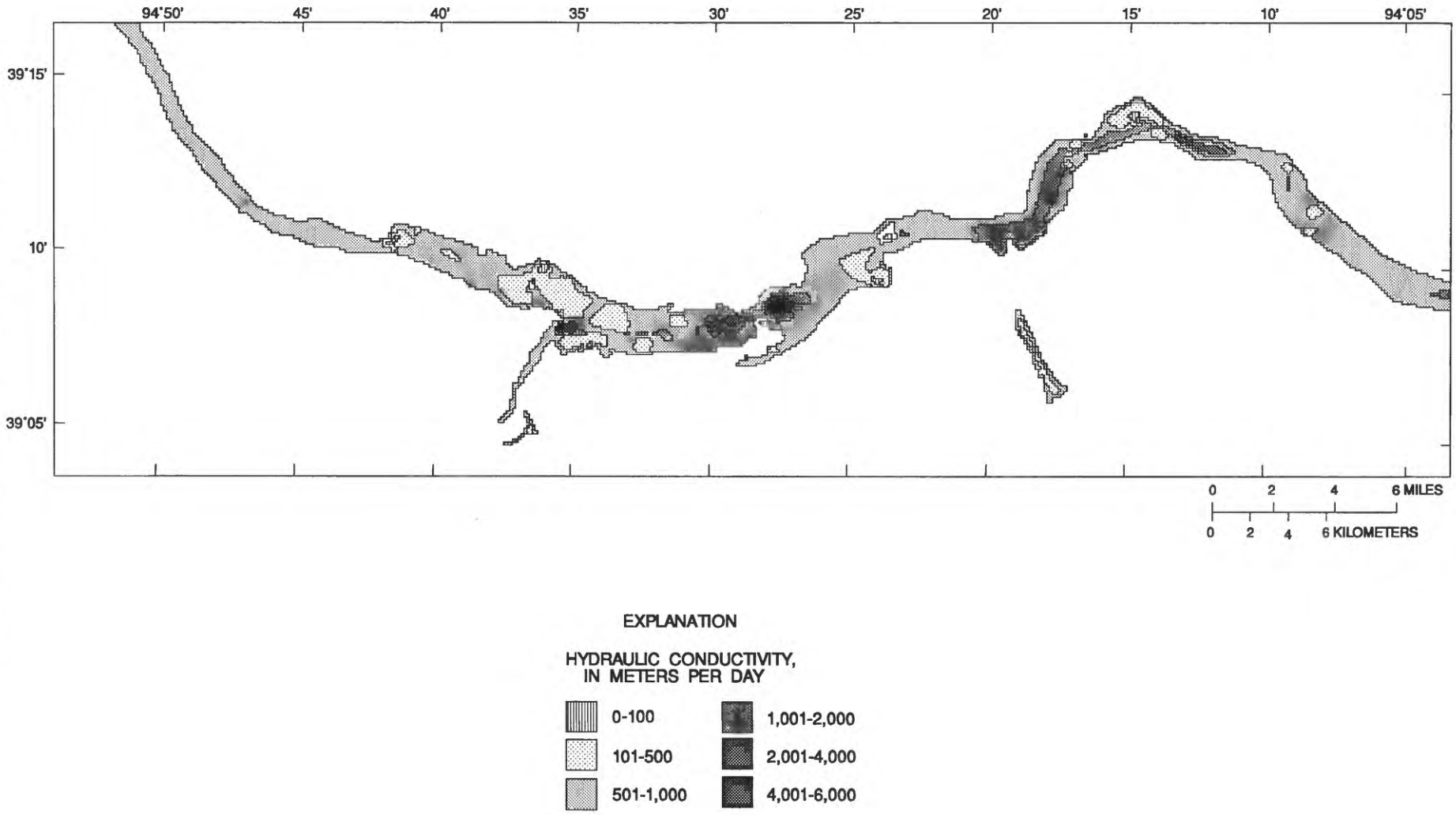

Figure 25. Hydraulic conductivity represented in model layer 4.

lithology (fig. 26). A specific storage of 0.001 was used for layers 2, 3, and 4 and represents conditions where water is released from storage due to expansion of the water or compaction of the aquifer material and not actual drainage of the aquifer.

Table 5. Typical specific yield values for clay, sand, sand and gravel, and gravel

Lithology	Specific yield range[1]
Clay	0.01 - 0.1
Sand	.1 - .3
Sand and gravel	.15 - .25
Gravel	.15 - .30

[1]Driscoll, 1986.

Calibration

The ground-water flow model was calibrated by adjusting model input data and model geometry to modify model output so that the results matched onsite observations within an acceptable level of accuracy (Konikow, 1978). Parameters that were changed during the calibration process include hydraulic conductivity, vertical conductance between model layers, specific yield, riverbed conductance, and recharge rates. Ground-water levels were simulated after each change in one of these parameters, and the simulated ground-water levels were compared to observed ground-water levels. The model accuracy was calculated using the root mean square (RMS) error between actual synoptic measurements of hydraulic head and model generated hydraulic head. Model accuracy is increased by minimizing the RMS error, a measure of the absolute value of the variation between measured and simulated hydraulic heads. The equation used to calculate the RMS error was:

$$RMS\ error = \sqrt{\frac{e_1^2 + e_2^2 + e_3^2 + \ldots + e_n^2}{n}} \quad ,$$

where

e is the difference between measured hydraulic heads and the simulated hydraulic heads, and

n is the number of control points.

The accuracy of measured water levels was the basis for choosing the RMS error used to determine if the model simulation was acceptable. Most water levels were measured with a steel tape or an electric water-level measuring tape to the nearest 3 mm (millimeters). Water levels of public-water-supply wells were measured onsite using air line methods. For these water-level measurements, the accuracy is assumed to be within 0.3 m, the largest possible error from measurement of water levels.

Water-level accuracy also depends on the accuracy of the reference point altitude from which the water level was measured. The reference point altitudes for most wells used in this study were obtained using standard surveying or global positioning system methods described in the report by Kelly and Blevins (1995). The accuracy of these measurements is between 0.01 and 0.15 m. The reference point altitude of a few wells in the study area was estimated from 1:24,000-scale topographic maps. The vertical accuracy of these measurements is one-half of the contour interval. The contour interval on topographic maps of the alluvial valley is 5 or 10 ft (feet; 1.5 or 3 m), so the accuracy of water-level measurements for these wells is 0.75 or 1.5 m, the largest possible error in water levels from reference point altitude measurements.

Another component of the accuracy of measured water levels is the change of water levels in the aquifer that can occur during the time required for a synoptic water-level measurement of numerous wells. Synoptic water-level measurements within the study area required at least 5 days. A hydrologic stress during this time, such as a change in river stage or increase in recharge that changed water levels in the aquifer, may have caused water levels measured in wells at the beginning of the synoptic measurements to not represent conditions after 5 days at the end of the measurement. Water levels change more quickly in wells located near the source of stress than in wells located at some distance from the stress.

Water-level changes in the Missouri River at the Kansas City gaging station during synoptic water-level measurements ranged from 0.11 m in January 1993 to 0.69 m in February 1994 (figs. 27–29). These changes were chosen to represent the effect of river-stage fluctuations on water-level measurement accuracy because Missouri River stage fluctuations recorded at this gage are indicative of changes in stage for the Missouri River for the entire study area. Also, this gage is located downstream from the mouth of the Kansas River in the middle of the study area where fluctuations of the Missouri River stage caused by changes in the Kansas River stage are recorded. During a synoptic water-level measurement, a change in

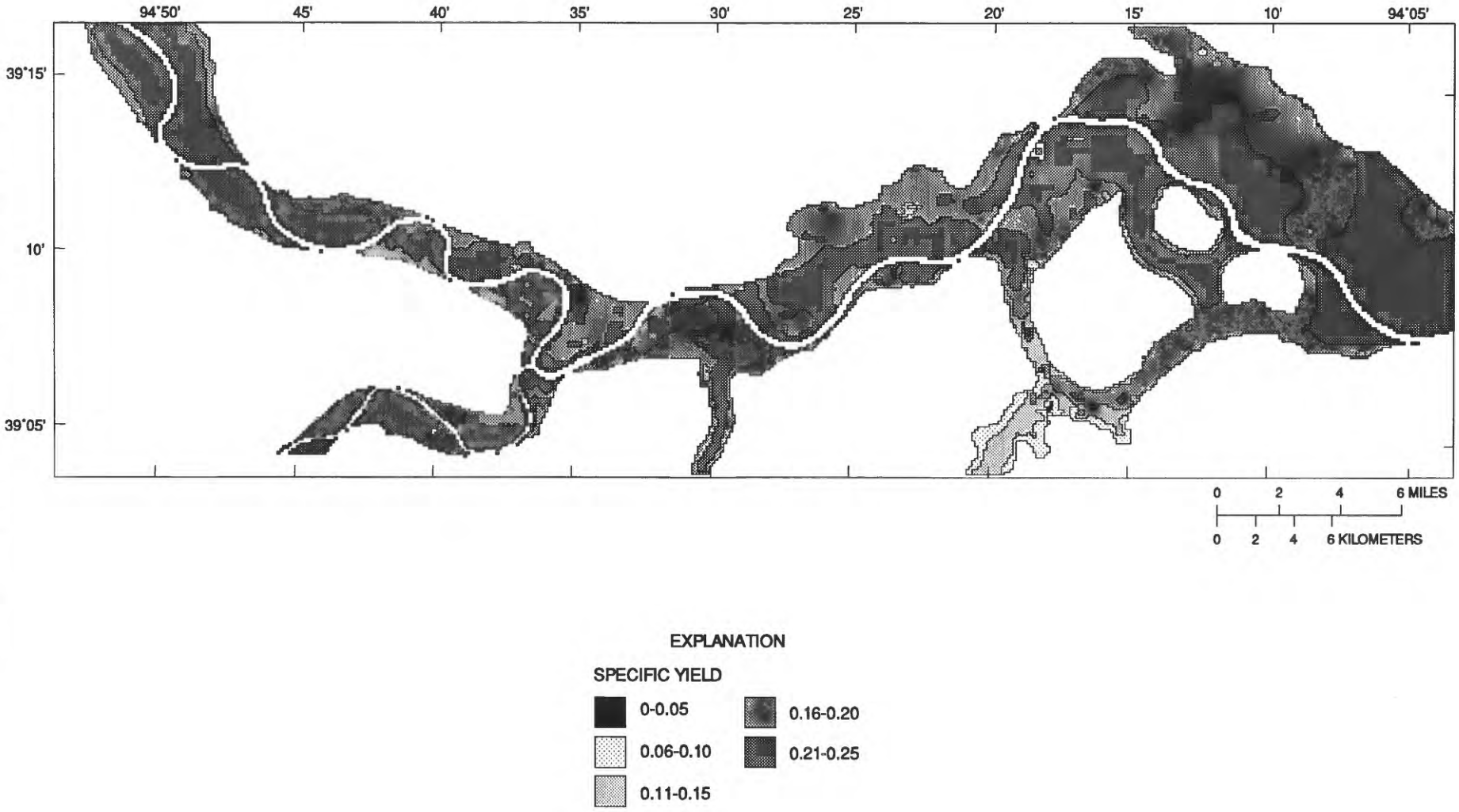

Figure 26. Specific yield represented in model layer 1.

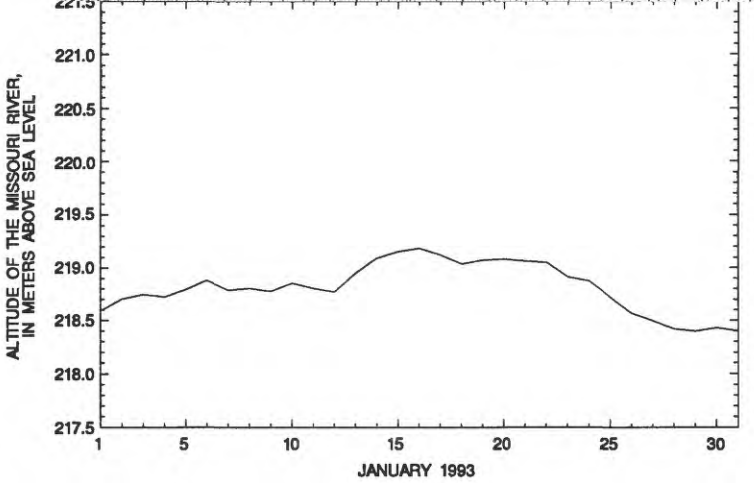

Figure 27. Altitude of the Missouri River at Kansas City, Missouri, January 1993 (ground-water levels measured between January 18 and 23, 1993).

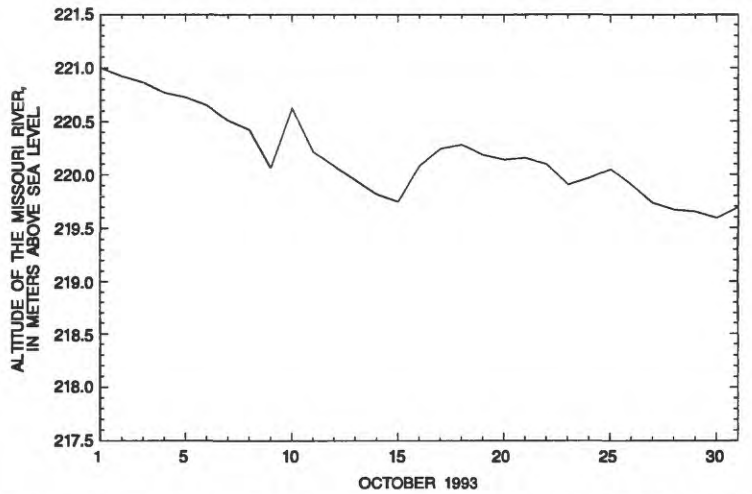

Figure 28. Altitude of the Missouri River at Kansas City, Missouri, October 1993 (ground-water levels measured between October 18 and 22, 1993).

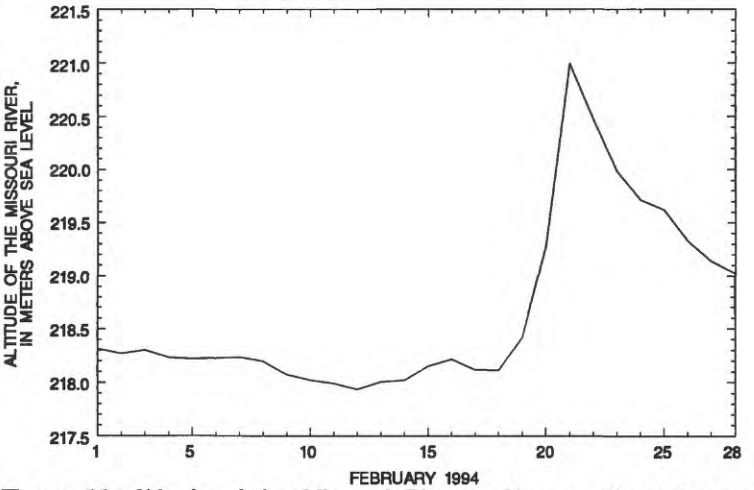

Figure 29. Altitude of the Missouri River at Kansas City, Missouri, February 1994 (ground-water levels measured between February 14 and 18, 1994).

river stage that changed water levels in wells near the river increased the error of the water-level measurement for those wells.

Recharge from precipitation also may affect ground-water levels during a synoptic water-level measurement. Precipitation was recorded daily at the Kansas City Municipal Airport and at Independence, Missouri (fig. 30), located near the center of the study area (pl. 1). The Independence rain gage also was used because of data gaps at the Kansas City Municipal Airport rain gage. For the following analysis, recharge was assumed to be 20 percent of precipitation and specific yield of the aquifer to be 0.2. Between January 18 and January 22, 1993, total precipitation was 0.014 m, so the estimated change in water levels from recharge for this time was about 0.014 m. Between October 18 and 22, 1993, total precipitation was 0.009 m, so estimated change in water levels from recharge for this time was about 0.009 m. Between February 14 and 18, 1994, no precipitation was recorded, so no changes in water levels occurred from recharge. The precipitation and water-level increases are equal in this analysis because the 20 percent of precipitation available for recharge and the 0.2 specific yield value cancel each other.

The maximum possible error for each synoptic water-level measurement is the sum of the maximum possible errors caused by water-level measurement errors, reference point altitude measurement errors, and errors introduced by changes in water level from river stage changes or recharge from precipitation during the time required for a synoptic water-level measurement. The chance that the maximum error would occur at any well is small because all of the measurement errors are unlikely to be maximum errors and because the errors are unlikely to be all positive or all negative with respect to the actual value. A combination of errors of varying value and sign is more likely to occur. Knowledge of these errors and their magnitude is necessary to compare model RMS error to ground-water level measurement accuracy. The calculated RMS errors for the model calibrations, discussed in the following sections, are less than the maximum measurement errors listed in table 6.

The strategy for calibration of the ground-water flow model was to use both quasi-steady state and transient hydraulic head data. The steady state calibration using quasi-steady state hydraulic head data was used to assess model geometry, confirm the conceptual model of ground-water flow, test the appropriateness of simulated boundary conditions, and obtain approximate transmissivity and recharge arrays in preparation for more rigorous transient calibration. The transient calibration was used to refine the input data for the model using simulations of a period of prolonged aquifer drainage from August 1993, immediately after the peak of the flood of 1993, to February 1994, when river stage and ground-water levels had approached typical conditions for that time of year.

Steady State Calibration

The quasi-steady state hydraulic head data were obtained from the January 1993 synoptic water-level measurement. The January 1993 data were considered to represent the closest approximation of steady state conditions where water levels, river stage, and pumped well data were readily available. Steady state conditions occur when total inflow is equal to total outflow, storage of water in the aquifer is constant, and water levels do not change with time. Because river stage fluctuates continually, precipitation is variable and intermittent, and well pumping rates are not constant, true steady state conditions probably never exist in the alluvial flow system.

The rationale for using a steady state calibration was based on the complexity and size of the model and the availability of synoptic water-level data for the study area for January 1993. Initial calibration simulations used uniform hydraulic conductivity values for each layer, uniform recharge rates for each soil group calculated from average annual precipitation, and no pumped wells. Errors in model geometry were corrected during this stage of calibration in several locations where data were limited. Large differences between measured and simulated hydraulic head in the area near Lake City Army Ammunition Plant and Buckner, Missouri (pl. 1), indicated that the buried alluvial channels in the eastern part of the study area needed to be included in the simulation as an outlet for ground-water flow. Other changes to the model geometry in areas where the depth to bedrock was unknown included the extension of layer 4 to the upstream and downstream model boundaries of the Missouri River alluvial aquifer and the lateral extension of layer 3 to more closely approximate the bowl shape of the alluvial aquifer. Numerical instabilities in initial simulations were caused by a large number of model cells in layer 1 going dry. To correct the instabilities, the thicknesses of layers 2 and 3 were decreased and the thickness of layer 1 was increased to allow more vertical

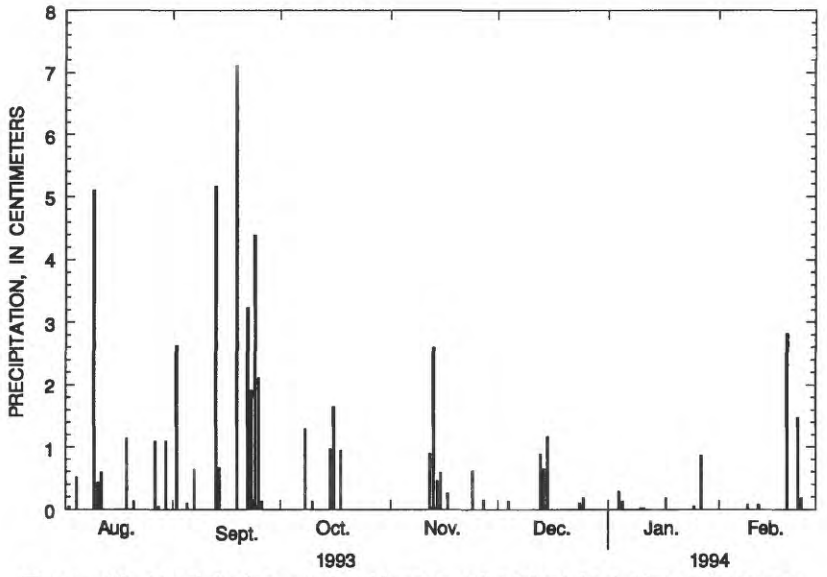

Figure 30. Precipitation at the Kansas City Municipal Airport between August 1 and October 31, 1993, and at Independence, Missouri, between November 1, 1993, and February 28, 1994.

Table 6. Water-level measurement error sources and maximum values

Synoptic water-level measurement	Water-level measurement error, in meter	Reference point altitude measurement error, in meters	Water-level change from river stage change, in meter	Water-level change from recharge, in meter
January 1993	0.3	1.5	0.16	0.014
October 1993	.3	1.5	.11	.009
February 1994	.3	1.5	.69	0

movement of the simulated water table during the iterative solution.

The assignment of hydraulic conductivity based on lithologic distribution, recharge rate based on the vertical permeability of soils, and inclusion of data for pumped wells reduced the RMS error of the steady state calibration simulation and more realistically simulated the January 1993 distribution of hydraulic head. Well pumping rates used in the steady state simulation for January 1993 depended on the availability of data and were either average pumping rates for the month of January 1993 or average annual pumping rates. These additional data were incorporated during the steady state calibration simulations. However, the RMS error for these simulations was still larger than the maximum measurement error. The effect of the smaller streams and constructed drainage ditches on ground-water flow was not included in the original model of the flow system. Model simulations indicated that these surface-water bodies had a considerable effect on ground-water flow and the hydraulic head distribution. The addition of these head-dependent flow boundaries to simulate the effects of small streams and ditches on ground-water flow reduced the RMS error to an acceptable value of 1.15 m. The maximum positive error was 4.11 m; the maximum negative error was -3.08 m.

The difference between inflow and outflow across all model boundaries was 0.13 percent of total flow for the steady state calibration. The volumetric budget for the steady state calibration simulation is shown in table 7. The level of accuracy of the simulation in representing the January 1993 hydraulic head distribution was accepted because conditions were not completely at steady state. Further calibration of the quasi-steady state model probably would have resulted

in erroneously changing model input parameters to match a hydraulic head distribution that partially resulted from transient conditions.

Transient Calibration

Transient calibration of the ground-water flow model to hydrologic conditions measured between August 1, 1993, and March 27, 1994, was completed by comparing the change of simulated hydraulic head distribution over time with the change of the measured hydraulic head distribution. The changes in various hydrologic stresses that affected the distribution of hydraulic head were measured and used in the simulation. A stress on the ground-water flow system was any change in river stage, recharge, or pumped wells that caused the ground-water flow system and, in particular, the distribution of hydraulic head to change. These changes actually occurred as gradual increases or decreases of river stage, intermittent and varying recharge rates from precipitation, and intermittent or constant well pumping at varying rates. Areal and temporal changes in stress to the ground-water flow system were applied to the ground-water flow model by using a series of stress periods. Within each stress

Table 7. Volumetric budget for the steady state calibration simulation

[Budget component volumes and rates from model output reported to five significant figures caused the discrepancies between totals and sum of individual budget components]

Budget component	Cumulative volumes, in cubic meters	Rates of flow, in cubic meters per day
	In	
Storage	0	0
Constant head	0	0
Wells	0	0
Drains	0	0
Recharge	182,620,000	500,330
River leakage	31,550,000	86,438
Head dependent boundaries	1,046,100	2,866.0
Total	215,220,000	589,630
	Out	
Storage	0	0
Constant head	0	0
Wells	43,864,000	120,180
Drains	4,491,700	12,306
Recharge	0	0
River leakage	165,240,000	452,720
Head dependent boundaries	1,343,600	3,681.2
Total	214,940,000	588,880
	In - Out	
	275,740	755.44
	Percent discrepancy	
	0.13	0.13

period, river stage, recharge, and well pumping rates were held constant. The transient calibration simulation was begun immediately after the July-August 1993 flood in the Missouri River Basin. At that time, the entire alluvial aquifer in the study area was at or near saturation from infiltrated flood waters and local precipitation. The initial hydraulic head for each active cell in the model was set equal to the corresponding land-surface altitude. The model was allowed to simulate 81 days using the August 1, 1993, pumping rates of wells and river stage parameters to produce an initial hydraulic head distribution for the beginning of the transient simulation.

After initial conditions were established, each subsequent stress period in the transient calibration was 7 days and was divided into three time steps to calculate the change of hydraulic head. In each stress period the first time step was 1.47 days, the second was 2.21 days, and the third was 3.32 days. Therefore, each stress period corresponded to a specific time and represented the average stress to the ground-water flow system for that time. The length of the stress periods was chosen based on the time intervals for data collection and the approximately 1-week period required to obtain the synoptic water-level measurements during October 1993 and February 1994.

Average river stage during each stress period was assigned to each river model cell using the interpolation methods previously discussed. Average river-stage altitudes for each gaging station in the study area are listed for each stress period in table 8 (at the back of this report). Average recharge for each stress period was assigned to the topmost active cell in each vertical column based on average precipitation and the vertical hydraulic conductivity class of soil at the cell (Kelly and Blevins, 1995). Total daily precipitation from August 1, 1993, to March 27, 1994, is shown in figure 30. The percentage of precipitation that was supplied to the model as recharge is shown for each vertical hydraulic conductivity class of soil (Kelly and Blevins, 1995) in table 3. The time between precipitation and recharge is variable and depends on the amount and intensity of precipitation, soil saturation, hydraulic conductivity of the soil, and depth to the water table. The soil vertical hydraulic conductivity ranges from less than 0.015 m/hr (meter per hour; 0.36 m/d) to greater than 0.152 m/hr (3.65 m/d). Assuming the average depth to the water table ranges from 4.5 to 7.6 m, ponded infiltration when soils are saturated would take between 1.2 to 21 days to reach the water table. Because precipitation was averaged over a 7-day stress period and precipitation intensity and soil saturation were unknown, the application of recharge during the stress period in which corresponding precipitation occurred was considered valid. An average well pumping rate for each stress period for each pumped well was assigned to the model cell that contained that well. The layer, row, column, and withdrawal rate for each well used in the transient calibration are listed for each stress period in tables 9 through 11 (at the back of this report).

The hydraulic head data used for transient calibration of the ground-water flow model were obtained from August 1993 flood data and two synoptic water-level measurements from 123 wells in October 1993 and from 98 wells in February 1994. Model results from stress periods that corresponded to the October 1993 and February 1994 synoptic water-level measurements were compared, and the RMS error was calculated for the corresponding stress periods of each transient calibration simulation. For the accepted calibration simulation, the RMS error for October 1993 was 0.71 m and for February 1994 was 0.80 m. These values are less than the maximum measurement errors previously discussed and indicate the acceptability of the calibrated model. The maximum positive error for October 1993 was 2.72 m and for February 1994 was 1.85 m. The maximum negative error for October 1993 was -2.56 m and for February 1994 was -1.92 m.

A comparison between the potentiometric surfaces determined from measured water levels and from model results for October 1993 and February 1994 are shown in figures 31 and 32. These maps indicate where the simulated potentiometric surface is lower or higher than the measured potentiometric surface. However, because the representation of the potentiometric surfaces from measured water levels was constructed by interpolation of water levels between well locations and the potentiometric surfaces from model simulations were constructed with results of the ground-water flow model, the maximum and minimum differences have a wider range of values than the actual RMS errors, indicating the maps can only provide a semi-quantitative comparison.

Sensitivity Analysis

A sensitivity analysis was performed to assess the response of the model simulation to changes in various model parameter values. The model is sensi-

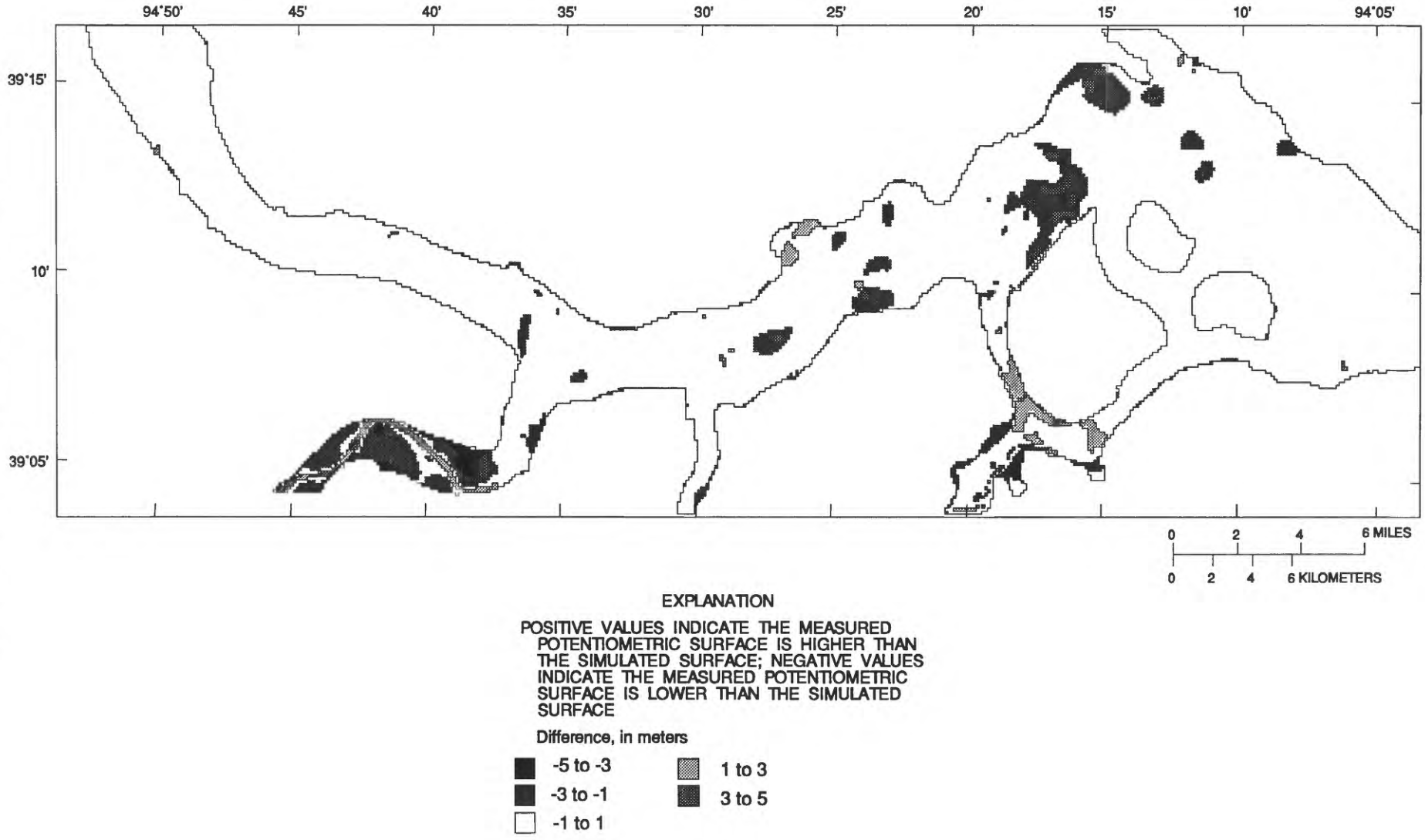

Figure 31. Difference map calculated by subtracting the altitude of the simulated potentiometric surface for October 1993 from the altitude of the potentiometric surface derived from synoptic water-level measurements of 123 wells in the Missouri River alluvial aquifer, October 1993.

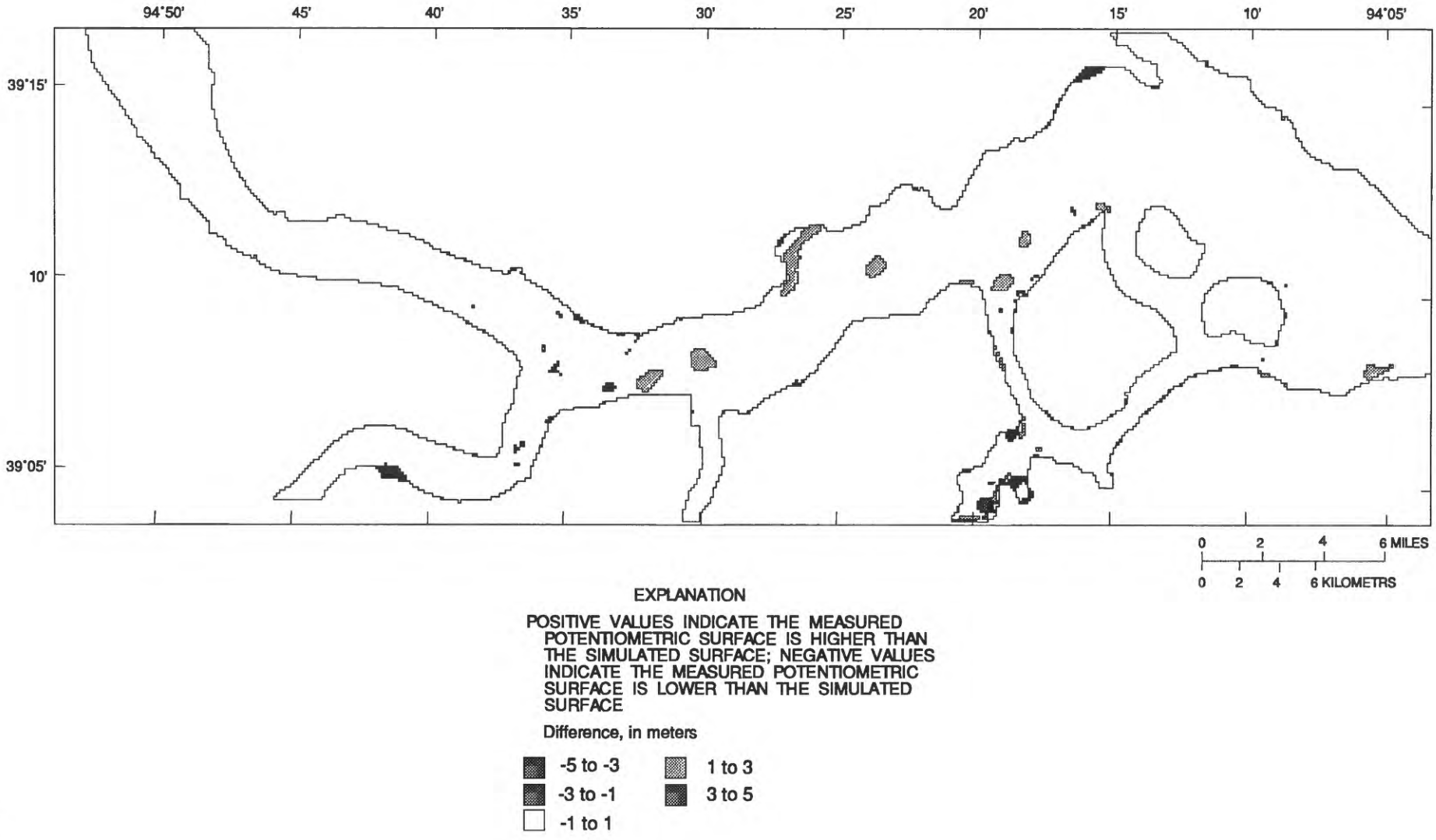

Figure 32. Difference map calculated by subtracting the altitude of simulated potentiometric surface for February 1994 from the altitude of the potentiometric surface derived from synoptic water-level measurements of 98 wells in the Missouri River alluvial aquifer, February 1994.

tive to a parameter when a change in that parameter substantially changes the distribution of simulated hydraulic head. When the model is sensitive to an input parameter, the value and distribution of that parameter within the model are more accurately determined during model calibration because small changes to the parameter value cause large changes in hydraulic head. If a change of parameter does not cause large changes in the simulated hydraulic head distribution, the model is insensitive to that parameter. When the model is insensitive to an input parameter, the value and distribution of that parameter within the model are more difficult to accurately determine from model calibration because large changes to the parameter do not cause large changes in hydraulic head. Therefore, the values of these parameters are less likely to represent actual values.

Results of the sensitivity analysis for each change in model parameter are given in table 12 and include the RMS errors and the increase or decrease in RMS error from the calibrated model RMS error for October 1993 (0.71 m) and February 1994 (0.80 m). Values of the hydraulic conductivity, the vertical conductance between layers, the specific yield of layer 1, the specific storage of layers 2, 3, and 4, the riverbed conductance, and the recharge rate were decreased by 50 percent below the calibrated parameter value (multiplier of 0.5) and increased by 50 percent above the calibrated parameter value (multiplier of 1.5) during the sensitivity analysis. In the following discussion the effect of these changes on model output was assessed with the transient calibration scenario, and percentage changes in RMS error are with respect to the accepted RMS error for October 1993 and February 1994.

The sensitivity of the model to changes in hydraulic conductivity is greatest when the hydraulic conductivity is decreased in all layers at the same time. Decreasing the hydraulic conductivity by 50 percent in all layers increased the RMS error for October 1993 by 64.8 percent and the RMS error for February 1994 by 13.8 percent. The sum of the percent changes in RMS errors caused by decreasing the hydraulic conductivity by 50 percent in each layer is 37.0 percent for October 1993 and 8.8 percent for February 1994. Increasing the hydraulic conductivity by 50 percent in all layers decreased the RMS error for October 1993 by 12.7 percent and increased the RMS error for February 1994 by 18.8 percent. The sum of the percent changes in RMS errors caused by increasing the hydraulic conductivity by 50 percent in each layer resulted in a 23.0 percent decrease for the RMS error for October 1993 and a 13.8 percent increase for the RMS error for February 1994. The model is more sensitive to the sum of individual increases of hydraulic conductivity for the October 1993 data than for the February 1994 data.

The model is sensitive to overall changes in the hydraulic conductivity as indicated by the large change of RMS error when the hydraulic conductivity is simultaneously changed in all layers. Also, the effect of changing the hydraulic conductivity for all layers and in each individual layer caused a larger change in the RMS error for October 1993 than in the RMS error for February 1994, indicating that the model is more sensitive to hydraulic conductivity earlier in the calibration simulation than later. Also, decreasing the hydraulic conductivity by 50 percent in all layers and in each layer caused the RMS error for October 1993 to increase and the RMS error for February 1994 to decrease. Increasing the hydraulic conductivity by 50 percent in all layers and in each layer caused the RMS error for October 1993 to decrease and the RMS error for February 1994 to increase.

The insensitivity of the model to changes in the vertical conductance between layers is evident when the small percent changes of the RMS errors are compared to the corresponding percent changes in vertical conductance during the sensitivity analysis. The only change in RMS error (1.0 percent) occurred in October 1993 when the vertical conductance was decreased by 50 percent between layers 1 and 2 and between layers 3 and 4.

The sensitivity of the model to changes in the specific yield in layer 1 is evident when the relatively large changes in the RMS errors are compared to the corresponding change of specific yield. The small change in the RMS errors indicates the model is insensitive to changes in the specific storage and riverbed conductance. The model is somewhat sensitive to changes in recharge rate, but large changes in recharge rate result in minor changes in the RMS error.

CONTRIBUTING RECHARGE AREAS

Particle-tracking analysis using the USGS particle-tracking program MODPATH (Pollock, 1994) was used to determine the CRAs and ground-water travel times for each known pumped well or well field in the study area. MODPATH uses the hydraulic heads and flow distribution output from MODFLOW to calculate

Table 12. Sensitivity analysis results for each model parameter

[RMS, root mean square]

Layer	Multiplier	RMS error		RMS error change	
		October 1993, in meters	February 1994, in meters	October 1993, in meter	February 1994, in meter
		Hydraulic conductivity			
All layers	0.5	1.17	0.91	0.46	0.11
	1.0	.71	.80	0	0
	1.5	.62	.95	-.09	.15
Layer 1	.5	.74	.79	.03	-.01
	1.0	.71	.80	0	0
	1.5	.68	.82	-.03	-.02
Layer 2	.5	.81	.78	.1	-.02
	1.0	.71	.80	0	0
	1.5	.65	.85	-.06	.05
Layer 3	.5	.79	.79	.08	-.01
	1.0	.71	.80	0	0
	1.5	.66	.84	-.05	.04
Layer 4	.5	.77	.76	.06	-.04
	1.0	.71	.80	0	0
	1.5	.68	.84	-.03	.04
		Vertical conductance between layers			
Layers 1 and 2	0.5	0.70	0.80	-0.01	0
	1.0	.71	.80	0	0
	1.5	.71	.80	0	0
Layers 2 and 3	.5	.71	.80	0	0
	1.0	.71	.80	0	0
	1.5	.71	.80	0	0
Layers 3 and 4	.5	.70	.80	-.01	0
	1.0	.71	.80	0	0
	1.5	.71	.80	0	0
		Specific yield			
Layer 1	0.5	0.63	1.06	-0.08	0.26
	1.0	.71	.80	0	0
	1.5	.96	.79	.25	-.01

Table 12. Sensitivity analysis results for each model parameter—Continued

Layer	Multiplier	RMS error		RMS error change	
		October 1993, in meters	February 1994, in meters	October 1993, in meter	February 1994, in meter
		Specific storage			
Layers 2, 3, and 4	0.5	0.70	0.80	-0.01	0
	1.0	.71	.80	0	0
	1.5	.71	.80	0	0
		Riverbed conductance			
Layers 1 and 2	0.5	0.71	0.80	0	0
	1.0	.71	.80	0	0
	1.5	.71	.80	0	0
		Recharge rate			
Layer 1	0.5	0.66	0.81	-0.05	0.01
	1.0	.71	.80	0	0
	1.5	.76	.79	.05	-.01

the flow paths and travel times of imaginary particles of water moving through the simulated ground-water flow system. Limitations of particle-tracking analysis are discussed by Pollock (1994), but several important factors that affect particle-tracking results are presented herein. Particle movement and ground-water travel times computed by MODPATH are based on advective ground-water flow, and no dispersion, diffusion, or chemical or microbiological retardation are incorporated into the calculations. Therefore, the movement of contaminants within ground water is not fully described by MODPATH results alone. The spatial discretization of the ground-water flow model also may limit the accuracy of particle-tracking results because cells containing sinks that do not discharge at a rate large enough to consume all the water entering the cell introduce uncertainty into the computed path of an imaginary water particle. However, the most significant factor affecting the particle-tracking analysis is the accuracy of the hydraulic head and flow distribution computed by the ground-water flow model. Therefore, all of the limitations associated with the ground-water flow model also apply to the particle-tracking analysis.

The porosity of the alluvial aquifer is necessary for MODPATH to compute ground-water velocities. At the same ground-water discharge through a unit cross-sectional area of porous material, a material with a high porosity will have a lower average ground-water flow velocity than a material with a low porosity. The higher porosity material has more openings per unit area of porous material than does a lower porosity material, thereby allowing the same amount of discharge at a lower average ground-water velocity than in a lower porosity material. Porosity was assigned to model cells based on the distribution of lithology (figs. 33–36) and typical values of porosity (Freeze and Cherry, 1979; Driscoll, 1986).

Pumping and River-Stage Scenarios

Steady state ground-water flow was simulated for five different combinations of well pumping rates and river stage. Particle-tracking analysis then determined the total CRA for pumped wells in each of the following scenarios: (1) low pumping rates and low river stage (LPLR; pl. 2); (2) low pumping rates and

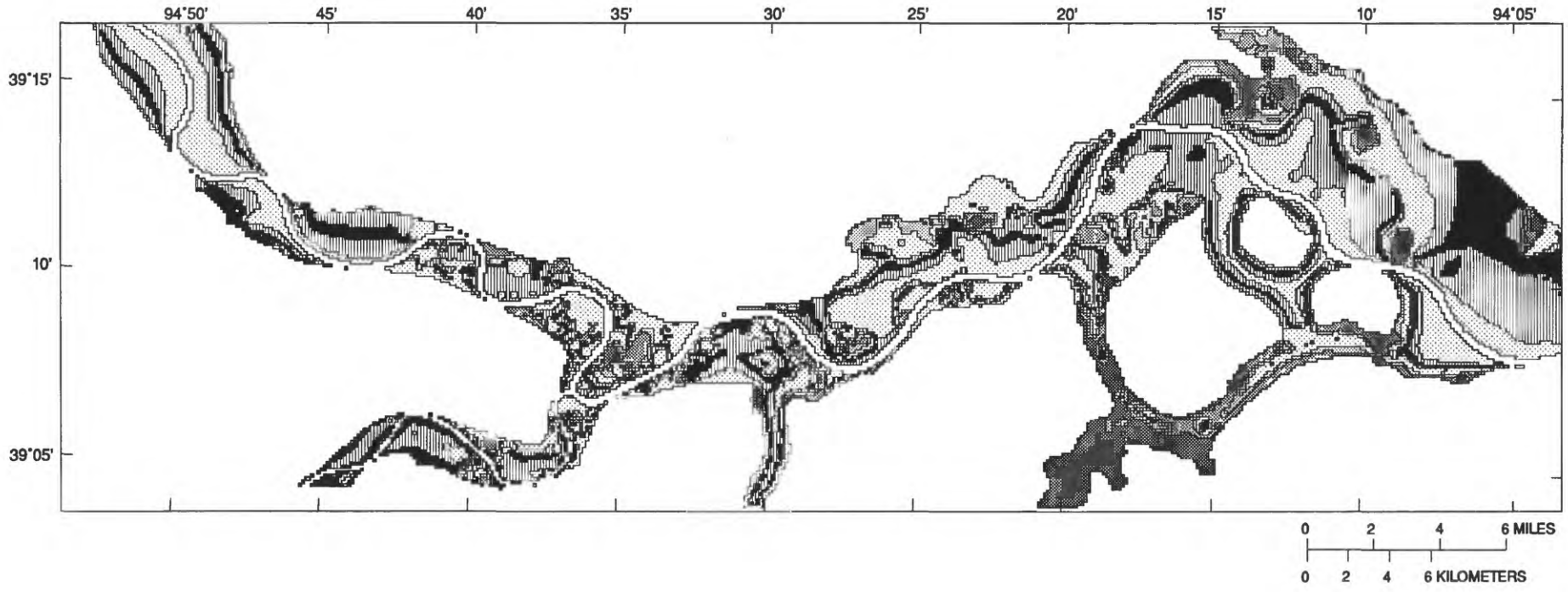

Figure 33. Porosity represented in model layer 1.

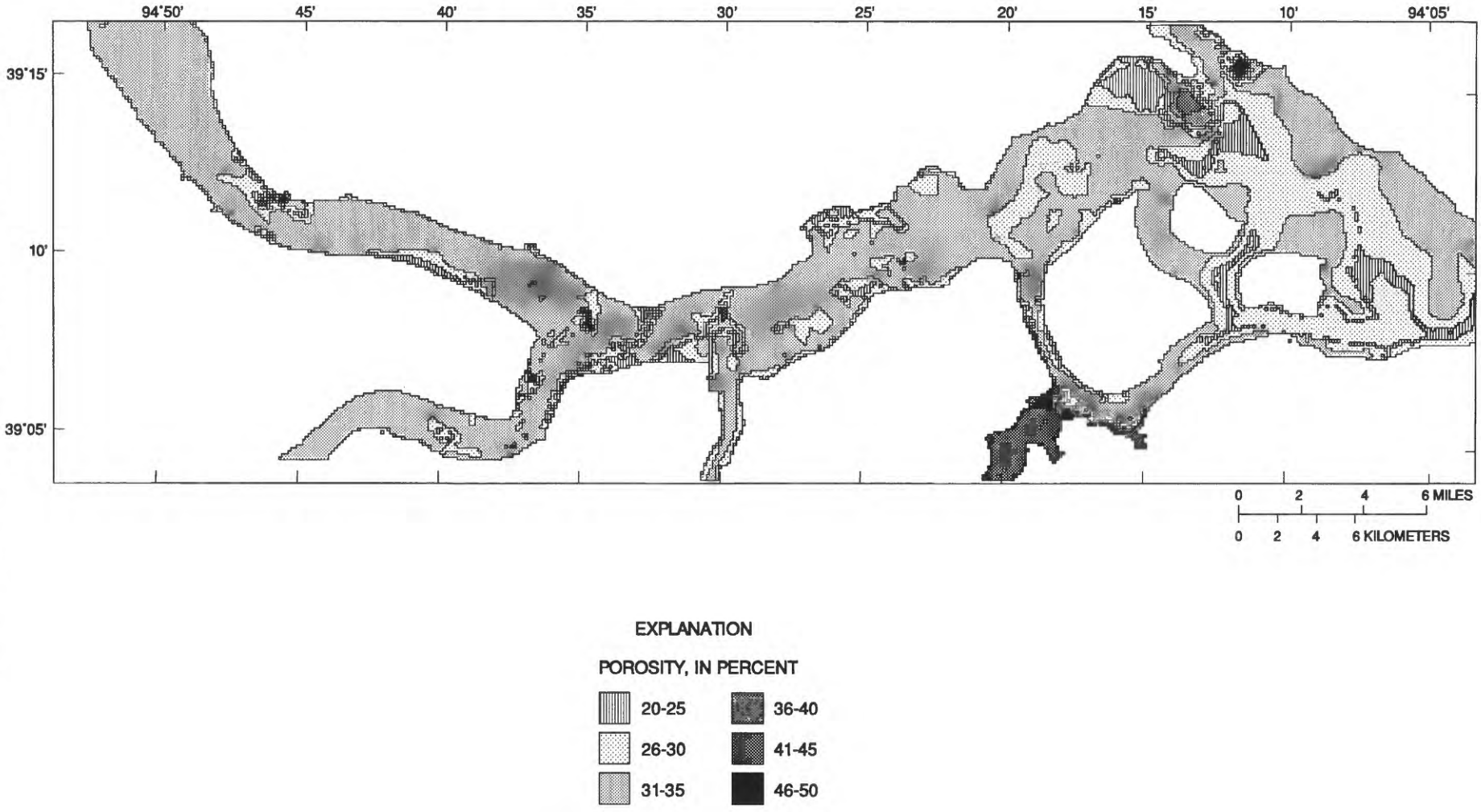

Figure 34. Porosity represented in model layer 2.

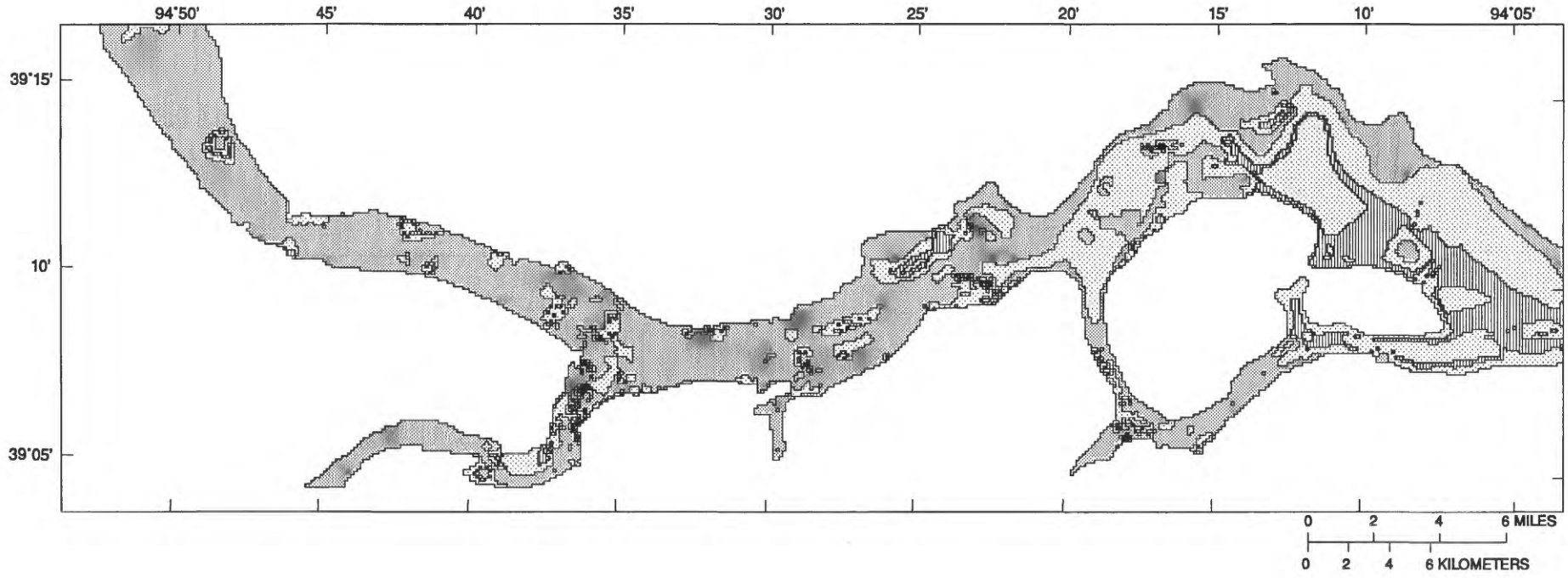

EXPLANATION

POROSITY, IN PERCENT

20-25	36-40
26-30	41-45
31-35	46-50

Figure 35. Porosity represented in model layer 3.

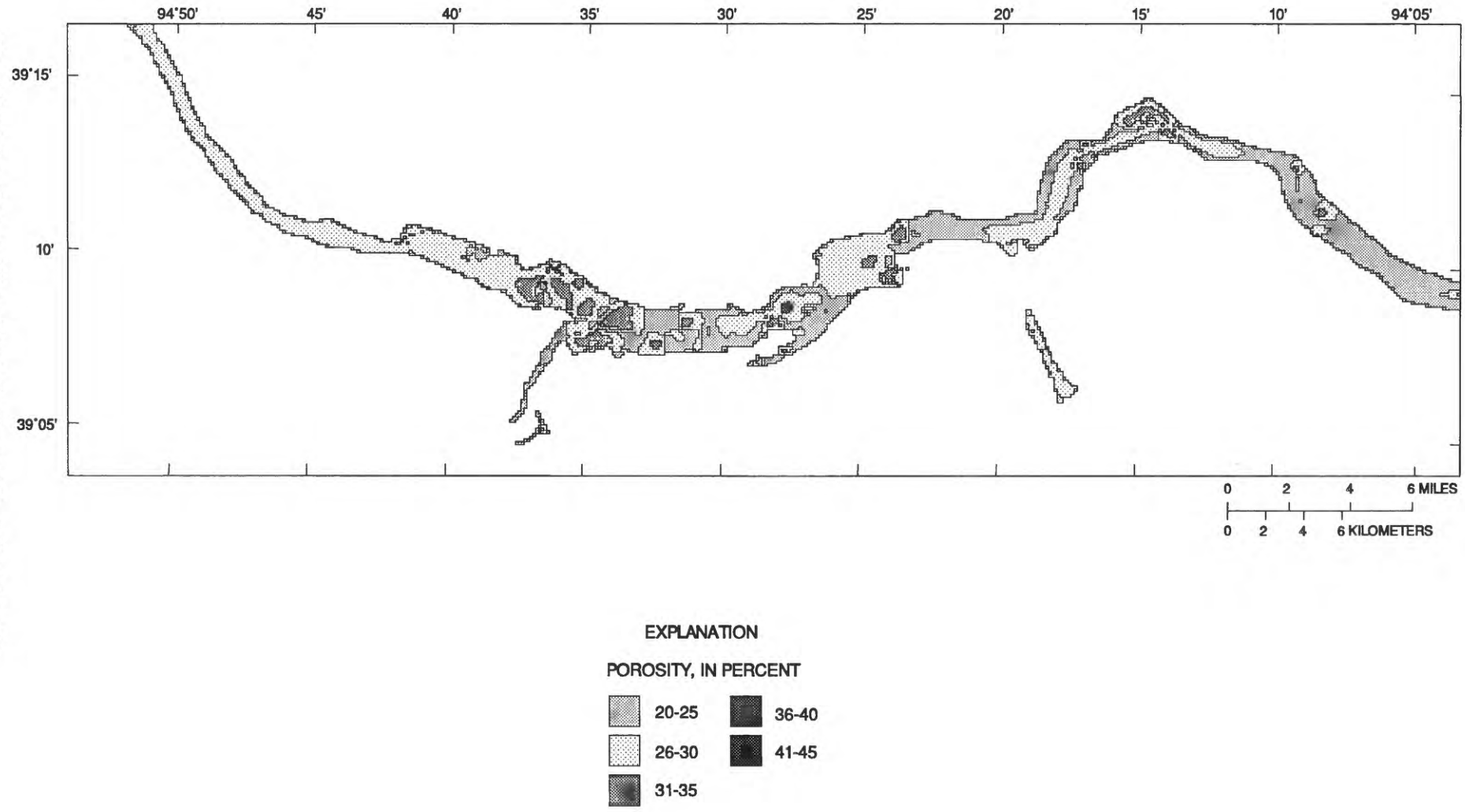

Figure 36. Porosity represented in model layer 4.

high river stage (LPHR; pl. 3); (3) quasi-steady state conditions of January 1993 (QUASI; pl. 4); (4) high pumping rates and low river stage (HPLR; pl. 5); and (5) high pumping rates and high river stage (HPHR; pl. 6).

The river-surface altitude was defined for each river cell in the model for the steady state calibration and for each stress period of the transient calibration. High and low river-stage data sets were chosen from the transient stress-period data based on a comparison of the Missouri River stage at the USGS gage located in Kansas City with the average annual high and low stages calculated from 1958 to 1994. The annual mean discharge was 54,890 ft^3/s (cubic feet per second), which corresponds to a river-surface altitude of 219.62 m at the gage. High river-stage conditions were represented by the September 26, 1993, river-stage data when the average river-surface altitude was 221.65 m (93,160 ft^3/s discharge). A discharge of 91,200 ft^3/s corresponds to a river-surface altitude of 221.55 m and was exceeded 10 percent of the time between 1958 and 1994 (Reed and others, 1995). The river-stage altitude at the USGS gage in Kansas City for the January 1993 quasi-steady state river-stage conditions was 218.51 m (39,930 ft^3/s discharge). Low river-stage conditions were represented by the January 16, 1994, river-stage data when the average river-surface altitude at the USGS gage in Kansas City was 217.95 m (28,980 ft^3/s discharge). A discharge of 23,400 ft^3/s corresponds to a river-surface altitude of 217.5 m and was exceeded 90 percent of the time between 1958 and 1994 (Reed and others, 1995).

High well pumping rates were set at 1.25 times the average annual pumping rates, and low pumping rates were set at 0.75 time the average annual pumping rates. Recharge was the same as used in the January 1993 steady state simulation.

For each scenario, one imaginary particle of water was placed on the water table in the center of each topmost active model cell and tracked to its eventual discharge point. Particles were placed in this manner for two reasons: (1) most water entering the alluvial aquifer comes from direct infiltration by precipitation or from the major rivers; and (2) the primary source of potential contamination to the alluvial aquifer is from leaks or spills that occur on the land surface. Consequently, the CRA computed by MODPATH includes the source area of water to each well or well field and ground-water travel times from the land surface and the major rivers to each well or well field. The starting location and travel times of the particles that discharged to a well were entered into the GIS. The model cell corresponding to each particle-starting location was assigned the travel time of that particle. Model cells with travel times from 0 to 1 year, 1 to 5 years, 5 to 10 years, 10 to 100 years, and 100 to 1,000 years were grouped to create 1-, 5-, 10-, 100-, and 1,000-year CRAs for each scenario (pls. 2–6). The total area of each CRA was determined by summing the areas of all model cells within each group for each well field.

Individual Well Field Results

The shape, size, and ground-water travel time within the total CRA for each well or well field are affected by changes in river stage and pumping rates and by the location of the well or well field with respect to the major rivers, alluvial valley walls, and other pumped wells. Similarities in the shapes of CRAs between different wells and well fields can be attributed to similarities in the pumping rate and the position of the wells or well fields in relation to the major rivers, the alluvial valley walls, or other well fields. A typical CRA for a well located within an aquifer so that effects from any hydrologic boundary are negligible will have a bull's-eye pattern. In the following discussion, the CRA for each public-water-supply well field will be discussed individually followed by a discussion of the CRAs for the industrial well fields.

Missouri Cities Water Company

The shape of the simulated total CRA for the Missouri Cities Water Company well field was approximately triangular for all pumping and river-stage scenarios and was affected by the proximity of the well field to both the Missouri River and the alluvial valley walls (well field number 1, pls. 2–6). Recharge to the well field was partially induced from the Missouri River by pumped wells and is shown by the location of the 1- and 5-year CRA below and next to the river. The Missouri River forms the eastern boundary of the total CRA, which extends west along the alluvial valley wall and away from the river for approximately 4 km for all pumping and river-stage scenarios. The capture of ground water by the pumped wells as the water moved downgradient toward the

Missouri River caused the long upvalley extent of the total CRA. The 1-year CRA is between the area south of the well field to the Missouri River because of the short distance ground water traveled from the bottom of the riverbed in layer 2 of the model to the screened interval of the wells in layer 3 of the model. The 5- and 10-year CRAs are centered around the well field, but are skewed toward the west away from the river.

Simulated pumping rates for the Missouri Cities Water Company well field (table 13) ranged from 5,180 m^3/d for the QUASI (pl. 4) scenario to 9,228 m^3/d for the high pumping-rate scenarios. The size of the total CRA (table 14) ranged from 2.611 km^2 (square kilometers) for the HPHR (pl. 6) scenario to 5.469 km^2 for the LPHR (pl. 3) scenario.

For the Missouri Cities Water Company well field, the 1-, 5-, and 10-year CRAs are larger in both the high pumping-rate scenarios, but the 100-year CRA is smaller. The 1,000-year CRA is largely unaffected by pumped wells. Typically, a CRA will increase in size with an increase in pumping rate. However, the largest total CRA for the Missouri Cities Water Company well field occurred during the LPHR scenario (pl. 3) and the smallest occurred during the HPHR scenario (pl. 6). The size of the 100-year CRA has the largest effect on the size of the total CRA because it ranges from 68 percent (HPHR, pl. 6) to 88 percent (LPHR, pl. 3) of the total CRA. The effect of river stage on the size of the CRA is not well understood. Low river stage did not affect the size of the 1-year CRA, but increased the size of the 5- and 10-year CRAs for the low pumping-rate scenarios and the 5-year CRA for the high pumping-rate scenario. High river stage increased the 100-year CRA during the low pumping scenarios but decreased the 100-year CRA during the high pumping scenarios. The 10-year CRA is larger for the LPLR scenario (pl. 2). Small changes in the potentiometric surface in this low gradient area can cause large changes in the direction of ground-water flow. The ground-water divide that defines the

Table 13. Simulated pumping rates for the Missouri Cities Water Company well field

	Well location in model			Pumping rate, in cubic meters per day			
	Layer	Row	Column	Low	Jan. 1993	Average	High
	3	69	120	1,384	1,295	1,846	2,307
	3	69	120	1,384	1,295	1,846	2,307
	3	69	121	1,384	1,295	1,846	2,307
	3	69	122	1,384	1,295	1,846	2,307
Total				5,536	5,180	7,384	9,228

Table 14. Contributing recharge areas for the Missouri Cities Water Company well field

Contributing recharge area	Area, in square kilometers				
	Low pumping rate		Jan. 1993 quasi-steady state	High pumping rate	
	Low river stage	High river stage		Low river stage	High river stage
1-year	0.068	0.068	0.068	0.09	0.09
5-year	.248	.18	.225	.315	.225
10-year	.383	.225	.405	.45	.495
100-year	3.29	4.793	3.285	3.195	1.778
1,000-year	.023	.203	0	.023	.023
Total	4.012	5.469	3.983	4.073	2.611

southern boundary of the 100-year CRA shifted northward and eastward during the HPHR scenario and decreased the size of the total CRA. A slight change in the potentiometric surface caused by high river stage and low ground-water gradient away from the well field is assumed to have caused the ground-water flow divide to move to the north.

Gladstone, Missouri, Well Field

The shape of the Gladstone, Missouri, well field (well field number 2, pls. 2–6) is elongated upgradient for all pumping and river-stage scenarios. This well field is similar to the Missouri Cities Water Company well field because it also is located next to the Missouri River and close to the alluvial valley walls. Induced recharge from the Missouri River is shown by the location of the 1- and 5-year CRAs next to and below the river. The total CRA extends for approximately 3 km to the northwest from the well field. Its long narrow shape was caused by the capture of ground water by the pumped wells as it flowed down the natural gradient toward the Missouri River and by the alluvial valley walls to the north that were a flow boundary. The 1-year CRA is next to or below the Missouri River for all scenarios because of the short distance ground water traveled from the bottom of the riverbed in layer 2 of the model to the screened interval of the wells in layers 3 and 4 of the model. The 5- and 10-year CRAs are centered around the well field but skewed to the northwest.

Simulated pumping rates for the Gladstone well field (table 15) ranged from 6,540 m^3/d for the low pumping-rate scenarios to 10,895 m^3/d for the high pumping-rate scenarios. The total CRA (table 16) ranged from 1.914 km^2 for the LPHR scenario (pl. 3) to 3.669 km^2 for the HPLR scenario (pl. 5). The total

Table 15. Simulated pumping rates for the Gladstone, Missouri, well field

	Well location in model			Pumping rate, in cubic meters per day			
	Layer	Row	Column	Low	Jan. 1993	Average	High
	3	87	171	1,308	1,526	1,743	2,179
	3	87	171	1,308	1,526	1,743	2,179
	4	88	172	1,308	1,526	1,743	2,179
	4	88	172	1,308	1,526	1,743	2,179
	4	88	172	1,308	1,526	1,743	2,179
Total				6,540	7,630	8,715	10,895

Table 16. Contributing recharge areas for the Gladstone, Missouri, well field

Contributing recharge area	Area, in square kilometers				
	Low pumping rate		Jan. 1993 quasi-steady state	High pumping rate	
	Low river stage	High river stage		Low river stage	High river stage
1-year	0.023	0.023	0.068	0.068	0.068
5-year	.18	.18	.18	.158	.158
10-year	.158	.045	.135	.158	.09
100-year	3.06	1.643	3.173	3.24	2.295
1,000-year	.09	.023	.045	.045	.023
Total	3.511	1.914	3.601	3.669	2.634

CRA for the Gladstone well field increased in response to increased well pumping rates and decreased with decreased well pumping rates. Low river stage increased the total CRA, and high river stage decreased the total CRA.

Kansas City, Missouri, Well Field

The shape of the total CRA for the Kansas City, Missouri, well field (well field number 3, pls. 2–6) is approximately circular, centered around the well field, and extends along the northern bank of the Missouri River for approximately 1 km for all pumping and river-stage scenarios. The total CRA is limited in extent by the nearness of the well field to the Missouri River and the alluvial valley walls. The location of the 1- and 5-year CRAs below and near the Missouri River and the relatively small total CRA indicate induced recharge from the Missouri River supplies a large part of the water for this well field.

Simulated pumping rates for the Kansas City well field ranged from 2,442 m^3/d for the QUASI scenario to 73,062 m^3/d for the high pumping-rate scenario (table 17). The total CRA ranged from 0 km^2 for the QUASI scenario (pl. 4) to 0.339 km^2 for HPHR scenario (table 18).

Table 17. Simulated pumping rates for the Kansas City, Missouri, well field

Well location			Pumping rate, in cubic meters per day			
Layer	Row	Column	Low	Jan. 1993	Average	High
4	90	176	3,985	222	5,314	6,642
4	90	176	3,985	222	5,314	6,642
4	90	180	3,985	222	5,314	6,642
4	91	180	3,985	222	5,314	6,642
4	92	178	3,985	222	5,314	6,642
4	92	178	3,985	222	5,314	6,642
4	92	178	3,985	222	5,314	6,642
4	93	179	3,985	222	5,314	6,642
4	93	179	3,985	222	5,314	6,642
4	93	179	3,985	222	5,314	6,642
4	94	179	3,985	222	5,314	6,642
Total			43,835	2,442	58,454	73,062

Table 18. Contributing recharge areas for the Kansas City, Missouri, well field

Contributing recharge area	Area, in square kilometers				
	Low pumping rate		Jan. 1993 quasi-steady state	High pumping rate	
	Low river stage	High river stage		Low river stage	High river stage
1-year	0.113	0.113	0	0.135	0.135
5-year	.18	.18	0	.158	.158
10-year	0	0	0	.045	.023
100-year	.045	.045	0	0	.023
Total	0.338	0.338	0	0.338	0.339

The total CRA for all pumping and river-stage scenarios remained about the same size except for the QUASI scenario when pumping rates were so low that a CRA was not apparent and for the HPHR scenario when the increase of the 100-year CRA slightly increased the total CRA. This result indicates that induced recharge from the Missouri River is the dominant source of water to the Kansas City well field. River stage changes did not affect the size of the 1-, 5-, 10-, or 100-year CRAs between the two low pumping-rate scenarios and only slightly changed the 10- and 100-year CRAs between the two high pumping-rate scenarios.

North Kansas City, Missouri, Well Field

The shape of the total CRA for the North Kansas City, Missouri, well field (well field number 4, pls. 2–6) is approximately circular and extends from the well field northwest toward the Missouri River. The length of the total CRA ranges from approximately 1 km for the LPLR scenario (pl. 2) to almost 1.5 km in the two high river-stage scenarios. The length of the total CRA is limited by the flow boundary of the Missouri River to the west and interference from an industrial well field (well field number 5, pls. 2–6) to the southeast. Unlike the Missouri Cities Water Company and the Gladstone well field CRAs that intersect ground water as it flows toward the Missouri River, the total CRA for the North Kansas City well field is bounded on the upgradient edge by the Missouri River. Induced recharge from the Missouri River is shown by the location of the 1- and 5-year CRAs. The 1-year CRA is next to and beneath the Missouri River for all pumping and river-stage scenarios. However, during the high pumping scenarios, the 1-year CRA is composed of two areas; one next to and beneath the river and another around the well field.

Simulated pumping rates for the North Kansas City well field ranged from 9,884 m^3/d for the low pumping-rate scenarios to 16,476 m^3/d for the high pumping-rate scenarios (table 19). The total CRA (table 20) ranged from 0.563 km^2 for the LPLR scenario (pl. 2) to 1.058 km^2 for the QUASI scenario.

Table 19. Simulated pumping rates for the North Kansas City, Missouri, well field

	Well location in model			Pumping rate, in cubic meters per day			
	Layer	Row	Column	Low	Jan. 1993	Average	High
	4	102	182	2,471	3,300	3,295	4,119
	4	103	182	2,471	3,300	3,295	4,119
	4	103	182	2,471	3,300	3,295	4,119
	4	104	182	2,471	3,300	3,295	4,119
Total				9,884	13,200	13,180	16,476

Table 20. Contributing recharge areas for the North Kansas City, Missouri, well field

Contributing recharge area	Area, in square kilometers				
	Low pumping rate		Jan. 1993 quasi-steady state	High pumping rate	
	Low river stage	High river stage		Low river stage	High river stage
1-year	0.09	0.068	0.158	0.27	0.203
5-year	.45	.54	.63	.54	.585
10-year	.023	.09	.135	.113	.135
100-year	0	.18	.135	.09	.113
Total	0.563	0.878	1.058	1.013	1.036

The total CRA for the North Kansas City well field increased with higher pumping, decreased with lower pumping, increased during high river stage, and decreased during low river stage. The 1-year CRA decreased with high river stage, but increased with increased pumping. The 5-, 10-, and 100-year CRAs increased with high pumping and increased with high river stage. The change in area of the total CRA for this well field with respect to pumping is normal because increased pumping increased the size of the total CRA. As discussed earlier, well fields located close to a major river obtain a large part of their water from induced recharge.The North Kansas City well field is located far enough from the river so that increased pumping required a larger area of the aquifer for water supply rather than an increased rate of induced recharge from the Missouri River. As the pumping rate increased, the rate of induced recharge from the river probably also increased, but that increased rate alone was not enough to supply the well field.

Independence, Missouri, Well Field

The shape of the total CRA for the Independence, Missouri, well field (well field number 8, pls. 2–6) is approximately a half-circle bounded by the alluvial valley wall to the south and by the Missouri River to the north. The part of the total CRA that extends across the Missouri River to the west for each pumping and river-stage scenario indicates that flow occurs beneath the river. The greatest changes in the total CRA occur in the area across the river and to the west of the well field. However, the entire river bend within the confines of the alluvial valley walls to the south and the Missouri River to the north, with the exception of a small area on the extreme eastern edge, are a part of the total CRA for all pumping and river-stage scenarios. Induced recharge from the Missouri River is indicated by the 1- and 5-year CRAs located next to the Missouri River for all scenarios.

The location and shape of the total CRA for the Independence well field across the Missouri River is different for each scenario and is affected not only by pumping rates and river stage, but also by the low ground-water gradient west of the well field across the river and the possible interference of pumping from the Liberty, Missouri, well field (well field number 9, pls. 2–6) located north of the Independence well field. The effect of this interference is illustrated by comparing the total CRA between the HPLR and LPLR scenarios. The component of the Independence well field total CRA across the Missouri River for the HPLR scenario (pl. 5) is a narrow band approximately 0.25 to 0.5 km wide and almost 5 km long adjacent to the southwest edge of the total CRA for the Liberty well field. When pumping rates decrease in the LPLR scenario (pl. 2), the component of the total CRA across the Missouri River for the Independence well field shifts north in response to the decrease in size of the total CRA of the Liberty well field and expands to approximately 0.5 to 1 km in width. The effect of changes in pumping rate on the location of the total CRA across the Missouri River is greater for the high river-stage scenarios because of the relatively low ground-water gradient. The total CRA across the Missouri River for the LPHR scenario (pl. 3) extends northwest of the well field and is approximately 6.5 km long and as much as 1 km wide. However, the total CRA across the Missouri River for the HPHR scenario (pl. 6) is much smaller and is composed of only a few isolated areas located along the southwestern edge of the Liberty well field total CRA and next to the north alluvial valley walls. The decrease in the total CRA for the Independence well field in the HPHR scenario (pl. 6) was caused by the diversion of ground water toward the Liberty well field as shown by the increase in the total CRA for the Liberty well field for this scenario.

Simulated pumping rates for the Independence well field (table 21) ranged from 38,816 m^3/d for the QUASI scenario (pl. 4) to 112,864 m^3/d for the high pumping-rate scenarios. The total CRA (table 22) ranged from 6.39 km^2 for the HPHR scenario (pl. 6) to 9.406 km^2 for the LPHR scenario (pl. 3).

The total CRA for the Independence well field decreased with increased pumping rates for both high and low river-stage scenarios, increased with an increase in river stage for the low pumping-rate scenarios and decreased with an increase in river stage for the high pumping-rate scenarios. The 1-year CRA was smallest for the QUASI scenario (pl. 4) when pumping rates also were small and increased for the two low pumping-rate scenarios to the same area.

The change in size of the total CRA for the Independence well field with respect to changes in pumping rates and river stage is similar to the changes in the total CRA for the Missouri Cities Water Company well field (well field number 1, pls. 2–6) when the ground-water gradient was low. As previously discussed, the decrease in the total CRA for the HPHR

Table 21. Simulated pumping rates for the Independence, Missouri, well field

	Well location in model			Pumping rate, in cubic meters per day			
	Layer	Row	Column	Low	Jan. 1993	Average	High
	3	85	294	2,116	1,213	2,821	3,527
	3	85	296	2,116	1,213	2,821	3,527
	3	85	298	2,116	1,213	2,821	3,527
	3	87	294	2,116	1,213	2,821	3,527
	3	89	293	2,116	1,213	2,821	3,527
	3	90	286	2,116	1,213	2,821	3,527
	4	86	189	2,116	1,213	2,821	3,527
	4	86	289	2,116	1,213	2,821	3,527
	4	87	288	2,116	1,213	2,821	3,527
	4	87	288	2,116	1,213	2,821	3,527
	4	87	289	2,116	1,213	2,821	3,527
	4	87	289	2,116	1,213	2,821	3,527
	4	88	285	2,116	1,213	2,821	3,527
	4	88	286	2,116	1,213	2,821	3,527
	4	88	286	2,116	1,213	2,821	3,527
	4	88	287	2,116	1,213	2,821	3,527
	4	88	288	2,116	1,213	2,821	3,527
	4	88	288	2,116	1,213	2,821	3,527
	4	88	289	2,116	1,213	2,821	3,527
	4	88	289	2,116	1,213	2,821	3,527
	4	88	289	2,116	1,213	2,821	3,527
	4	88	290	2,116	1,213	2,821	3,527
	4	89	284	2,116	1,213	2,821	3,527
	4	89	286	2,116	1,213	2,821	3,527
	4	89	286	2,116	1,213	2,821	3,527
	4	89	287	2,116	1,213	2,821	3,527
	4	89	291	2,116	1,213	2,821	3,527
	4	90	286	2,116	1,213	2,821	3,527
	4	90	287	2,116	1,213	2,821	3,527
	4	90	285	2,116	1,213	2,821	3,527
	4	91	285	2,116	1,213	2,821	3,527
	4	91	285	2,116	1,213	2,821	3,527
Total				67,712	38,816	90,272	112,864

Table 22. Contributing recharge areas for the Independence, Missouri, well field

Contributing recharge area	Area, in square kilometers				
	Low pumping rate		Jan. 1993 quasi-steady state	High pumping rate	
	Low river stage	High river stage		Low river stage	High river stage
1-year	0.293	0.293	0.203	0.428	0.36
5-year	1.215	1.035	.765	1.665	1.395
10-year	1.058	.99	.878	.99	.99
100-year	4.86	6.773	4.59	4.163	3.195
1,000-year	.293	.315	.54	.405	.45
Total	7.719	9.406	6.976	7.651	6.39

scenario (pl. 6) is explained by the combined effect of a low ground-water gradient across the Missouri River, west of the Independence well field caused by increased river stage, and the increased pumping of the Liberty well field (well field number 9, pls. 2–6). Therefore, the gradient beneath the Missouri River toward the well field decreased so that water that previously discharged to the well field during low-river stage instead discharged into the Missouri River during high-river stage.

Liberty, Missouri, Well Field

The shape of the total CRA for the Liberty, Missouri, well field (well field number 9, pls. 2–6) is approximately oval, is longest in an east-west orientation, and is bounded on the north by the alluvial valley walls. The dimensions of the total CRA range from approximately 6.5 km long by 3 km wide (LPHR scenario, pl. 3) to approximately 8 km long by 4 km wide (HPLR scenario, pl. 5). The total CRA is skewed to the west, and, for the HPLR scenario, the well field is approximately 5 km from the western edge and approximately 3 km from the eastern edge of the total CRA. The total CRA for the Liberty well field is large as compared to other total CRAs in the study area. This size difference is because little or no water is supplied to the well field through induced recharge from the Missouri River. Therefore, the total CRA extends into the surrounding aquifer. No 1-year CRA exists for any of the pumping and river-stage scenarios because the area where the wells are located has a relatively thick upper layer of clay and silty clay that inhibits rapid downward movement of water from the surface of the water table to the screened interval of the pumped wells. The 5-year CRA is centered around the well field for all pumping and river-stage scenarios. The 10-year CRA is located in two general areas; one centered around the well field and the other approximately 1 km to the southwest of the well field. The presence of the 10-year CRA to the southwest of the well field is caused by an area of silt and sand with a higher hydraulic conductivity in the same location in the upper part of the aquifer. Surface recharge from rainfall can enter the aquifer and move to the screened interval of the wells more quickly in this area than in other nearby areas. The 100- and 1,000-year CRAs include most of the total CRA in all scenarios.

Simulated pumping rates for the Liberty well field (table 23) ranged from 7,950 m^3/d for the low pumping rate scenarios to 13,254 m^3/d for the high pumping-rate scenarios. The total CRA (table 24) ranged from 14.874 km^2 for the LPHR scenario (pl. 3) to 23.469 km^2 for the HPHR scenario (pl. 6). The total CRA for the Liberty well field increased with increased pumping rates for both river-stage scenarios, decreased with increased river stage in the low pumping-rate scenarios, and increased slightly with increased river stage for the high pumping-rate scenarios.

Community Water Company Well Field

The shape of the total CRA for the Community Water Company well field (well field number 10, pls. 2–6) is long and relatively narrow for both of the low river-stage scenarios (pls. 2, 5) and the QUASI scenario (pl. 4), extends into the Little Blue River valley

Table 23. Simulated pumping rates for the Liberty, Missouri, well field

	Well location in model			Pumping rate, in cubic meters per day			
	Layer	Row	Column	Low	Jan. 1993	Average	High
	3	60	296	1,325	1,363	1,766	2,209
	3	61	296	1,325	1,363	1,766	2,209
	3	61	296	1,325	1,363	1,766	2,209
	3	62	296	1,325	1,363	1,766	2,209
	3	63	296	1,325	1,362	1,766	2,209
	3	64	296	1,325	1,362	1,766	2,209
Total				7,950	8,176	10,596	13,254

Table 24. Contributing recharge areas for the Liberty, Missouri, well field

Contributing recharge area	Area, in square kilometers				
	Low pumping rate		Jan. 1993 quasi-steady state	High pumping rate	
	Low river stage	High river stage		Low river stage	High river stage
5-year	0.135	0.113	0.18	0.293	0.248
10-year	.858	.315	.855	2.115	.968
100-year	14.378	13.973	14.558	20.543	21.465
1,000-year	.54	.473	.563	.495	.788
Total	15.911	14.874	16.156	23.446	23.469

approximately 6.5 km south of the well field, and is 0.25 to 0.5 km wide. The shape for the LPHR scenario (pl. 3) is a smaller oval that extends toward the Missouri River and is approximately 2.5 km long and 1 km wide. The shape of the total CRA for the HPHR scenario (pl. 6) is elongated to the south and divides into two arms approximately 1.5 km south of the well field. One arm extends south for 4.5 km from the divide and the other arm extends to the southwest for almost 3 km from the divide.

The relatively long narrow shape of the total CRA for the LPLR, HPLR, and QUASI scenarios (pls. 2, 4, 5) was caused by the interception of ground water by the Community Water Company well field as the water moved downgradient toward the Missouri River. The absence of a 1- or 5-year CRA and the fact that the total CRA does not intersect the Missouri River for these scenarios indicates the relatively small effect that pumping this well field has on ground-water flow. The increase of river stage alters the shape of the total CRA because the regional ground-water gradient near the well field becomes lower. The increase of river stage for the low pumping-rate scenarios changed the total CRA from the long narrow shape for the LPLR scenario (pl. 2) to the smaller shorter shape of the LPHR scenario (pl. 3). The increase of river stage for the high pumping-rate scenarios caused the total CRA from the HPLR scenario (pl. 5) to expand for the HPHR scenario (pl. 6) to include an additional arm to the southwest. The branching of the total CRA for the HPHR scenario (pl. 6) was caused by the presence of a silty clay deposit with low hydraulic conductivity in the aquifer represented in layer 3 of the model.

Simulated pumping rates for the Community Water Company well field (table 25) ranged from 852 m^3/d for the low pumping-rate scenarios to 1,420 m^3/d for the high pumping-rate scenarios. The total CRA (table 26) ranged from 1.396 km^2 for the LPHR scenario (pl. 3) to 3.173 km^2 for the HPHR scenario (pl. 6).

Table 25. Simulated pumping rates for the Community Water Company well field

Well location in model			Pumping rate, in cubic meters per day			
Layer	Row	Column	Low	Jan. 1993	Average	High
3	66	337	426	568	568	710
3	66	337	426	568	568	710
Total			852	1,136	1,136	1,420

Table 26. Contributing recharge areas for the Community Water Company well field

Contributing recharge area	Area, in square kilometers				
	Low pumping rate		Jan. 1993 quasi-steady state	High pumping rate	
	Low river stage	High river stage		Low river stage	High river stage
10-year	0	0	0.045	0.068	0
100-year	1.508	1.148	1.778	2.003	2.835
1,000-year	0	.248	.023	0	.338
Total	1.508	1.396	1.846	2.071	3.173

The total CRA for the Community Water Company well field increased with increased pumping rates, decreased with increased river stage for the low pumping-rate scenarios (pls. 2, 3), and increased with increased river stage for the high pumping-rate scenarios (pls. 5, 6). The 1- and 5-year CRAs were absent for all pumping and river-stage scenarios because of the relatively low pumping rate of the well field. The 10-year CRA existed for only the QUASI (pl. 4) and HPLR (pl. 5) scenarios and was centered around the well field.

Tri-County Water Company Well Field

The shape of the total CRA for the Tri-County Water Company well field (well field number 11, pls. 2–6) is approximately oval for the low river stage and QUASI scenarios (pls. 2, 4, 5), extends approximately 4.5 km from the well field to the west, and is approximately 2 km wide. The total CRA for the LPHR scenario (pl. 3) extends into a buried alluvial channel approximately 5.5 km to the south and is approximately 1 km wide. The total CRA for the HPHR scenario (pl. 6) is divided into two arms. The divide occurs approximately 2.5 km to the southwest of the well field where the aquifer splits between the main aquifer and a buried alluvial channel to the south. The western arm extends approximately 3 km and the southern arm extends approximately 4 km from the divide.

The extent of the total CRA for all scenarios is controlled on the south edge by the alluvial valley walls and by the Missouri River, which supplies water to the well field from the east. The long upgradient extent of the total CRA for all pumping and river-stage scenarios was caused by the interception of ground water by the well field as water moved downgradient toward the Missouri River.

The 1-year CRA is located next to the Missouri River for all pumping and river-stage scenarios and indicates that the well field induced recharge from the Missouri River. The 5-year CRA is centered around the well field but skewed to the west upgradient. The 10-, 100-, and 1,000-year CRAs extend toward the west or southwest for all scenarios.

Simulated pumping rates for the Tri-County Water Company (table 27) ranged from 4,257 m^3/d for the low pumping-rate scenarios to 7,095 m^3/d for the high pumping-rate scenarios. The total CRA (table 28) ranged from 5.535 km^2 for the LPLR scenario (pl. 2) to 10.621 km^2 for the HPLR scenario (pl. 5). The total

Table 27. Simulated pumping rates for the Tri-County Water Company well field

	Well location in model			Pumping rate, in cubic meters per day			
	Layer	Row	Column	Low	Jan. 1993	Average	High
	3	50	381	1,419	1,892	1,892	2,365
	3	50	382	1,419	1,892	1,892	2,365
	3	50	382	1,419	1,892	1,892	2,365
Total				4,257	5,676	5,676	7,095

Table 28. Contributing recharge areas for the Tri-County Water Company well field

Contributing recharge area	Area, in square kilometers				
	Low pumping rate		Jan. 1993 quasi-steady state	High pumping rate	
	Low river stage	High river stage		Low river stage	High river stage
1-year	0.023	0.045	0.045	0.113	0.068
5-year	.63	.405	.923	.855	.653
10-year	.63	.405	.743	.81	.698
100-year	8.123	3.51	7.853	8.528	7.448
1,000-year	.518	1.17	.225	.315	1.373
Total	9.924	5.535	9.789	10.621	10.240

CRA decreased with an increase in river stage and increased with an increase in well pumping rates for all pumping and river-stage scenarios.

Ray County Public Water Supply District Number 2 Well Field

The shape of the Ray County Public Water Supply District Number 2 well field (Ray County PWSD No. 2; well field number 12, pls. 2–6) is an elongated oval, extends approximately 6.5 km northwest from the well field, and is approximately 1.5 km wide for all pumping and river-stage scenarios. The extent of the total CRA is controlled by the alluvial valley wall to the northeast that is a ground-water flow barrier and to some degree by the Fishing River, which supplies water to the well field from induced recharge. The west edge of total CRA for all pumping and river-stage scenarios coincides with the course of the Fishing River. The long upgradient extent of the total CRA was caused by the interception of ground water by the well field as water flowed downgradient toward the Missouri River.

Simulated pumping rates for the Ray County PWSD No. 2 well field (table 29) ranged from 2,460 m^3/d for the QUASI scenario (pl. 4) to 4,558 m^3/d for the HPHR scenario (pl. 6). The total CRA (table 30) ranged from 4.636 km^2 for the QUASI scenario (pl. 4) to 7.404 km^2 for the HPHR scenario (pl. 6). The total CRA increased with an increase in pumping rates and river stage for all pumping and river-stage scenarios.

Excelsior Springs, Missouri, Well Field

The shape of the total CRA for the Excelsior Springs, Missouri, well field (well field number 13, pls. 2–6) is circular and has an approximate diameter of 2 km with an arm extending northward into the Fishing River alluvial valley for approximately 3 km for all pumping and river-stage scenarios. The long northern arm of the total CRA was caused by the interception of water by the well field as water moved downgradient toward the Missouri River. The extent

Table 29. Simulated pumping rates for the Ray County Public Water Supply District Number 2 well field

	Well location in model			Pumping rate, in cubic meters per day			
	Layer	Row	Column	Low	Jan. 1993	Average	High
	2	40	437	1,016	615	1,354	1,693
	2	40	437	352	615	469	586
	2	41	435	703	615	937	1,172
	2	41	437	664	615	885	1,107
Total				2,735	2,460	3,645	4,558

Table 30. Contributing recharge areas for the Ray County Public Water Supply District Number 2 well field

Contributing recharge area	Area, in square kilometers				
	Low pumping rate		Jan. 1993 quasi-steady state	High pumping rate	
	Low river stage	High river stage		Low river stage	High river stage
5-year	0.18	0.135	0.135	0.405	0.203
10-year	.428	.293	.518	.518	.428
100-year	4.32	5.535	3.735	5.445	6.323
1,000-year	.27	.405	.248	.225	.36
Total	5.198	6.368	4.636	6.593	7.404

of the total CRA is controlled by the alluvial valley wall to the north that is a flow barrier and by Cooley Lake, which supplies water to the well field through induced recharge. The 1-year CRA is non-existent for all scenarios because of low pumping rates. The 5-year CRA is centered around the well field for all scenarios. Part of the 5-year CRA is next to Cooley Lake for the LPLR, HPLR, and QUASI scenarios and indicates induced recharge. A small part of the 5-year CRA is located north of the well field in the Fishing River alluvial valley for the QUASI (pl. 4) and HPLR (pl. 5) scenarios, which was caused by the presence of a sand with a high hydraulic conductivity at that location that allowed water to enter the lower parts of the aquifer where water then traveled more quickly to the well field. The 10-year CRA is centered around the well field and has a small northern part in the Fishing River alluvial valley for all scenarios and a small part located near Cooley Lake for the LPLR, QUASI, HPLR, and HPHR scenarios (pls. 2, 4, 5, 6). The 100-year CRA extends toward Cooley Lake to the west and to the Fishing River alluvial valley to the north for all scenarios. The 100-year CRA is divided into two parts for the LPLR (pl. 2) and QUASI (pl. 4) scenarios because of the presence of a clay with a low hydraulic conductivity at the surface that limited the rate of water movement downward into the lower parts of the aquifer. The 1,000-year CRA is located north of the well field in the Fishing River alluvial valley for all scenarios.

Simulated pumping rates for the Excelsior Springs well field (table 31) ranged from 4,332 m^3/d for the low pumping-rate scenario to 7,216 m^3/d for the high pumping-rate scenario. The total CRA (table 32) ranged from 3.309 km^2 for the LPLR scenario (pl. 2) to 8.483 km^2 for the HPHR scenario (pl. 6). The total CRA increased with increased pumping rates and river stage for all pumping and river-stage scenarios.

Lake City Army Ammunition Plant Well Field

The shape of the total CRA for the Lake City Army Ammunition Plant well field changes substantially between each of the pumping and river-stage scenarios (well field number 14, pls. 2–6). The extent of the total CRA is limited by the alluvial valley walls

Table 31. Simulated pumping rates for the Excelsior Springs, Missouri, well field

	Well location in model			Pumping rate, in cubic meters per day			
	Layer	Row	Column	Low	Jan. 1993	Average	High
	2	23	391	1,083	1,246	1,443	1,804
	2	23	391	1,083	1,246	1,443	1,804
	2	24	391	1,083	1,246	1,443	1,804
	2	25	391	1,083	1,246	1,443	1,804
Total				4,332	4,984	5,772	7,216

Table 32. Contributing recharge areas for the Excelsior Springs, Missouri, well field

Contributing recharge area	Area, in square kilometers				
	Low pumping rate		Jan. 1993 quasi-steady state	High pumping rate	
	Low river stage	High river stage		Low river stage	High river stage
5-year	0.203	0.27	0.248	0.518	0.315
10-year	.428	.36	.473	.495	.72
100-year	2.385	6.188	2.768	4.703	6.593
1,000-year	.293	.518	.158	.495	.855
Total	3.309	7.336	3.647	6.211	8.483

of the Little Blue River alluvial valley to the north and west, the walls of the abandoned Missouri River alluvial valley now occupied by Fire Prairie Creek to the east, areas of low vertical hydraulic conductivity, and local drainage.

The effect of river stage on the shape of the total CRA is evident between the low river-stage scenarios and the high river-stage scenarios. The total CRA is divided into multiple parts for low river-stage scenarios (LPLR, pl. 2; HPLR, pl. 5). The areas between the total CRA do not contribute water to the well field. High river-stage scenarios (LPHR, pl. 3; HPHR, pl. 6) have an undivided total CRA. The most probable explanation for these differences is the change in ground-water gradient and flow direction between the low river-stage scenarios and the high river-stage scenarios in the vicinity of the well field. During the low river-stage scenarios, the total CRA for the well field extends to the Little Blue River, indicating induced recharge as a source of water. The divide between the northern and southern total CRA was most probably caused by lower pumping rates and the eastward flow of shallow ground water to Fire Prairie Creek, where the water discharged. During the high river-stage scenarios, the total CRA is undivided because the low regional ground-water gradient in the vicinity of the well field decreased the lateral movement of water eastward toward Fire Prairie Creek and increased the effect of pumping rates on the potentiometric surface by creating an extremely broad, but shallow, cone of depression.

Simulated pumping rates for the Lake City Army Ammunition Plant well field (table 33) ranged from 3,055 m^3/d for the low pumping-rate scenarios to 5,092 m^3/d for the high pumping-rate scenarios. The total CRA (table 34) ranged from 3.173 km^2 for the QUASI scenario (pl. 4) to 10.779 km^2 for the HPHR scenario (pl. 6). The total CRA increased with increased pumping rates and river stage for all pumping and river-stage scenarios.

Industrial Well Fields

Nineteen industrial well fields with 37 wells are known to be present within the study area (table 35). The six industrial well fields that have large

Table 33. Simulated pumping rates for the Lake City Army Ammunition Plant well field

	Well location in model			Pumping rate, in cubic meters per day			
	Layer	Row	Column	Low	Jan. 1993	Average	High
	2	131	359	524	491	698	873
	3	130	368	629	491	839	1,049
	3	130	372	146	491	194	243
	3	133	365	518	491	690	863
	3	133	370	0	491	0	0
	3	134	356	440	491	587	734
	3	135	360	53	491	70	88
	3	137	356	0	491	0	0
	3	137	365	313	491	419	523
	3	137	369	432	491	575	719
Total				3,055	4,910	4,072	5,092

Table 34. Contributing recharge areas for the Lake City Army Ammunition Plant well field

Contributing recharge area	Area, in square kilometers				
	Low pumping rate		Jan. 1993 quasi-steady state	High pumping rate	
	Low river stage	High river stage		Low river stage	High river stage
10-year	0.068	0	0	0.315	0.068
100-year	4.05	4.568	1.328	4.275	8.123
1,000-year	.833	.54	1.845	1.283	2.588
Total	4.951	5.108	3.173	5.873	10.779

CRAs (table 36; pls. 2–6) include the National Starch Company, Inc. well field (well field number 5), the Chevron Chemical Company well field (well number 7), Phillips Petroleum well fields (well field number 18 and well number 23), the Sealright Company well field (well number 25), and the Reichhold Chemicals, Inc./Certain-Teed Corp. well field (well field number 27). The total CRA for the Chloride Industrial Batteries well field (well number 29) is small and present in model results only during the HPHR scenario (pl. 6). The Phillips Petroleum wells were grouped into two well fields because well number 23 (pls. 2–6) developed an individual CRA because of its distance from other pumped wells. The Reichhold Chemicals, Inc./Certain-Teed Corp. wells were combined into one well field because of their proximity to each other. The pumping rates of the remaining industrial wells were not sufficient to produce individual CRAs from the model results. Most of the industrial wells are north of the junction of the Missouri and Kansas Rivers in North Kansas City, Missouri, and Kansas City, Kansas, where the effects of industrial well pumping on the CRAs of the public-water-supply well fields are evident. The total CRA of each of the 19 industrial well fields is not presented individually, but is described as part of the overall effect of pumping rates and river stage on the alluvial aquifer in the following section.

Table 35. Simulated pumping rates of the industrial well fields

	Well location in model			Pumping rate, in cubic meters per day			
	Layer	Row	Column	Low	Jan. 1993	Average	High
Well field 5	3	115	188	817	1,090	1,090	1,363
	3	115	189	817	1,090	1,090	1,363
	4	114	183	817	1,090	1,090	1,263
	4	112	188	817	1,090	1,090	1,363
	4	113	188	817	1,090	1,090	1,363
	4	113	188	817	1,090	1,090	1,363
	4	114	188	817	1,090	1,090	1,363
	4	114	188	817	1,090	1,090	1,363
	4	115	186	817	1,090	1,090	1,363
	4	116	184	817	1,090	1,090	1,363
Total				8,170	10,900	10,900	13,530
Well 6	3	114	245	204	273	273	341
Well 7	3	109	269	409	545	545	681
Well 15	3	135	343	0	55	0	0
Well 16	2	46	54	0	545	0	0
Well 17	4	99	183	409	545	545	681
Well field 18	2	108	169	409	545	545	681
	2	109	168	409	545	545	681
	2	110	168	409	545	545	681
	2	110	169	409	545	545	681
	2	111	169	409	545	545	681
	3	109	171	409	545	545	681
	3	110	170	409	545	545	681
Total				2,863	3,815	3,815	4,767
Well field 19	4	108	195	245	327	327	409
	4	109	195	1,226	1,635	1,635	2,044
Total				1,471	1,962	1,962	2,453
Well 20	4	101	196	204	273	273	341
Well 21	4	106	188	102	136	136	170
Well 22	4	108	183	102	136	136	170
Well 23	3	102	175	1,226	1,635	1,635	2,044

Table 35. Simulated pumping rates of the industrial well fields—Continued

	Well location in model			Pumping rate, in cubic meters per day			
	Layer	Row	Column	Low	Jan. 1993	Average	High
Well 24	3	102	169	102	136	136	170
Well 25	3	104	166	818	1,090	1,090	1,363
Well 26	3	86	165	102	136	136	170
Well field 27	3	101	162	409	545	545	681
	4	100	162	1,022	545	1,363	1,703
	4	101	163	409	545	545	681
Total				1,840	1,635	2,453	3,065
Well 28	4	98	163	409	545	545	681
Well 29	4	99	166	204	273	273	341
Well 30	4	95	165	409	545	545	681

Effects of Pumping Rates and River Stage on Contributing Recharge Areas

The effect of well pumping rates and river stage on the total CRA of well fields in the study area is complex because (1) each well field has a unique orientation with respect to the geometry of the aquifer, the alluvial valley walls, the rivers, and the other pumped wells in the study area; (2) the hydraulic properties of the aquifer in the vicinity of each well field are different in both magnitude and spatial distribution; and (3) each well field has a different pumping rate. For most well fields, an increase in pumping rates increases the total CRA for both low and high river-stage scenarios (fig. 37). However, the total CRAs for well fields of National Starch Company, Inc. and Phillips Petroleum (well field number 18) decreased with increased pumping rates for the low river-stage scenarios, and the total CRAs for well fields of the Missouri Cities Water Company, Independence, and National Starch Company, Inc. decreased with increased pumping rates for the high river-stage scenarios.

A change in river stage has a large effect on the potentiometric surface gradient of the aquifer. Typically, an increased river stage lowers the regional ground-water gradient between the alluvial valley walls and the rivers in the study area. Most total CRAs increased with increased river stage (fig. 38). However, the effect of a change in the ground-water gradient on the total CRAs is different for each well field. For instance, the total CRAs for the well fields of Gladstone, Chevron Chemical Company, Liberty, Community Water Company, Tri-County Water Company, and Phillips Petroleum (well field number 18) decreased with increased river stage for the low pumping-rate scenarios and the total CRAs for well fields of the Missouri Cities Water Company, Gladstone, Independence, Tri-County Water Company, Phillips Petroleum (well number 23), Sealright Company, and Reichhold Chemicals, Inc./Certain-Teed Corp. decreased with increased river stage for the high pumping-rate scenarios.

In general, ground water flows away from the alluvial valley walls, toward the Missouri River, and down the river valley. Well fields without close hydrologic boundaries upgradient of the regional flow direction, such as the Missouri River or the alluvial valley walls, have relatively long elliptically shaped total CRAs in the simulation because ground water traveled a long distance along the flow gradient before it was intercepted by the pumped wells. These include well fields of the Missouri Cities Water Company, Gladstone, Independence, Community Water Company, Tri-County Water Company, Ray County PWSD No. 2, and Excelsior Springs. Wells located close to

Table 36. Contributing recharge areas of the industrial well fields

Well field number	Contributing recharge area	Area, in square kilometers				
		Low pumping rate		Jan. 1993 quasi-steady state	High pumping rate	
		Low river stage	High river stage		Low river stage	High river stage
5	1-year	0.023	0.023	0	0	0
	5-year	.158	.09	.203	.383	.293
	10-year	.315	.473	.63	.45	.45
	100-year	3.6	3.51	3.735	2.34	2.61
	1,000-year	0	0	0	0	.023
	Total	4.096	4.096	4.568	3.173	3.376
7	1-year	0.045	0.045	0.045	0.045	0.045
	5-year	.023	.023	.023	.023	.023
	10-year	.09	.045	.09	.09	.045
	100-year	.18	0	.135	.203	0
	1,000-year	.068	0	0	.045	.225
	Total	0.406	0.113	0.293	0.406	0.338
18	1-year	0	0	0	0	0
	5-year	.36	.293	.585	.698	.54
	10-year	.743	.473	.495	.63	.495
	100-year	3.285	2.475	2.205	2.048	2.498
	1,000-year	.023	.023	0	0	0
	Total	4.411	3.264	3.285	3.376	3.533
23	1-year	0	0	0	0	0
	5-year	.068	.068	.09	.158	.113
	10-year	.27	.135	.293	.54	.428
	100-year	.54	.855	.788	1.755	1.733
	Total	0.878	1.058	1.171	2.453	2.274
25	1-year	0	0	0	0	0
	5-year	0	.068	.09	.113	.09
	10-year	0	.113	.248	.36	.248
	100-year	0	.698	.54	.54	.63
	1,000-year	0	.045	0	0	0
	Total	0	0.924	0.878	1.013	0.968

Table 36. Contributing recharge areas of the industrial well fields—Continued

Well field number	Contributing recharge area	Area, in square kilometers				
		Low pumping rate		Jan. 1993 quasi-steady state	High pumping rate	
		Low river stage	High river stage		Low river stage	High river stage
27	1-year	0	0	0	0	0
	5-year	.045	.113	.203	.293	.203
	10-year	.203	.27	.473	.675	.45
	100-year	.72	1.35	1.328	1.305	1.508
	Total	0.968	1.733	2.004	2.273	2.161
29	1-year	0	0	0	0	0
	5-year	0	0	0	0	0
	10-year	0	0	0	0	.023
	Total	0	0	0	0	0.023

the alluvial walls, like the Liberty well field, have total CRAs that extend long distances away from the alluvial valley walls because little water is available from this boundary and recharge is unavailable from a nearby river.

Proximity to a major river decreases the size of a total CRA because the well or well field obtains a large part of its water from recharge induced from the river, as illustrated by the North Kansas City well field. The simulated high pumping rate for the North Kansas City well field of 16,476 m^3/d corresponds to a total CRA of just greater than 1 km^2 for both low and high river-stage scenarios. In comparison, the simulated high pumping rate for the Liberty well field (farther from the river) is 13,254 m^3/d, which corresponds to a total CRA of more than 23 km^2 for both the low and high river-stage scenarios.

Induced recharge because of proximity of a well field to a river also may affect the spatial distribution of individual CRAs associated with a specific time within the total CRA for each well field. For example, the Independence well field is located close to the Missouri River and has the 1-year CRA located near the river, but the 5- or 10-year CRAs are located in the area closest to the wells for all scenarios because the distance from the bottom of the riverbed to the screened interval of the well is less than the distance from the land surface to the screened interval of the well. Also, because the bottoms of larger rivers typically intersect alluvial material of higher hydraulic conductivity, ground water travels more quickly at this depth than at shallower depths where alluvial deposits of lower hydraulic conductivity are located.

The value of the vertical conductance term limits water flow between layers of the model to simulate the vertical anisotropy of hydraulic conductivity within the alluvial aquifer. This anisotropy is greatest in the heterogeneously distributed finer-grained deposits present at shallow depths and represented in the model by layer 1 and, to a lesser degree, in the more homogeneously distributed silt and sand present in deeper parts of the aquifer and represented in the model by layers 2 and 3. The distribution of vertical conductance between layers 1 and 2 and between layers 2 and 3 affects the relative distribution of a CRA within the total CRA of each well or well field. For example, the Liberty well field has a part of the 100-year CRA located closer to the well field than a part of the 10-year CRA because a low rate of vertical water movement caused by the presence of clay near the land surface increased the travel time of water from the water table to deeper parts of the aquifer. The part of the 10-year CRA located farther from the well field is present because a high rate of vertical water movement caused by coarse deposits at the land surface decreased the travel time of water from the water table to deeper parts of the aquifer. Because the hydraulic conductivity values in the deeper parts of the aquifer are higher and more uniformly distributed than in the shallower parts, the rate of water movement is faster and more uniform. Therefore, the rate of vertical water flow from the shallower parts of the aquifer to the

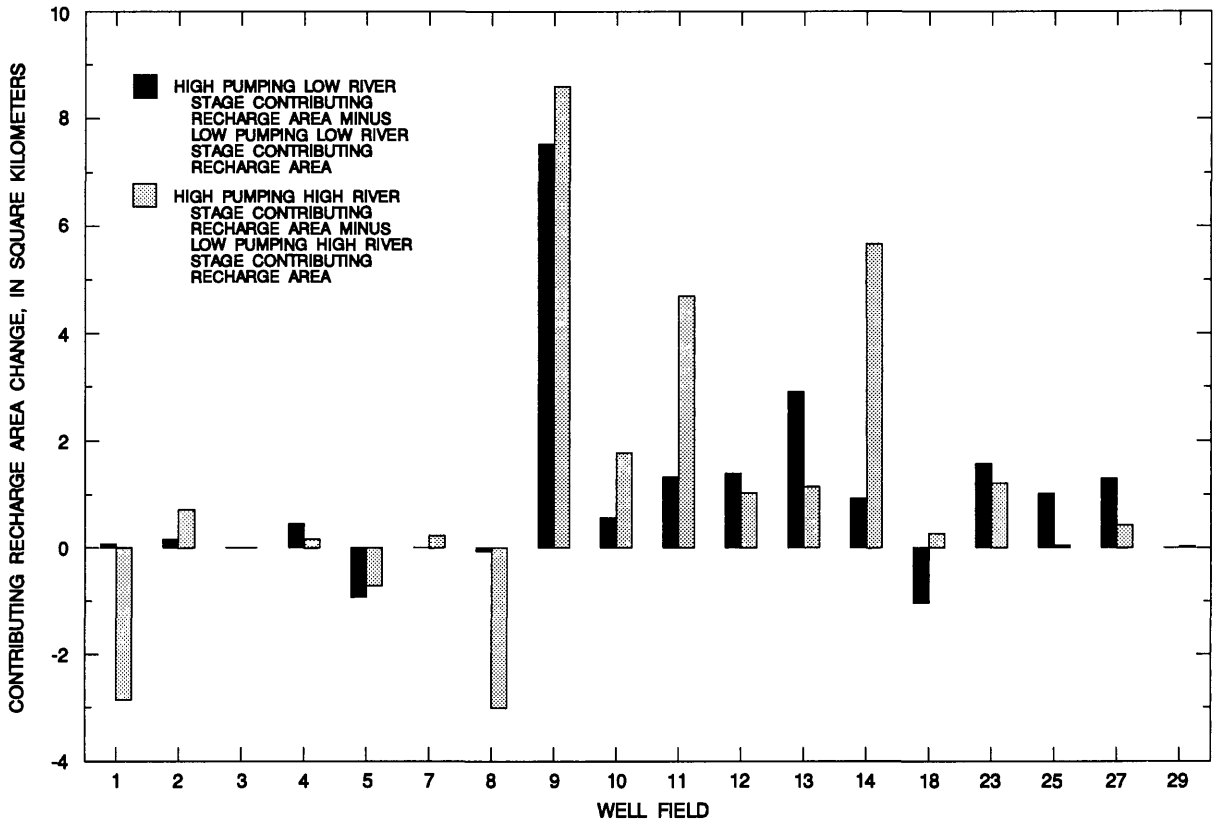

Figure 37. Change in contributing recharge area size in relation to well pumping rate for each well field.

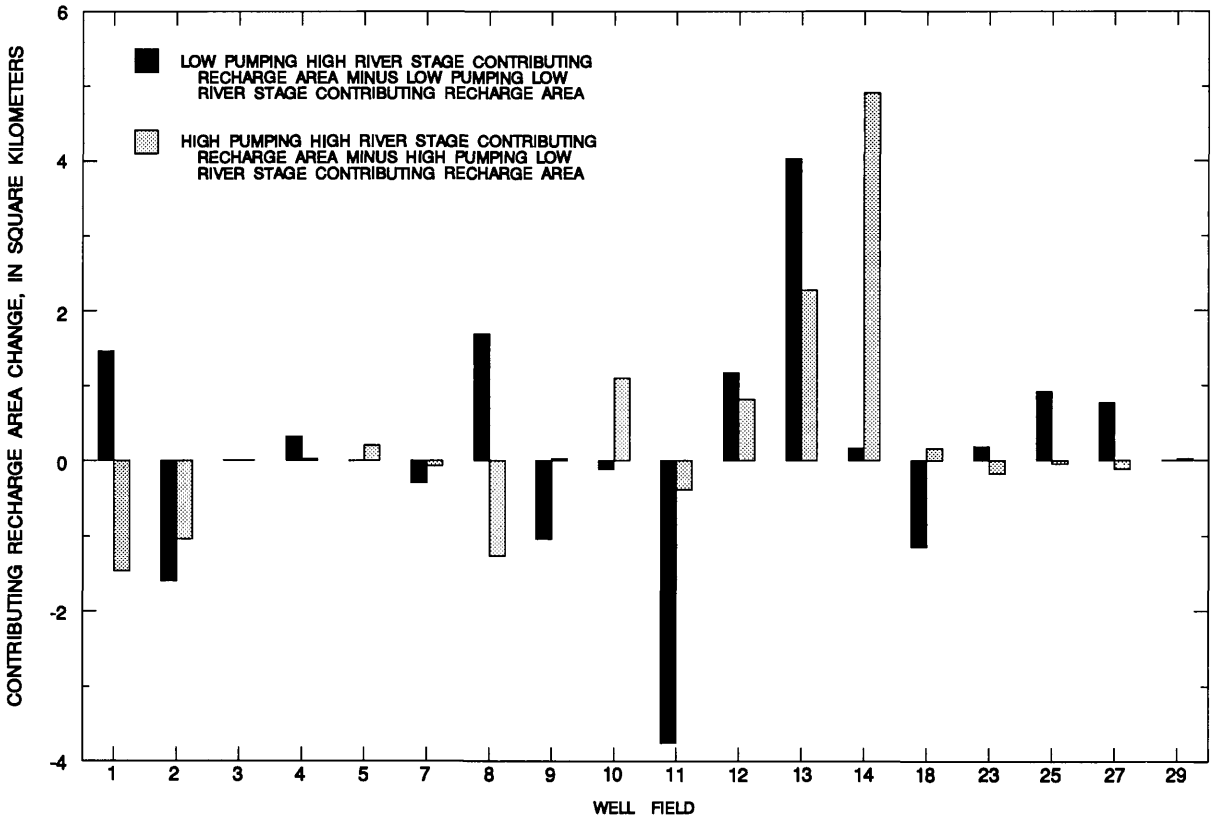

Figure 38. Change in contributing recharge area size in relation to river altitude.

deeper parts often controls the time of travel of water from the water table to the screened interval of a pumped well and the distribution of the total CRA of a well or well field.

Interference between pumped well fields also affects the size and shape of total CRAs of well fields. Well interference between the Independence well field and Liberty well field has already been discussed. However, the total CRAs of well fields located immediately north of the junction of the Missouri and Kansas Rivers show the greatest well interference effects. Well fields located upgradient of the regional flow system will intercept ground water before it reaches well fields located downgradient. This limits the groundwater supply and the extent of the CRAs of well fields located downgradient in the system. This is exemplified by the Phillips Petroleum, Sealright Company, and Reichhold Chemicals, Inc./Certain-Teed Corp. well fields (well field numbers 18, 25, and 27, pls. 2–6).

SUMMARY AND CONCLUSIONS

The Missouri River alluvial aquifer in the Kansas City metropolitan area supplies all or part of the drinking water for more than 900,000 people in 90 municipalities and public-water-supply districts and is the only aquifer in the area that can supply large quantities of ground water for public and industrial use. Because of the importance of this resource to the metropolitan area, a comprehensive ground-water protection plan is being developed for the Missouri River alluvial aquifer. As a basis for this plan, hydrogeologic data collected and compiled for more than 1,400 locations in the study area were entered into a geographic information system and interfaced with a groundwater flow model and a particle-tracking program to determine the contributing recharge areas for public-water-supply well fields.

The floodplains of the Missouri, Kansas, Blue, Little Blue, and Fishing Rivers are underlain by alluvial deposits of clay, silt, sand, gravel, cobbles, and boulders that form the alluvial aquifer and lie atop shale, limestone, and sandstone bedrock. Several abandoned alluvial channels are hydraulically connected to the Missouri River alluvial aquifer and exist as a result of changes in the course of the Missouri River and its tributaries during glacial and interglacial periods. The aquifer thickness ranges from less than 1 to about 59 meters. Average thickness is about 25 meters. The potentiometric surface is free to move vertically over time in the unconfined Missouri River alluvial aquifer and is the boundary across which recharge from precipitation flows into the aquifer and discharge from evapotranspiration flows out of the aquifer. However, because ground water usually is deeper than 4.5 meters, evapotranspiration is not considered an important source of discharge. Recharge has been estimated in several previous studies to be between 2 and 25 percent of precipitation. Because the study area has low local relief, topography has little effect on the areal distribution of recharge. Rather, the vertical hydraulic conductivity of soils directly controls the rate of infiltration. Flooding, irrigation, pumped wells, and dewatering during construction can alter ground-water flow directions.

Reported hydraulic conductivity values for the aquifer are between 0.1 and 1,400 meters per day; transmissivity values are as large as 7,400 meters squared per day, and specific yield is between 0.15 and 0.2. Ground-water flow between the aquifer and bedrock is thought to be minimal in comparison to the total flow of ground water in the aquifer because the bedrock units have estimated hydraulic conductivities between 0.003 and 3 meters per day.

A ground-water flow model of the Missouri River alluvial aquifer in the Kansas City metropolitan area was developed using the U.S. Geological Survey model MODFLOWARC, a modified version of MODFLOW. The model has a uniform grid size of 150 by 150 meters and contains 310,400 cells in 4 layers, 160 rows, and 485 columns. Hydrogeologic data from within the study area were entered into the geographic information system and assigned to each model cell by interpolation. The model was calibrated to both quasi-steady state hydraulic head data from the January 1993 synoptic water-level measurement and transient hydraulic head data from river-stage data of August 1993 and synoptic water-level measurements from October 1993 and February 1994. The steady state calibration was used to assess model geometry, confirm the conceptual model of ground-water flow, test the appropriateness of simulated boundary conditions, and obtain approximate transmissivity and recharge arrays. The root mean square error for the steady state calibration was 1.15 meters. The transient calibration was used to refine hydraulic properties of the model through simulation of a period of prolonged aquifer drainage from August 1993, immediately after the peak of the flood of 1993, to February 1994, when

river stage and ground-water levels had approached typical conditions for that time of year. The root mean square error for October 1993 was 0.71 meter and for February 1994 was 0.80 meter. Sensitivity analysis indicates that the model is most sensitive to increases and decreases in calibrated hydraulic conductivity values and least sensitive to decreases in vertical conductance between layers 1 and 2 and increases in river conductance.

Ground-water flow was simulated for five different well pumping-rate and river-stage scenarios to represent the range of conditions expected to occur. These scenarios include: (1) low pumping rates and low river stage; (2) low pumping rates and high river stage; (3) quasi-steady state conditions of January 1993; (4) high pumping rates and low river stage; and (5) high pumping rates and high river stage. The 1-, 5-, 10-, 100-, and 1,000-year contributing recharge areas (CRA) to each public-water-supply well field for each of the five scenarios were determined with the U.S. Geological Survey particle tracking program MODPATH.

The effect of well pumping and river stage on the total CRA of each well field in the study area is different because of (1) the unique relation of each well field to the geometry of the aquifer, the alluvial valley walls, the rivers, and other pumped wells; (2) the magnitude and spatial orientation of the hydraulic properties of the aquifer in the vicinity of each well field; and (3) the pumping rate of each well field. The ground-water flow model and the particle-tracking program results simulated these effects to determine the total CRAs of each well field.

Several conclusions can be made based on the results of particle-tracking analysis for the Missouri River alluvial aquifer in the study area:

1. The interception of ground water by pumped wells as it moved downgradient toward the Missouri River caused the long upvalley extent of some CRAs.
2. Well fields located near alluvial valley walls have total CRAs that extend from the walls because little water is available from this boundary.
3. Induced recharge caused by proximity to a major river reduces the size of the total CRA when compared to the CRAs of other wells or well fields with similar pumping rates but located farther from a major river.
4. Induced recharge from a river affects the spatial distribution of the individual CRA associated with a specific time within the total CRA for each well field.
5. The distribution of vertical anisotropy of hydraulic conductivity in the aquifer affects the relative distribution of each CRA associated with a specific time within the total CRA of each well or well field.
6. Low regional ground-water gradient in the vicinity of a well field caused by high river stage may increase the CRAs of those well fields by increasing the effect of well pumping on the potentiometric surface.
7. Movement of ground water beneath rivers because of pumped wells occurs in several locations in the study area.

REFERENCES CITED

Bevans, H.E., Skelton, John, Kenny, J.F., and Davis, J.V., 1984, Hydrology of Area 39, Western Region, Interior Coal Province, Kansas and Missouri: U.S. Geological Survey Water-Resources Investigations Report 83–851, 83 p.

Crabtree, J.D., and Older, Kathleen, 1985, Impacts of waste disposal at the Conservation Chemical Company, Kansas City, Missouri, on the regional hydrologic regime: Vicksburg, Miss., unpublished U.S. Army Corps of Engineers Waterways Experiment Station Technical Report.

Driscoll, F.G., 1986, Groundwater and wells: St. Paul, Minn., Johnson Filtration Systems Inc., 1,089 p.

Emmett, L.F., and Jeffery, H.G., 1969, Reconnaissance of the ground-water resources of the Missouri River alluvium between Kansas City, Missouri, and the Iowa border: U.S. Geological Survey Hydrologic Investigations Atlas HA–336, 1 sheet, scale 1:250,000.

———1970, Reconnaissance of the ground-water resources of the Missouri River alluvium between Miami and Kansas City, Missouri: U.S. Geological Survey Hydrologic Investigations Atlas HA–344, 1 sheet, scale 1:250,000.

Fischel, V.C., 1948, Ground-water resources of the Kansas City, Kansas area: Lawrence, Kansas Geological Survey Bulletin 71, 52 p.

Fischel, V.C., Searcy, J.K., and Rainwater, F.H., 1953, Water resources of the Kansas City area, Missouri and Kansas: U.S. Geological Survey Circular 273, 52 p.

Franke, L.O., Reilly, T.E., and Bennett, G.D., 1984, Definition of boundary and initial conditions in the analysis of saturated ground-water flow systems—An introduction: U.S. Geological Survey Open-File Report 84–458, 26 p.

Freeze, R.A., and Cherry, J.A., 1979, Groundwater: Englewood Cliffs, N.J., Prentice-Hall, 604 p.

Gann, E.E., Harvey, E.J., Barks, J.H., and Fuller, D.L., 1973, Water resources of northeastern Missouri: U.S. Geological Survey Hydrologic Investigations Atlas HA–444, 4 sheets.

Gann, E.E., Harvey, E.J., Barks, J.H., Fuller, D.L., and Miller, D.E., 1974 Water resources of west-central Missouri: U.S. Geological Survey Hydrologic Investigations Atlas HA–491, 4 sheets.

Gentile, R.J., Moberly, R.L., and Barnes, S.K., 1994, Geology along the Trans-Missouri River Tunnel, Kansas City, Missouri: Bulletin of the Association of Engineering Geologists, v. 31, no. 4, p. 483–504.

Grannemann, N.G., and Sharp, J.M., 1979, Alluvial hydrology of the lower Missouri River valley: Journal of Hydrology, v. 40, p. 85–99.

Hasan, S.E., Moberly, R.L., and Caoile, J.A., 1988, Geology of greater Kansas City, Missouri and Kansas, United States of America: Bulletin of the Association of Engineering Geologists, v. 25, no. 3, p. 277–341.

Hedman, E.R., and Jorgensen, D.G., 1990, Surface- and ground-water interaction and hydrologic budget of the Missouri River Valley aquifer between Yankton, South Dakota, and St. Louis, Missouri: U.S. Geological Survey Hydrologic Investigations Atlas HA–721, 1 sheet, scale 1:1,500,000.

Kelly, B.P., and Blevins, D.W., 1995, Vertical hydraulic conductivity of soil and potentiometric surface of the Missouri River alluvial aquifer at Kansas City, Missouri and Kansas—August 1992 and January 1993: U.S. Geological Survey Open-File Report 95–322, 19 p.

Konikow, L.F., 1978, Calibration of ground-water models, *in* Specialty Conference on Verification of Mathematical and Physical Models in Hydraulic Engineering, College Park, Md., 1978, Proceedings: American Society of Civil Engineering, p. 87–93.

McCourt, W.E., Albertson, M., and Benne, J.E., 1917, The geology of Jackson County: Rolla, Missouri Division of Geology and Land Survey, v. 14, 2nd series, 158 p.

McDonald, M.G., and Harbaugh, A.W., 1988, A modular three-dimensional finite-difference ground-water flow model: U.S. Geological Survey Techniques of Water-Resources Investigations, book 6, chap. A 1, 576 p.

Missouri Department of Natural Resources, 1991, Census of Missouri public water systems 1991: Jefferson City, Division of Environmental Quality, Public Drinking Water Program, 181 p.

Orzol, L.L., and McGrath, T.S., 1992, Modifications of the U.S. Geological Survey modular, finite-difference, ground-water flow model to read and write geographic information system files: U.S. Geological Survey Open-File Report 92–50, 201 p.

Pollock, D.W., 1994, User's guide for MODPATH/MODPATH-PLOT, version 3—A particle tracking post-processing package for MODFLOW, the U.S Geological Survey finite-difference ground-water flow model: U.S. Geological Survey Open-File Report 94–464.

Reed, H.L., Perkins, T.J., and Gray, G.L., 1995, Water resources data—Missouri water year 1994: U.S. Geological Survey Water-Data Report MO–94–1, 338 p.

Zheng, C., 1994, Analysis of particle tracking errors associated with spatial discretization: Groundwater, v. 32, no. 5, p. 821–828.

TABLES

~PAGE 77 FOLLOWS~

Table 8. Average river altitude at gaging stations in study area for each transient simulation stress period

Begin date for stress period	Average river altitude, in meters above sea level									
	Missouri River at Napoleon, Missouri	Misouri River at Sibley, Missouri	Missouri River at Hawthorne Power Plant	Missouri River at Kansas City, Missouri	Missouri River at Kansas City, Missouri, water plant	Missouri River at Nearman Power Plant	Missouri River at St. Joseph, Missouri	Kansas River at 23rd St., Kansas City, Kansas	Blue River at 12th St., Kansas City, Missouri	Little Blue River at Independence, Missouri
08-01-93	214.92	218.18	224.62	227.61	229.24	230.88	247.62	229.93	225.00	220.31
08-08-93	213.53	216.10	222.30	224.03	225.50	227.13	245.30	226.26	222.43	220.12
08-15-93	212.93	215.12	220.99	222.56	223.91	225.34	244.51	224.67	221.12	219.99
08-22-93	212.77	214.65	220.99	222.68	223.81	225.34	244.57	224.76	221.15	220.08
08-29-93	212.52	214.42	220.52	222.20	223.45	225.35	244.83	224.07	220.73	219.96
09-05-93	212.78	214.69	221.01	222.40	223.92	225.76	245.02	224.05	221.01	219.98
09-12-93	212.35	215.04	220.00	221.49	222.87	224.86	243.99	223.41	220.47	220.09
09-19-93	212.30	215.35	219.86	221.65	222.95	224.77	244.33	223.08	220.71	220.81
09-26-93	213.32	215.37	221.52	223.36	224.91	227.02	245.12	225.02	222.11	221.88
10-03-93	212.07	214.89	219.47	220.94	222.59	224.86	243.89	230.03	220.06	220.38
10-10-93	211.57	214.41	218.81	220.31	222.02	224.62	243.90	224.56	219.91	220.10
10-17-93	211.40	213.96	218.65	220.05	221.75	224.45	243.88	221.23	220.20	220.32
10-24-93	211.35	213.48	218.62	220.00	221.73	224.35	243.67	220.83	219.92	220.09
10-31-93	211.06	213.07	218.22	219.64	221.43	224.08	243.47	220.58	219.79	219.98
11-07-93	210.80	212.85	218.00	219.35	221.22	223.81	243.34	220.58	219.75	219.93
11-14-93	210.91	212.67	218.04	219.43	221.31	223.78	243.40	220.54	220.34	220.46
11-21-93	210.85	212.50	217.96	219.41	221.30	223.61	243.36	220.39	220.11	220.22
11-28-93	210.56	212.34	217.61	219.08	220.91	223.37	242.73	220.03	220.20	220.07
12-05-93	210.37	212.39	217.26	218.71	220.68	223.07	242.94	219.66	220.22	220.02

Table 8. Average river altitude at gaging stations in study area for each transient simulation stress period—Continued

Begin date for stress period	Average river altitude, in meters above sea level									
	Missouri River at Napoleon, Missouri	Missouri River at Sibley, Missouri	Missouri River at Hawthorne Power Plant	Missouri River at Kansas City, Missouri	Missouri River at Kansas City, Missouri, water plant	Missouri River at Nearman Power Plant	Missouri River at St. Joseph, Missouri	Kansas River at 23rd St., Kansas City, Kansas	Blue River at 12th St., Kansas City, Missouri	Little Blue River at Independence, Missouri
12-12-93	211.30	212.39	217.38	218.81	220.82	223.34	242.93	219.73	220.10	220.09
12-19-93	211.40	212.35	217.62	219.09	220.71	223.34	242.96	219.92	220.10	220.10
12-26-93	210.92	211.99	217.24	218.86	220.36	223.13	242.59	219.62	220.23	220.02
01-02-94	210.11	211.43	216.93	218.39	220.23	223.00	242.58	219.31	220.24	219.99
01-09-94	210.04	211.31	216.86	218.41	219.95	222.67	242.23	219.30	220.29	219.97
01-16-94	209.86	210.98	216.29	218.00	219.77	222.61	242.31	219.30	220.33	219.95
01-23-94	209.80	210.92	216.26	217.85	219.84	222.28	242.28	219.30	220.30	219.97
01-30-94	210.01	211.40	216.81	218.40	220.20	222.60	242.49	219.31	220.22	219.96
02-06-94	209.72	211.12	216.54	218.27	219.98	222.39	242.36	219.37	220.33	219.92
02-13-94	209.67	210.96	216.40	218.10	219.91	222.18	242.27	219.43	220.35	219.90
02-20-94	210.34	211.24	217.68	219.34	221.02	223.43	243.55	220.13	219.88	220.52
02-27-94	210.53	212.12	217.74	219.25	221.01	223.23	243.16	220.03	220.00	220.28
03-06-94	211.15	212.12	218.72	220.45	221.96	224.15	244.49	220.58	219.86	220.71
03-13-94	211.36	212.75	218.85	220.25	222.14	224.35	244.30	221.03	220.16	220.26
03-20-94	210.74	212.28	217.92	219.71	221.49	223.71	243.76	220.24	220.24	220.12
03-27-94	210.50	212.01	217.67	219.78	221.26	223.57	243.57	218.98	220.26	220.07

Table 9. Well pumping rates for transient stress periods 1 to 17

			Well pumping rates, in cubic meters per day, for each stress period in the transient calibration Pumping rates from stress period 08-01-93 were used for stress periods 1-6											
			1-6	7	8	9	10	11	12	13	14	15	16	17
Layer	Row	Column	08-01-93	08-08-93	08-15-93	08-22-93	08-29-93	09-05-93	09-12-93	09-19-93	09-26-93	10-03-93	10-10-93	10-17-93
2	23	391	1,607.27	1,607.27	1,607.27	1,607.27	1,481.17	1,481.17	1,481.17	1,481.17	1,481.17	1,511.25	1,511.25	1,511.25
2	23	391	1,607.27	1,607.27	1,607.27	1,607.27	1,481.17	1,481.17	1,481.17	1,481.17	1,481.17	1,511.25	1,511.25	1,511.25
2	24	391	1,607.27	1,607.27	1,607.27	1,607.27	1,481.17	1,481.17	1,481.17	1,481.17	1,481.17	1,511.25	1,511.25	1,511.25
2	25	391	1,607.27	1,607.27	1,607.27	1,607.27	1,481.17	1,481.17	1,481.17	1,481.17	1,481.17	1,511.25	1,511.25	1,511.25
2	40	437	1,822.9	1,822.9	1,822.9	1,822.9	1,822.9	1,822.9	1,822.9	1,822.9	1,822.9	1,822.9	1,822.9	1,822.9
2	41	435	1,822.9	0	0	0	0	0	1,822.9	1,822.9	1,822.9	1,822.9	1,822.9	1,822.9
2	41	437	0	1,822.9	1,822.9	1,822.9	1,822.9	1,822.9	0	0	0	0	0	0
2	74	71	272.5	272.5	272.5	272.5	272.5	272.5	272.5	272.5	272.5	272.5	272.5	272.5
2	108	169	545	545	545	545	545	545	545	545	545	545	545	545
2	109	168	545	545	545	545	545	545	545	545	545	545	545	545
2	110	168	545	545	545	545	545	545	545	545	545	545	545	545
2	110	169	545	545	545	545	545	545	545	545	545	545	545	545
2	111	169	545	545	545	545	545	545	545	545	545	545	545	545
2	131	359	698.15	698.15	698.15	698.15	698.15	698.15	698.15	698.15	698.15	698.15	698.15	698.15
3	50	381	1,892.361	1,892.361	1,892.361	1,892.361	1,892.361	1,892.361	1,892.361	1,892.361	1,892.361	1,892.361	1,892.361	1,892.361
3	50	382	1,892.361	1,892.361	1,892.361	1,892.361	1,892.361	1,892.361	1,892.361	1,892.361	1,892.361	1,892.361	1,892.361	1,892.361
3	50	382	1,892.361	1,892.361	1,892.361	1,892.361	1,892.361	1,892.361	1,892.361	1,892.361	1,892.361	1,892.361	1,892.361	1,892.361
3	60	296	2,053.4	1,875.1	2,071.75	2,139.7	1,955.13	1,757.41	1,791.3	1,653.14	1,719.3	1,931.7	1,739.84	1,655.04
3	61	296	2,053.4	1,875.1	2,071.75	2,139.7	1,955.13	1,757.41	1,791.3	1,653.14	1,719.3	1,931.7	1,739.84	1,655.04
3	61	296	2,053.4	1,875.1	2,071.75	2,139.7	1,955.13	1,757.41	1,791.3	1,653.14	1,719.3	1,931.7	1,739.84	1,655.04
3	62	296	2,053.4	1,875.1	2,071.75	2,139.7	1,955.13	1,757.41	1,791.3	1,653.14	1,719.3	1,931.7	1,739.84	1,655.04
3	63	296	2,053.4	1,875.1	2,071.75	2,139.7	1,955.13	1,757.41	1,791.3	1,653.14	1,719.3	1,931.7	1,739.84	1,655.04
3	64	296	2,053.4	1,875.1	2,071.75	2,139.7	1,955.13	1,757.41	1,791.3	1,653.14	1,719.3	1,931.7	1,739.84	1,655.04
3	66	337	567.7	567.7	567.7	567.7	567.7	567.7	567.7	567.7	567.7	567.7	567.7	567.7

Table 9. Well pumping rates for transient stress periods 1 to 17—Continued

			Well pumping rates, in cubic meters per day, for each stress period in the transient calibration. Pumping rates from stress period 08-01-93 were used for stress periods 1-6											
			1-6	7	8	9	10	11	12	13	14	15	16	17
Layer	Row	Column	08-01-93	08-08-93	08-15-93	08-22-93	08-29-93	09-05-93	09-12-93	09-19-93	09-26-93	10-03-93	10-10-93	10-17-93
3	66	337	567.7	567.7	567.7	567.7	567.7	567.7	567.7	567.7	567.7	567.7	567.7	567.7
3	69	120	0	2,183.13	2,454.98	2,769.13	1,715.42	2,173.54	2,088.24	2,011.73	2,106.22	2,242.61	2,074.72	2,172.05
3	69	120	0	2,183.13	2,454.98	2,769.13	1,715.42	2,173.54	2,088.24	2,011.73	2,106.22	2,242.61	2,074.72	2,172.05
3	69	121	0	2,183.13	2,454.98	2,769.13	1,715.42	2,173.54	2,088.24	2,011.73	2,106.22	2,242.61	2,074.72	2,172.05
3	69	122	0	2,183.13	2,454.98	2769.13	1,715.42	2,173.54	2,088.24	2,011.73	2,106.22	2,242.61	2,074.72	2,172.05
3	85	294	2,941.03	3,051.67	3,279.36	3,122.03	3,035.71	2,868.62	2,805.75	2,656.63	2,739.82	2,863.98	2,738.67	2,655.99
3	85	296	2,941.03	3,051.67	3,279.36	3,122.03	3,035.71	2,868.62	2,805.75	2,656.63	2,739.82	2,863.98	2,738.67	2,655.99
3	85	298	2,941.03	3,051.67	3,279.36	3,122.03	3,035.71	2,868.62	2,805.75	2,656.63	2,739.82	2,863.98	2,738.67	2,655.99
3	86	165	136.25	136.25	136.25	136.25	136.25	136.25	136.25	136.25	136.25	136.25	136.25	136.25
3	87	171	1,994.7	2,062.83	2,270.24	2,180.92	1,906.13	1,834.97	1,769.87	1,663.13	1,714.61	1,873.58	1,673.73	1,627.55
3	87	171	1,994.7	2,062.83	2,270.24	2,180.92	1,906.13	1,834.97	1,769.87	1,663.13	1,714.61	1,873.58	1,673.73	1,627.55
3	87	294	2,941.03	3,051.67	3,279.36	3,122.03	3,035.71	2,868.62	2,805.75	2,656.63	2,739.82	2,863.98	2,738.67	2,655.99
3	89	293	2,941.03	3,051.67	3,279.36	3,122.03	3,035.71	2,868.62	2,805.75	2,656.63	2,739.82	2,863.98	2,738.67	2,655.99
3	101	162	545	545	545	545	545	545	545	545	545	545	545	545
3	101	276	408.75	408.75	408.75	408.75	408.75	408.75	408.75	408.75	408.75	408.75	408.75	408.75
3	102	169	136.25	136.25	136.25	136.25	136.25	136.25	136.25	136.25	136.25	136.25	136.25	136.25
3	102	175	1,635	1,635	1,635	1,635	1,635	1,635	1635	1,635	1,635	1,635	1,635	1,635
3	104	166	1,090	1,090	1,090	1,090	1,090	1,090	1,090	1,090	1,090	1,090	1,090	1,090
3	109	171	545	545	545	545	545	545	545	545	545	545	545	545
3	109	269	545	545	545	545	545	545	545	545	545	545	545	545
3	110	170	545	545	545	545	545	545	545	545	545	545	545	545
3	114	245	272.5	272.5	272.5	272.5	272.5	272.5	272.5	272.5	272.5	272.5	272.5	272.5
3	115	188	1,090	1,090	1,090	1,090	1,090	1,090	1,090	1,090	1,090	1,090	1,090	1,090
3	115	189	1,090	1,090	1,090	1,090	1,090	1,090	1,090	1,090	1,090	1,090	1,090	1,090
3	130	368	839.19	839.19	839.19	839.19	839.19	839.19	839.19	839.19	839.19	839.19	839.19	839.19

Table 9. Well pumping rates for transient stress periods 1 to 17—Continued

			Well pumping rates, in cubic meters per day, for each stress period in the transient calibration. Pumping rates from stress period 08-01-93 were used for stress periods 1-6											
			1-6	7	8	9	10	11	12	13	14	15	16	17
Layer	Row	Column	08-01-93	08-08-93	08-15-93	08-22-93	08-29-93	09-05-93	09-12-93	09-19-93	09-26-93	10-03-93	10-10-93	10-17-93
3	130	372	194.29	194.29	194.29	194.29	194.29	194.29	194.29	194.29	194.29	194.29	194.29	194.29
3	131	362	54.17	54.17	54.17	54.17	54.17	54.17	54.17	54.17	54.17	54.17	54.17	54.17
3	131	367	78.86	78.86	78.86	78.86	78.86	78.86	78.86	78.86	78.86	78.86	78.86	78.86
3	133	365	690.35	690.35	690.35	690.35	690.35	690.35	690.35	690.35	690.35	690.35	690.35	690.35
3	134	356	586.91	586.91	586.91	586.91	586.91	586.91	586.91	586.91	586.91	586.91	586.91	586.91
3	135	360	70.14	70.14	70.14	70.14	70.14	70.14	70.14	70.14	70.14	70.14	70.14	70.14
3	137	365	418.45	418.45	418.45	418.45	418.45	418.45	418.45	418.45	418.45	418.45	418.45	418.45
3	137	369	575.36	575.36	575.36	575.36	575.36	575.36	575.36	575.36	575.36	575.36	575.36	575.36
4	86	289	2,941.03	3,051.67	3,279.36	3,122.03	3,035.71	2,868.62	2,805.75	2,656.63	2,739.82	2,863.98	2,738.67	2,655.99
4	86	289	2,941.03	3,051.67	3,279.36	3,122.03	3,035.71	2,868.62	2,805.75	2,656.63	2,739.82	2,863.98	2,738.67	2,655.99
4	87	288	2,941.03	3,051.67	3,279.36	3,122.03	3,035.71	2,868.62	2,805.75	2,656.63	2,739.82	2,863.98	2,738.67	2,655.99
4	87	288	2,941.03	3,051.67	3,279.36	3,122.03	3,035.71	2,868.62	2,805.75	2,656.63	2,739.82	2,863.98	2,738.67	2,655.99
4	87	289	2,941.03	3,051.67	3,279.36	3,122.03	3,035.71	2,868.62	2,805.75	2,656.63	2,739.82	2,863.98	2,738.67	2,655.99
4	87	289	2,941.03	3,051.67	3,279.36	3,122.03	3,035.71	2,868.62	2,805.75	2,656.63	2,739.82	2,863.98	2,738.67	2,655.99
4	88	172	1,994.7	2,062.83	2,270.24	2,180.92	1,906.13	1,834.97	1,769.87	1,663.13	1,714.61	1,873.58	1,673.73	1,627.55
4	88	172	1,994.7	2,062.83	2,270.24	2,180.92	1,906.13	1,834.97	1,769.87	1,663.13	1,714.61	1,873.58	1,673.73	1,627.55
4	88	172	1,994.7	2,062.83	2,270.24	2,180.92	1,906.13	1,834.97	1,769.87	1,663.13	1,714.61	1,873.58	1,673.73	1,627.55
4	88	285	2,941.03	3,051.67	3,279.36	3,122.03	3,035.71	2,868.62	2,805.75	2,656.63	2,739.82	2,863.98	2,738.67	2,655.99
4	88	286	2,941.03	3,051.67	3,279.36	3,122.03	3,035.71	2,868.62	2,805.75	2,656.63	2,739.82	2,863.98	2,738.67	2,655.99
4	88	286	2,941.03	3,051.67	3,279.36	3,122.03	3,035.71	2,868.62	2,805.75	2,656.63	2,739.82	2,863.98	2,738.67	2,655.99
4	88	287	2,941.03	3,051.67	3,279.36	3,122.03	3,035.71	2,868.62	2,805.75	2,656.63	2,739.82	2,863.98	2,738.67	2,655.99
4	88	288	2,941.03	3,051.67	3,279.36	3,122.03	3,035.71	2,868.62	2,805.75	2,656.63	2,739.82	2,863.98	2,738.67	2,655.99
4	88	288	2,941.03	3,051.67	3,279.36	3,122.03	3,035.71	2,868.62	2,805.75	2,656.63	2,739.82	2,863.98	2,738.67	2,655.99
4	88	289	2,941.03	3,051.67	3,279.36	3,122.03	3,035.71	2,868.62	2,805.75	2,656.63	2,739.82	2,863.98	2,738.67	2,655.99
4	88	289	2,941.03	3,051.67	3,279.36	3,122.03	3,035.71	2,868.62	2,805.75	2,656.63	2,739.82	2,863.98	2,738.67	2,655.99

Table 9. Well pumping rates for transient stress periods 1 to 17—Continued

			Well pumping rates, in cubic meters per day, for each stress period in the transient calibration. Pumping rates from stress period 08-01-93 were used for stress periods 1-6											
			1-6	7	8	9	10	11	12	13	14	15	16	17
Layer	Row	Column	08-01-93	08-08-93	08-15-93	08-22-93	08-29-93	09-05-93	09-12-93	09-19-93	09-26-93	10-03-93	10-10-93	10-17-93
4	88	289	2,941.03	3,051.67	3,279.36	3,122.03	3,035.71	2,868.62	2,805.75	2,656.63	2,739.82	2,863.98	2,738.67	2,655.99
4	88	290	2,941.03	3,051.67	3,279.36	3,122.03	3,035.71	2,868.62	2,805.75	2,656.63	2,739.82	2,863.98	2,738.67	2,655.99
4	89	284	2,941.03	3,051.67	3,279.36	3,122.03	3,035.71	2,868.62	2,805.75	2,656.63	2,739.82	2,863.98	2,738.67	2,655.99
4	89	286	2,941.03	3,051.67	3,279.36	3,122.03	3,035.71	2,868.62	2,805.75	2,656.63	2,739.82	2,863.98	2,738.67	2,655.99
4	89	286	2,941.03	3,051.67	3,279.36	3,122.03	3,035.71	2,868.62	2,805.75	2,656.63	2,739.82	2,863.98	2,738.67	2,655.99
4	89	287	2,941.03	3,051.67	3,279.36	3,122.03	3,035.71	2,868.62	2,805.75	2,656.63	2,739.82	2,863.98	2,738.67	2,655.99
4	89	291	2,941.03	3,051.67	3,279.36	3,122.03	3,035.71	2,868.62	2,805.75	2,656.63	2,739.82	2,863.98	2,738.67	2,655.99
4	90	176	0	4,545.44	6,926.55	6,042.24	7,521.83	10,198.85	7,683.55	0	0	0	0	0
4	90	176	0	4,545.44	6,926.55	6,042.24	7,521.83	10,198.85	7,683.55	0	0	0	0	0
4	90	180	0	4,545.44	6,926.55	6,042.24	7,521.83	10,198.85	7,683.55	0	0	0	0	0
4	90	286	2,941.03	3,051.67	3,279.36	3,122.03	3,035.71	2,868.62	2,805.75	2,656.63	2,739.82	2,863.98	2,738.67	2,655.99
4	90	286	2,941.03	3,051.67	3,279.36	3,122.03	3,035.71	2,868.62	2,805.75	2,656.63	2,739.82	2,863.98	2,738.67	2,655.99
4	90	287	2,941.03	3,051.67	3,279.36	3,122.03	3,035.71	2,868.62	2,805.75	2,656.63	2,739.82	2,863.98	2,738.67	2,655.99
4	91	180	0	4,545.44	6,926.55	6,042.24	7,521.83	10,198.85	7,683.55	0	0	0	0	0
4	91	285	2,941.03	3,051.67	3,279.36	3,122.03	3,035.71	2,868.62	2,805.75	2,656.63	2,739.82	2,863.98	2,738.67	2,655.99
4	91	285	2,941.03	3,051.67	3,279.36	3,122.03	3,035.71	2,868.62	2,805.75	2,656.63	2,739.82	2,863.98	2,738.67	2,655.99
4	91	285	2,941.03	3,051.67	3,279.36	3,122.03	3,035.71	2,868.62	2,805.75	2,656.63	2,739.82	2,863.98	2,738.67	2,655.99
4	92	178	0	4,545.44	6,926.55	6,042.24	7,521.83	10,198.85	7,683.55	0	0	0	0	0
4	92	178	0	4,545.44	6,926.55	6,042.24	7,521.83	10,198.85	7,683.55	0	0	0	0	0
4	92	178	0	4,545.44	6,926.55	6,042.24	7,521.83	10,198.85	7,683.55	0	0	0	0	0
4	93	179	0	4,545.44	6,926.55	6,042.24	7,521.83	10,198.85	7,683.55	0	0	0	0	0
4	93	179	0	4,545.44	6,926.55	6,042.24	7,521.83	10,198.85	7,683.55	0	0	0	0	0
4	93	179	0	4,545.44	6,926.55	6,042.24	7,521.83	10,198.85	7,683.55	0	0	0	0	0
4	94	179	0	4,545.44	6,926.55	6,042.24	7,521.83	10,198.85	7,683.55	0	0	0	0	0
4	95	165	545	545	545	545	545	545	545	545	545	545	545	545

Table 9. Well pumping rates for transient stress periods 1 to 17—Continued

			Well pumping rates, in cubic meters per day, for each stress period in the transient calibration Pumping rates from stress period 08-01-93 were used for stress periods 1-6											
			1-6	7	8	9	10	11	12	13	14	15	16	17
Layer	Row	Column	08-01-93	08-08-93	08-15-93	08-22-93	08-29-93	09-05-93	09-12-93	09-19-93	09-26-93	10-03-93	10-10-93	10-17-93
4	98	163	545	545	545	545	545	545	545	545	545	545	545	545
4	99	166	272.5	272.5	272.5	272.5	272.5	272.5	272.5	272.5	272.5	272.5	272.5	272.5
4	99	183	545	545	545	545	545	545	545	545	545	545	545	545
4	100	162	1,362.5	1,362.5	1,362.5	1,362.5	1,362.5	1,362.5	1,362.5	1,362.5	1,362.5	1,362.5	1,362.5	1,362.5
4	101	163	545	545	545	545	545	545	545	545	545	545	545	545
4	101	196	272.5	272.5	272.5	272.5	272.5	272.5	272.5	272.5	272.5	272.5	272.5	272.5
4	102	182	3,698.03	3,636.25	3687	3,594.26	3,463.14	3,095.18	3,278.63	3,193.19	3,295.39	3,421.38	3,126	3,229.15
4	103	182	3,698.03	3,636.25	3687	3,594.26	3,463.14	3,095.18	3,278.63	3,193.19	3,295.39	3,421.38	3,126	3,229.15
4	103	182	3,698.03	3,636.25	3687	3,594.26	3,463.14	3,095.18	3,278.63	3,193.19	3,295.39	3,421.38	3,126	3,229.15
4	104	182	3,698.03	3,636.25	3,687	3,594.26	3,463.14	3,095.18	3,278.63	3,193.19	3,295.39	3,421.38	3,126	3,229.15
4	106	188	136.25	136.25	136.25	136.25	136.25	136.25	136.25	136.25	136.25	136.25	136.25	136.25
4	108	183	136.25	136.25	136.25	136.25	136.25	136.25	136.25	136.25	136.25	136.25	136.25	136.25
4	108	195	327	327	327	327	327	327	327	327	327	327	327	327
4	109	195	1,635	1,635	1,635	1,635	1,635	1,635	1,635	1,635	1,635	1,635	1,635	1,635
4	112	188	1,090	1,090	1,090	1,090	1,090	1,090	1,090	1,090	1,090	1,090	1,090	1,090
4	113	188	1,090	1,090	1,090	1,090	1,090	1,090	1,090	1,090	1,090	1,090	1,090	1,090
4	113	188	1,090	1,090	1,090	1,090	1,090	1,090	1,090	1,090	1,090	1,090	1,090	1,090
4	114	188	1,090	1,090	1,090	1,090	1,090	1,090	1,090	1,090	1,090	1,090	1,090	1,090
4	114	188	1,090	1,090	1,090	1,090	1,090	1,090	1,090	1,090	1,090	1,090	1,090	1,090
4	115	186	1,090	1,090	1,090	1,090	1,090	1,090	1,090	1,090	1,090	1,090	1,090	1,090
4	116	184	1,090	1,090	1,090	1,090	1,090	1,090	1,090	1,090	1,090	1,090	1,090	1,090

Table 10. Well pumping rates for transient stress periods 18 to 29

			Well pumping rates, in cubic meters per day, for each stress period in the transient calibration											
			18	19	20	21	22	23	24	25	26	27	28	29
Layer	Row	Column	10-24-93	10-31-93	11-07-93	11-14-93	11-21-93	11-28-93	12-05-93	12-12-93	12-19-93	12-26-93	01-02-94	01-09-94
2	23	391	1,511.25	1,458.8	1,458.8	1,458.8	1,458.8	1,371.76	1,371.76	1,371.76	1,371.76	1,371.76	1,527.43	1,527.43
2	23	391	1,511.25	1,458.8	1,458.8	1,458.8	1,458.8	1,371.76	1,371.76	1,371.76	1,371.76	1,371.76	1,527.43	1,527.43
2	24	391	1,511.25	1,458.8	1,458.8	1,458.8	1,458.8	1,371.76	1,371.76	1,371.76	1,371.76	1,371.76	1,527.43	1,527.43
2	25	391	1,511.25	1,458.8	1,458.8	1,458.8	1,458.8	1,371.76	1,371.76	1,371.76	1,371.76	1,371.76	1,527.43	1,527.43
2	40	437	1,822.9	1,822.9	1,822.9	1,822.9	1,822.9	1,822.9	1,822.9	0	0	0	0	0
2	40	437	0	0	0	0	0	0	0	1,822.9	1,822.9	1,822.9	1,822.9	1,822.9
2	41	435	1,822.9	1,822.9	1,822.9	1,822.9	1,822.9	1,822.9	1,822.9	0	0	0	0	0
2	41	437	0	0	0	0	0	0	0	1,822.9	1,822.9	1,822.9	1,822.9	1,822.9
2	74	71	272.5	272.5	272.5	272.5	272.5	272.5	272.5	272.5	272.5	272.5	272.5	272.5
2	108	169	545	545	545	545	545	545	545	545	545	545	545	545
2	109	168	545	545	545	545	545	545	545	545	545	545	545	545
2	110	168	545	545	545	545	545	545	545	545	545	545	545	545
2	110	169	545	545	545	545	545	545	545	545	545	545	545	545
2	111	169	545	545	545	545	545	545	545	545	545	545	545	545
2	131	359	698.15	698.15	698.15	698.15	698.15	698.15	698.15	698.15	698.15	698.15	698.15	698.15
3	50	381	1,892.361	1,892.361	1,892.361	1,892.361	1,892.361	1,892.361	1,892.361	1,892.361	1,892.361	1,892.361	1,892.361	1,892.361
3	50	382	1,892.361	1,892.361	1,892.361	1,892.361	1,892.361	1,892.361	1,892.361	1,892.361	1,892.361	1,892.361	1,892.361	1,892.361
3	50	382	1,892.361	1,892.361	1,892.361	1,892.361	1,892.361	1,892.361	1,892.361	1,892.361	1,892.361	1,892.361	1,892.361	1,892.361
3	60	296	1,698.56	1,597.27	1,668.2	1,544.64	1,514.81	1,323.94	1,529.77	1,733.53	1,674.05	1,709.74	1,801.75	1,797.88
3	61	296	1,698.56	1,597.27	1,668.2	1,544.64	1,514.81	1,323.94	1,529.77	1,733.53	1,674.05	1,709.74	1,801.75	1,797.88
3	61	296	1,698.56	1,597.27	1,668.2	1,544.64	1,514.81	1,323.94	1,529.77	1,733.53	1,674.05	1,709.74	1,801.75	1,797.88
3	62	296	1,698.56	1,597.27	1,668.2	1,544.64	1,514.81	1,323.94	1,529.77	1,733.53	1,674.05	1,709.74	1,801.75	1,797.88
3	63	296	1,698.56	1,597.27	1,668.2	1,544.64	1,514.81	1,323.94	1,529.77	1,733.53	1,674.05	1,709.74	1,801.75	1,797.88
3	64	296	1,698.56	1,597.27	1,668.2	1,544.64	1,514.81	1,323.94	1,529.77	1,733.53	1,674.05	1,709.74	1,801.75	1,797.88
3	66	337	567.7	567.7	567.7	567.7	567.7	567.7	567.7	567.7	567.7	567.7	567.7	567.7
3	66	337	567.7	567.7	567.7	567.7	567.7	567.7	567.7	567.7	567.7	567.7	567.7	567.7

Table 10. Well pumping rates for transient stress periods 18 to 29—Continued

			Well pumping rates, in cubic meters per day, for each stress period in the transient calibration											
			18	19	20	21	22	23	24	25	26	27	28	29
Layer	Row	Column	10-24-93	10-31-93	11-07-93	11-14-93	11-21-93	11-28-93	12-05-93	12-12-93	12-19-93	12-26-93	01-02-94	01-09-94
3	69	120	2,090.54	1,966.85	1,916.29	1,823.56	1,886.96	1,833.56	1,966.98	1,970.5	1,932.65	1,976.45	1,638.36	1,583.75
3	69	120	2,090.54	1,966.85	1,916.29	1,823.56	1,886.96	1,833.56	1,966.98	1,970.5	1,932.65	1,976.45	1,638.36	1,583.75
3	69	121	2,090.54	1,966.85	1,916.29	1,823.56	1,886.96	1,833.56	1,966.98	1,970.5	1,932.65	1,976.45	1,638.36	1,583.75
3	69	122	2,090.54	1,966.85	1,916.29	1,823.56	1,886.96	1,833.56	1,966.98	1,970.5	1,932.65	1,976.45	1,638.36	1,583.75
3	85	294	2,743.8	2,646.09	2,706.87	2,671.15	2,837.74	2,772.7	2,854.68	2,771.5	2,751.99	2,887.62	2,859.47	2,828.73
3	85	296	2,743.8	2,646.09	2,706.87	2,671.15	2,837.74	2,772.7	2,854.68	2,771.5	2,751.99	2,887.62	2,859.47	2,828.73
3	85	298	2,743.8	2,646.09	2,706.87	2,671.15	2,837.74	2,772.7	2,854.68	2,771.5	2,751.99	2,887.62	2,859.47	2,828.73
3	86	165	136.25	136.25	136.25	136.25	136.25	136.25	136.25	136.25	136.25	136.25	136.25	136.25
3	87	171	1,763.05	1,675.24	1,673.73	1,600.3	1,675.24	1,608.63	1,609.38	1,629.82	1,691.9	1,735.8	1,669.19	1,669.94
3	87	171	1,763.05	1,675.24	1,673.73	1,600.3	1,675.24	1,608.63	1,609.38	1,629.82	1,691.9	1,735.8	1,669.19	1,669.94
3	87	294	2,743.8	2,646.09	2,706.87	2,671.15	2,837.74	2,772.7	2,854.68	2,771.5	2,751.99	2,887.62	2,859.47	2,828.73
3	89	293	2,743.8	2,646.09	2,706.87	2,671.15	2,837.74	2,772.7	2,854.68	2,771.5	2,751.99	2,887.62	2,859.47	2,828.73
3	101	162	545	545	545	545	545	545	545	545	545	545	545	545
3	101	276	408.75	408.75	408.75	408.75	408.75	408.75	408.75	408.75	408.75	408.75	408.75	408.75
3	102	169	136.25	136.25	136.25	136.25	136.25	136.25	136.25	136.25	136.25	136.25	136.25	136.25
3	102	175	1,635	1,635	1,635	1,635	1,635	1,635	1,635	1,635	1,635	1,635	1,635	1,635
3	104	166	1,090	1,090	1,090	1,090	1,090	1,090	1,090	1,090	1,090	1,090	1,090	1,090
3	109	171	545	545	545	545	545	545	545	545	545	545	545	545
3	109	269	545	545	545	545	545	545	545	545	545	545	545	545
3	110	170	545	545	545	545	545	545	545	545	545	545	545	545
3	114	245	272.5	272.5	272.5	272.5	272.5	272.5	272.5	272.5	272.5	272.5	272.5	272.5
3	115	188	1,090	1,090	1,090	1,090	1,090	1,090	1,090	1,090	1,090	1,090	1,090	1,090
3	115	189	1,090	1,090	1,090	1,090	1,090	1,090	1,090	1,090	1,090	1,090	1,090	1,090
3	130	368	839.19	839.19	839.19	839.19	839.19	839.19	839.19	839.19	839.19	839.19	839.19	839.19
3	130	372	194.29	194.29	194.29	194.29	194.29	194.29	194.29	194.29	194.29	194.29	194.29	194.29
3	131	362	54.17	54.17	54.17	54.17	54.17	54.17	54.17	54.17	54.17	54.17	54.17	54.17

Table 10. Well pumping rates for transient stress periods 18 to 29—Continued

			Well pumping rates, in cubic meters per day, for each stress period in the transient calibration											
			18	19	20	21	22	23	24	25	26	27	28	29
Layer	Row	Column	10-24-93	10-31-93	11-07-93	11-14-93	11-21-93	11-28-93	12-05-93	12-12-93	12-19-93	12-26-93	01-02-94	01-09-94
3	131	367	78.86	78.86	78.86	78.86	78.86	78.86	78.86	78.86	78.86	78.86	78.86	78.86
3	133	365	690.35	690.35	690.35	690.35	690.35	690.35	690.35	690.35	690.35	690.35	690.35	690.35
3	134	356	586.91	586.91	586.91	586.91	586.91	586.91	586.91	586.91	586.91	586.91	586.91	586.91
3	135	360	70.14	70.14	70.14	70.14	70.14	70.14	70.14	70.14	70.14	70.14	70.14	70.14
3	137	365	418.45	418.45	418.45	418.45	418.45	418.45	418.45	418.45	418.45	418.45	418.45	418.45
3	137	369	575.36	575.36	575.36	575.36	575.36	575.36	575.36	575.36	575.36	575.36	575.36	575.36
4	86	289	2,743.8	2,646.09	2,706.87	2,671.15	2,837.74	2,772.7	2,854.68	2,771.5	2,751.99	2,887.62	2,859.47	2,828.73
4	86	289	2,743.8	2,646.09	2,706.87	2,671.15	2,837.74	2,772.7	2,854.68	2,771.5	2,751.99	2,887.62	2,859.47	2,828.73
4	87	288	2,743.8	2,646.09	2,706.87	2,671.15	2,837.74	2,772.7	2,854.68	2,771.5	2,751.99	2,887.62	2,859.47	2,828.73
4	87	288	2,743.8	2,646.09	2,706.87	2,671.15	2,837.74	2,772.7	2,854.68	2,771.5	2,751.99	2,887.62	2,859.47	2,828.73
4	87	289	2,743.8	2,646.09	2,706.87	2,671.15	2,837.74	2,772.7	2,854.68	2,771.5	2,751.99	2,887.62	2,859.47	2,828.73
4	87	289	2,743.8	2,646.09	2,706.87	2,671.15	2,837.74	2,772.7	2,854.68	2,771.5	2,751.99	2,887.62	2,859.47	2,828.73
4	88	172	1,763.05	1,675.24	1,673.73	1,600.3	1,675.24	1,608.63	1,609.38	1,629.82	1,691.9	1,735.8	1,669.19	1,669.94
4	88	172	1,763.05	1,675.24	1,673.73	1,600.3	1,675.24	1,608.63	1,609.38	1,629.82	1,691.9	1,735.8	1,669.19	1,669.94
4	88	172	1,763.05	1,675.24	1,673.73	1,600.3	1,675.24	1,608.63	1,609.38	1,629.82	1,691.9	1,735.8	1,669.19	1,669.94
4	88	285	2,743.8	2,646.09	2,706.87	2,671.15	2,837.74	2,772.7	2,854.68	2,771.5	2,751.99	2,887.62	2,859.47	2,828.73
4	88	286	2,743.8	2,646.09	2,706.87	2,671.15	2,837.74	2,772.7	2,854.68	2,771.5	2,751.99	2,887.62	2,859.47	2,828.73
4	88	286	2,743.8	2,646.09	2,706.87	2,671.15	2,837.74	2,772.7	2,854.68	2,771.5	2,751.99	2,887.62	2,859.47	2,828.73
4	88	287	2,743.8	2,646.09	2,706.87	2,671.15	2,837.74	2,772.7	2,854.68	2,771.5	2,751.99	2,887.62	2,859.47	2,828.73
4	88	288	2,743.8	2,646.09	2,706.87	2,671.15	2,837.74	2,772.7	2,854.68	2,771.5	2,751.99	2,887.62	2,859.47	2,828.73
4	88	288	2,743.8	2,646.09	2,706.87	2,671.15	2,837.74	2,772.7	2,854.68	2,771.5	2,751.99	2,887.62	2,859.47	2,828.73
4	88	289	2,743.8	2,646.09	2,706.87	2,671.15	2,837.74	2,772.7	2,854.68	2,771.5	2,751.99	2,887.62	2,859.47	2,828.73
4	88	289	2,743.8	2,646.09	2,706.87	2,671.15	2,837.74	2,772.7	2,854.68	2,771.5	2,751.99	2,887.62	2,859.47	2,828.73
4	88	289	2,743.8	2,646.09	2,706.87	2,671.15	2,837.74	2,772.7	2,854.68	2,771.5	2,751.99	2,887.62	2,859.47	2,828.73
4	88	290	2,743.8	2,646.09	2,706.87	2,671.15	2,837.74	2,772.7	2,854.68	2,771.5	2,751.99	2,887.62	2,859.47	2,828.73
4	89	284	2,743.8	2,646.09	2,706.87	2,671.15	2,837.74	2,772.7	2,854.68	2,771.5	2,751.99	2,887.62	2,859.47	2,828.73

Table 10. Well pumping rates for transient stress periods 18 to 29—Continued

			Well pumping rates, in cubic meters per day, for each stress period in the transient calibration											
			18	19	20	21	22	23	24	25	26	27	28	29
Layer	Row	Column	10-24-93	10-31-93	11-07-93	11-14-93	11-21-93	11-28-93	12-05-93	12-12-93	12-19-93	12-26-93	01-02-94	01-09-94
4	89	286	2,743.8	2,646.09	2,706.87	2,671.15	2,837.74	2,772.7	2,854.68	2,771.5	2,751.99	2,887.62	2,859.47	2,828.73
4	89	286	2,743.8	2,646.09	2,706.87	2,671.15	2,837.74	2,772.7	2,854.68	2,771.5	2,751.99	2,887.62	2,859.47	2,828.73
4	89	287	2,743.8	2,646.09	2,706.87	2,671.15	2,837.74	2,772.7	2,854.68	2,771.5	2,751.99	2,887.62	2,859.47	2,828.73
4	89	291	2,743.8	2,646.09	2,706.87	2,671.15	2,837.74	2,772.7	2,854.68	2,771.5	2,751.99	2,887.62	2,859.47	2,828.73
4	90	176	0	0	0	0	244.3	5,880.51	4,875.77	4,600.5	6,155.79	8,602.27	8,856.9	9,724.01
4	90	176	0	0	0	0	244.3	5,880.51	4,875.77	4,600.5	6,155.79	8,602.27	8,856.9	9,724.01
4	90	180	0	0	0	0	244.3	5,880.51	4,875.77	4,600.5	6,155.79	8,602.27	8,856.9	9,724.01
4	90	286	2,743.8	2,646.09	2,706.87	2,671.15	2,837.74	2,772.7	2,854.68	2,771.5	2,751.99	2,887.62	2,859.47	2,828.73
4	90	286	2,743.8	2,646.09	2,706.87	2,671.15	2,837.74	2,772.7	2,854.68	2,771.5	2,751.99	2,887.62	2,859.47	2,828.73
4	90	287	2,743.8	2,646.09	2,706.87	2,671.15	2,837.74	2,772.7	2,854.68	2,771.5	2,751.99	2,887.62	2,859.47	2,828.73
4	91	180	0	0	0	0	244.3	5,880.51	4,875.77	4,600.5	6,155.79	8,602.27	8,856.9	9,724.01
4	91	285	2,743.8	2,646.09	2,706.87	2,671.15	2,837.74	2,772.7	2,854.68	2,771.5	2,751.99	2,887.62	2,859.47	2,828.73
4	91	285	2,743.8	2,646.09	2,706.87	2,671.15	2,837.74	2,772.7	2,854.68	2,771.5	2,751.99	2,887.62	2,859.47	2,828.73
4	91	285	2,743.8	2,646.09	2,706.87	2,671.15	2,837.74	2,772.7	2,854.68	2,771.5	2,751.99	2,887.62	2,859.47	2,828.73
4	92	178	0	0	0	0	244.3	5,880.51	4,875.77	4,600.5	6,155.79	8,602.27	8,856.9	9,724.01
4	92	178	0	0	0	0	244.3	5,880.51	4,875.77	4,600.5	6,155.79	8,602.27	8,856.9	9,724.01
4	92	178	0	0	0	0	244.3	5,880.51	4,875.77	4,600.5	6,155.79	8,602.27	8,856.9	9,724.01
4	93	179	0	0	0	0	244.3	5,880.51	4,875.77	4,600.5	6,155.79	8,602.27	8,856.9	9,724.01
4	93	179	0	0	0	0	244.3	5,880.51	4,875.77	4,600.5	6,155.79	8,602.27	8,856.9	9,724.01
4	93	179	0	0	0	0	244.3	5,880.51	4,875.77	4,600.5	6,155.79	8,602.27	8,856.9	9,724.01
4	94	179	0	0	0	0	244.3	5,880.51	4,875.77	4,600.5	6,155.79	8,602.27	8,856.9	9,724.01
4	95	165	545	545	545	545	545	545	545	545	545	545	545	545
4	98	163	545	545	545	545	545	545	545	545	545	545	545	545
4	99	166	272.5	272.5	272.5	272.5	272.5	272.5	272.5	272.5	272.5	272.5	272.5	272.5
4	99	183	545	545	545	545	545	545	545	545	545	545	545	545
4	100	162	1,362.5	1,362.5	1,362.5	1,362.5	1,362.5	1,362.5	1,362.5	1,362.5	1,362.5	1,362.5	1,362.5	1,362.5

Table 10. Well pumping rates for transient stress periods 18 to 29—Continued

			Well pumping rates, in cubic meters per day, for each stress period in the transient calibration											
			18	19	20	21	22	23	24	25	26	27	28	29
Layer	Row	Column	10-24-93	10-31-93	11-07-93	11-14-93	11-21-93	11-28-93	12-05-93	12-12-93	12-19-93	12-26-93	01-02-94	01-09-94
4	101	163	545	545	545	545	545	545	545	545	545	545	545	545
4	101	196	272.5	272.5	272.5	272.5	272.5	272.5	272.5	272.5	272.5	272.5	272.5	272.5
4	102	182	3,304.04	3,394.48	3,245.91	3,248.34	3,121	3,377.3	3,408.94	3,116.28	2,879.3	3,026.65	3,137.63	3,379.2
4	103	182	3,304.04	3,394.48	3,245.91	3,248.34	3,121	3,377.3	3,408.94	3,116.28	2,879.3	3,026.65	3,137.63	3,379.2
4	103	182	3,304.04	3,394.48	3,245.91	3,248.34	3,121	3,377.3	3,408.94	3,116.28	2,879.3	3,026.65	3,137.63	3,379.2
4	104	182	3,304.04	3,394.48	3,245.91	3,248.34	3,121	3,377.3	3408.94	3,116.28	2,879.3	3,026.65	3,137.63	3,379.2
4	106	188	136.25	136.25	136.25	136.25	136.25	136.25	136.25	136.25	136.25	136.25	136.25	136.25
4	108	183	136.25	136.25	136.25	136.25	136.25	136.25	136.25	136.25	136.25	136.25	136.25	136.25
4	108	195	327	327	327	327	327	327	327	327	327	327	327	327
4	109	195	1,635	1,635	1,635	1,635	1,635	1,635	1,635	1,635	1,635	1,635	1,635	1,635
4	112	188	1,090	1,090	1,090	1,090	1,090	1,090	1,090	1,090	1,090	1,090	1,090	1,090
4	113	188	1,090	1,090	1,090	1,090	1,090	1,090	1,090	1,090	1,090	1,090	1,090	1,090
4	113	188	1,090	1,090	1,090	1,090	1,090	1,090	1,090	1,090	1,090	1,090	1,090	1,090
4	114	188	1,090	1,090	1,090	1,090	1,090	1,090	1,090	1,090	1,090	1,090	1,090	1,090
4	114	188	1,090	1,090	1,090	1,090	1,090	1,090	1,090	1,090	1,090	1,090	1,090	1,090
4	115	186	1,090	1,090	1,090	1,090	1,090	1,090	1,090	1,090	1,090	1,090	1,090	1,090
4	116	184	1,090	1,090	1,090	1,090	1,090	1,090	1,090	1,090	1,090	1,090	1,090	1,090

Table 11. Well pumping rates for transient stress periods 30 to 40

			Well pumping rates, in cubic meters per day, for each stress period in the transient calibration										
			30	31	32	33	34	35	36	37	38	39	40
Layer	Row	Column	01-16-94	01-23-94	01-30-94	02-06-94	02-13-94	02-20-94	02-27-94	03-06-94	03-13-94	03-20-94	03-27-94
2	23	391	1,527.43	1,527.43	1,312.58	1,312.58	1,312.58	1,312.58	1,320.17	1,320.17	1,320.17	1,320.17	1,320.17
2	23	391	1,527.43	1,527.43	1,312.58	1,312.58	1,312.58	1,312.58	1,320.17	1,320.17	1,320.17	1,320.17	1,320.17
2	24	391	1,527.43	1,527.43	1,312.58	1,312.58	1,312.58	1,312.58	1,320.17	1,320.17	1,320.17	1,320.17	1,320.17
2	25	391	1,527.43	1,527.43	1,312.58	1,312.58	1,312.58	1,312.58	1,320.17	1,320.17	1,320.17	1,320.17	1,320.17
2	40	437	0	1,822.9	1,822.9	1,822.9	1,822.9	1,822.9	1,822.9	1,822.9	0	0	0
2	40	437	1,822.9	0	0	0	0	0	0	0	1,822.9	1,822.9	1,822.9
2	41	435	0	1,822.9	0	0	0	0	0	0	1,822.9	1,822.9	1,822.9
2	41	437	1,822.9	0	1,822.9	1,822.9	1,822.9	1,822.9	1,822.9	1,822.9	0	0	0
2	74	71	272.5	272.5	272.5	272.5	272.5	272.5	272.5	272.5	272.5	272.5	272.5
2	108	169	545	545	545	545	545	545	545	545	545	545	545
2	109	168	545	545	545	545	545	545	545	545	545	545	545
2	110	168	545	545	545	545	545	545	545	545	545	545	545
2	110	169	545	545	545	545	545	545	545	545	545	545	545
2	111	169	545	545	545	545	545	545	545	545	545	545	545
2	131	359	698.15	698.15	698.15	698.15	698.15	698.15	698.15	698.15	698.15	698.15	698.15
3	50	381	1,892.361	1,892.361	1,892.361	1,892.361	1,892.361	1,892.361	1,892.361	1,892.361	1,892.361	1,892.361	1,892.361
3	50	382	1,892.361	1,892.361	1,892.361	1,892.361	1,892.361	1,892.361	1,892.361	1,892.361	1,892.361	1,892.361	1,892.361
3	50	382	1,892.361	1,892.361	1,892.361	1,892.361	1,892.361	1,892.361	1,892.361	1,892.361	1,892.361	1,892.361	1,892.361
3	60	296	1,815.09	1,840.77	1,875.02	1,814.99	1,861.14	1,773.45	1,762.28	1,809.95	1,795.89	1,787.51	1,768.14
3	61	296	1,815.09	1,840.77	1,875.02	1,814.99	1,861.14	1,773.45	1,762.28	1,809.95	1,795.89	1,787.51	1,768.14
3	61	296	1,815.09	1,840.77	1,875.02	1,814.99	1,861.14	1,773.45	1,762.28	1,809.95	1,795.89	1,787.51	1,768.14
3	62	296	1,815.09	1,840.77	1,875.02	1,814.99	1,861.14	1,773.45	1,762.28	1,809.95	1,795.89	1,787.51	1,768.14
3	63	296	1,815.09	1,840.77	1,875.02	1,814.99	1,861.14	1,773.45	1,762.28	1,809.95	1,795.89	1,787.51	1,768.14
3	64	296	1,815.09	1,840.77	1,875.02	1,814.99	1,861.14	1,773.45	1,762.28	1,809.95	1,795.89	1,787.51	1,768.14
3	66	337	567.7	567.7	567.7	567.7	567.7	567.7	567.7	567.7	567.7	567.7	567.7

Table 11. Well pumping rates for transient stress periods 30 to 40—Continued

			Well pumping rates, in cubic meters per day, for each stress period in the transient calibration										
			30	31	32	33	34	35	36	37	38	39	40
Layer	Row	Column	01-16-94	01-23-94	01-30-94	02-06-94	02-13-94	02-20-94	02-27-94	03-06-94	03-13-94	03-20-94	03-27-94
3	66	337	567.7	567.7	567.7	567.7	567.7	567.7	567.7	567.7	567.7	567.7	567.7
3	69	120	1,699.6	1,620.12	1,607.41	1,697.84	1,537.79	1,566.85	1,623.77	1,669.19	1,734.88	1,671.21	1,595.76
3	69	120	1,699.6	1,620.12	1,607.41	1,697.84	1,537.79	1,566.85	1,623.77	1,669.19	1,734.88	1,671.21	1,595.76
3	69	121	1,699.6	1,620.12	1,607.41	1,697.84	1,537.79	1,566.85	1,623.77	1,669.19	1,734.88	1,671.21	1,595.76
3	69	122	1,699.6	1,620.12	1,607.41	1,697.84	1,537.79	1,566.85	1,623.77	1,669.19	1,734.88	1,671.21	1,595.76
3	85	294	3,009.31	2,815.36	2,895.31	2,873.82	3,011.25	2,626.1	2,680.44	2,692.82	2,733.02	2,755.4	2,566.16
3	85	296	3,009.31	2,815.36	2,895.31	2,873.82	3,011.25	2,626.1	2,680.44	2,692.82	2,733.02	2,755.4	2,566.16
3	85	298	3,009.31	2,815.36	2,895.31	2,873.82	3,011.25	2,626.1	2,680.44	2,692.82	2,733.02	2,755.4	2,566.16
3	86	165	136.25	136.25	136.25	136.25	136.25	136.25	136.25	136.25	136.25	136.25	136.25
3	87	171	1,716.88	1,656.32	1,752.46	1,646.48	1,640.42	1,611.65	1,676.76	1,725.2	1,653.29	1,703.25	1,660.86
3	87	171	1,716.88	1,656.32	1,752.46	1,646.48	1,640.42	1,611.65	1,676.76	1,725.2	1,653.29	1,703.25	1,660.86
3	87	294	3,009.31	2,815.36	2,895.31	2,873.82	3,011.25	2,626.1	2,680.44	2,692.82	2,733.02	2,755.4	2,566.16
3	89	293	3,009.31	2,815.36	2,895.31	2,873.82	3,011.25	2,626.1	2,680.44	2,692.82	2,733.02	2,755.4	2,566.16
3	101	162	545	545	545	545	545	545	545	545	545	545	545
3	101	276	408.75	408.75	408.75	408.75	408.75	408.75	408.75	408.75	408.75	408.75	408.75
3	102	169	136.25	136.25	136.25	136.25	136.25	136.25	136.25	136.25	136.25	136.25	136.25
3	102	175	1,635	1,635	1,635	1,635	1,635	1,635	1,635	1,635	1,635	1,635	1,635
3	104	166	1,090	1,090	1,090	1,090	1,090	1,090	1,090	1,090	1,090	1,090	1,090
3	109	171	545	545	545	545	545	545	545	545	545	545	545
3	109	269	545	545	545	545	545	545	545	545	545	545	545
3	110	170	545	545	545	545	545	545	545	545	545	545	545
3	114	245	272.5	272.5	272.5	272.5	272.5	272.5	272.5	272.5	272.5	272.5	272.5
3	115	188	1,090	1,090	1,090	1,090	1,090	1,090	1,090	1,090	1,090	1,090	1,090
3	115	189	1,090	1,090	1,090	1,090	1,090	1,090	1,090	1,090	1,090	1,090	1,090
3	130	368	839.19	839.19	839.19	839.19	839.19	839.19	839.19	839.19	839.19	839.19	839.19
3	130	372	194.29	194.29	194.29	194.29	194.29	194.29	194.29	194.29	194.29	194.29	194.29

Table 11. Well pumping rates for transient stress periods 30 to 40—Continued

			Well pumping rates, in cubic meters per day, for each stress period in the transient calibration										
			30	31	32	33	34	35	36	37	38	39	40
Layer	Row	Column	01-16-94	01-23-94	01-30-94	02-06-94	02-13-94	02-20-94	02-27-94	03-06-94	03-13-94	03-20-94	03-27-94
3	131	362	54.17	54.17	54.17	54.17	54.17	54.17	54.17	54.17	54.17	54.17	54.17
3	131	367	78.86	78.86	78.86	78.86	78.86	78.86	78.86	78.86	78.86	78.86	78.86
3	133	365	690.35	690.35	690.35	690.35	690.35	690.35	690.35	690.35	690.35	690.35	690.35
3	134	356	586.91	586.91	586.91	586.91	586.91	586.91	586.91	586.91	586.91	586.91	586.91
3	135	360	70.14	70.14	70.14	70.14	70.14	70.14	70.14	70.14	70.14	70.14	70.14
3	137	365	418.45	418.45	418.45	418.45	418.45	418.45	418.45	418.45	418.45	418.45	418.45
3	137	369	575.36	575.36	575.36	575.36	575.36	575.36	575.36	575.36	575.36	575.36	575.36
4	86	289	3,009.31	2,815.36	2,895.31	2,873.82	3,011.25	2,626.1	2,680.44	2,692.82	2,733.02	2,755.4	2,566.16
4	86	289	3,009.31	2,815.36	2,895.31	2,873.82	3,011.25	2,626.1	2,680.44	2,692.82	2,733.02	2,755.4	2,566.16
4	87	288	3,009.31	2,815.36	2,895.31	2,873.82	3,011.25	2,626.1	2,680.44	2,692.82	2,733.02	2,755.4	2,566.16
4	87	288	3,009.31	2,815.36	2,895.31	2,873.82	3,011.25	2,626.1	2,680.44	2,692.82	2,733.02	2,755.4	2,566.16
4	87	289	3,009.31	2,815.36	2,895.31	2,873.82	3,011.25	2,626.1	2,680.44	2,692.82	2,733.02	2,755.4	2,566.16
4	87	289	3,009.31	2,815.36	2,895.31	2,873.82	3,011.25	2,626.1	2,680.44	2,692.82	2,733.02	2,755.4	2,566.16
4	88	172	1,716.88	1,656.32	1,752.46	1,646.48	1,640.42	1,611.65	1,676.76	1,725.2	1,653.29	1,703.25	1,660.86
4	88	172	1,716.88	1,656.32	1,752.46	1,646.48	1,640.42	1,611.65	1,676.76	1,725.2	1,653.29	1,703.25	1,660.86
4	88	172	1,716.88	1,656.32	1,752.46	1,646.48	1,640.42	1,611.65	1,676.76	1,725.2	1,653.29	1,703.25	1,660.86
4	88	285	3,009.31	2,815.36	2,895.31	2,873.82	3,011.25	2,626.1	2,680.44	2,692.82	2,733.02	2,755.4	2,566.16
4	88	286	3,009.31	2,815.36	2,895.31	2,873.82	3,011.25	2,626.1	2,680.44	2,692.82	2,733.02	2,755.4	2,566.16
4	88	286	3,009.31	2,815.36	2,895.31	2,873.82	3,011.25	2,626.1	2,680.44	2,692.82	2,733.02	2,755.4	2,566.16
4	88	287	3,009.31	2,815.36	2,895.31	2,873.82	3,011.25	2,626.1	2,680.44	2,692.82	2,733.02	2,755.4	2,566.16
4	88	288	3,009.31	2,815.36	2,895.31	2,873.82	3,011.25	2,626.1	2,680.44	2,692.82	2,733.02	2,755.4	2,566.16
4	88	288	3,009.31	2,815.36	2,895.31	2,873.82	3,011.25	2,626.1	2,680.44	2,692.82	2,733.02	2,755.4	2,566.16
4	88	289	3,009.31	2,815.36	2,895.31	2,873.82	3,011.25	2,626.1	2,680.44	2,692.82	2,733.02	2,755.4	2,566.16
4	88	289	3,009.31	2,815.36	2,895.31	2,873.82	3,011.25	2,626.1	2,680.44	2,692.82	2,733.02	2,755.4	2,566.16
4	88	289	3,009.31	2,815.36	2,895.31	2,873.82	3,011.25	2,626.1	2,680.44	2,692.82	2,733.02	2,755.4	2,566.16
4	88	290	3,009.31	2,815.36	2,895.31	2,873.82	3,011.25	2,626.1	2,680.44	2,692.82	2,733.02	2,755.4	2,566.16

Table 11. Well pumping rates for transient stress periods 30 to 40—Continued

			Well pumping rates, in cubic meters per day, for each stress period in the transient calibration										
			30	31	32	33	34	35	36	37	38	39	40
Layer	Row	Column	01-16-94	01-23-94	01-30-94	02-06-94	02-13-94	02-20-94	02-27-94	03-06-94	03-13-94	03-20-94	03-27-94
4	89	284	3,009.31	2,815.36	2,895.31	2,873.82	3,011.25	2,626.1	2,680.44	2,692.82	2,733.02	2,755.4	2,566.16
4	89	286	3,009.31	2,815.36	2,895.31	2,873.82	3,011.25	2,626.1	2,680.44	2,692.82	2,733.02	2,755.4	2,566.16
4	89	286	3,009.31	2,815.36	2,895.31	2,873.82	3,011.25	2,626.1	2,680.44	2,692.82	2,733.02	2,755.4	2,566.16
4	89	287	3,009.31	2,815.36	2,895.31	2,873.82	3,011.25	2,626.1	2,680.44	2,692.82	2,733.02	2,755.4	2,566.16
4	89	291	3,009.31	2,815.36	2,895.31	2,873.82	3,011.25	2,626.1	2,680.44	2,692.82	2,733.02	2,755.4	2,566.16
4	90	176	11,286.2	11,286.2	12,022.54	11,778.23	12,270.28	11,286.2	11,286.2	11,286.2	1,613.79	0	0
4	90	176	11,286.2	11,286.2	12,022.54	11,778.23	12,270.28	11,286.2	11,286.2	11,286.2	1,613.79	0	0
4	90	180	11,286.2	11,286.2	12,022.54	11,778.23	12,270.28	11,286.2	11,286.2	11,286.2	1,613.79	0	0
4	90	286	3,009.31	2,815.36	2,895.31	2,873.82	3,011.25	2,626.1	2,680.44	2,692.82	2,733.02	2,755.4	2,566.16
4	90	286	3,009.31	2,815.36	2,895.31	2,873.82	3,011.25	2,626.1	2,680.44	2,692.82	2,733.02	2,755.4	2,566.16
4	90	287	3,009.31	2,815.36	2,895.31	2,873.82	3,011.25	2,626.1	2,680.44	2,692.82	2,733.02	2,755.4	2,566.16
4	91	180	11,286.2	11,286.2	12,022.54	11,778.23	12,270.28	11,286.2	11,286.2	11,286.2	1,613.79	0	0
4	91	285	3,009.31	2,815.36	2,895.31	2,873.82	3,011.25	2,626.1	2,680.44	2,692.82	2,733.02	2,755.4	2,566.16
4	91	285	3,009.31	2,815.36	2,895.31	2,873.82	3,011.25	2,626.1	2,680.44	2,692.82	2,733.02	2,755.4	2,566.16
4	91	285	3,009.31	2,815.36	2,895.31	2,873.82	3,011.25	2,626.1	2,680.44	2,692.82	2,733.02	2,755.4	2,566.16
4	92	178	11,286.2	11,286.2	12,022.54	11,778.23	12,270.28	11,286.2	11,286.2	11,286.2	1,613.79	0	0
4	92	178	11,286.2	11,286.2	12,022.54	11,778.23	12,270.28	11,286.2	11,286.2	11,286.2	1,613.79	0	0
4	92	178	11,286.2	11,286.2	12,022.54	11,778.23	12,270.28	11,286.2	11,286.2	11,286.2	1,613.79	0	0
4	93	179	11,286.2	11,286.2	12,022.54	11,778.23	12,270.28	11,286.2	11,286.2	11,286.2	1,613.79	0	0
4	93	179	11,286.2	11,286.2	12,022.54	11,778.23	12,270.28	11,286.2	11,286.2	11,286.2	1,613.79	0	0
4	93	179	11,286.2	11,286.2	12,022.54	11,778.23	12,270.28	11,286.2	11,286.2	11,286.2	1,613.79	0	0
4	94	179	11,286.2	11,286.2	12,022.54	11,778.23	12,270.28	11,286.2	11,286.2	11,286.2	1,613.79	0	0
4	95	165	545	545	545	545	545	545	545	545	545	545	545
4	98	163	545	545	545	545	545	545	545	545	545	545	545
4	99	166	272.5	272.5	272.5	272.5	272.5	272.5	272.5	272.5	272.5	272.5	272.5
4	99	183	545	545	545	545	545	545	545	545	545	545	545

Table 11. Well pumping rates for transient stress periods 30 to 40—Continued

			Well pumping rates, in cubic meters per day, for each stress period in the transient calibration										
			30	31	32	33	34	35	36	37	38	39	40
Layer	Row	Column	01-16-94	01-23-94	01-30-94	02-06-94	02-13-94	02-20-94	02-27-94	03-06-94	03-13-94	03-20-94	03-27-94
4	100	162	1,362.5	1,362.5	1,362.5	1,362.5	1,362.5	1,362.5	1,362.5	1,362.5	1,362.5	1,362.5	1,362.5
4	101	163	545	545	545	545	545	545	545	545	545	545	545
4	101	196	272.5	272.5	272.5	272.5	272.5	272.5	272.5	272.5	272.5	272.5	272.5
4	102	182	3,353.78	3,215.63	3,199.54	3,180.89	3,395.42	3,368.11	3,116.54	3,433.67	3,233.61	3,370.27	3,105.59
4	103	182	3,353.78	3,215.63	3,199.54	3,180.89	3,395.42	3,368.11	3,116.54	3,433.67	3,233.61	3,370.27	3,105.59
4	103	182	3,353.78	3,215.63	3,199.54	3,180.89	3,395.42	3,368.11	3,116.54	3,433.67	3,233.61	3,370.27	3,105.59
4	104	182	3,353.78	3,215.63	3,199.54	3,180.89	3,395.42	3,368.11	3,116.54	3,433.67	3,233.61	3,370.27	3,105.59
4	106	188	136.25	136.25	136.25	136.25	136.25	136.25	136.25	136.25	136.25	136.25	136.25
4	108	183	136.25	136.25	136.25	136.25	136.25	136.25	136.25	136.25	136.25	136.25	136.25
4	108	195	327	327	327	327	327	327	327	327	327	327	327
4	109	195	1,635	1,635	1,635	1,635	1,635	1,635	1,635	1,635	1,635	1,635	1,635
4	112	188	1,090	1,090	1,090	1,090	1,090	1,090	1,090	1,090	1,090	1,090	1,090
4	113	188	1,090	1,090	1,090	1,090	1,090	1,090	1,090	1,090	1,090	1,090	1,090
4	113	188	1,090	1,090	1,090	1,090	1,090	1,090	1,090	1,090	1,090	1,090	1,090
4	114	188	1,090	1,090	1,090	1,090	1,090	1,090	1,090	1,090	1,090	1,090	1,090
4	114	188	1,090	1,090	1,090	1,090	1,090	1,090	1,090	1,090	1,090	1,090	1,090
4	115	186	1,090	1,090	1,090	1,090	1,090	1,090	1,090	1,090	1,090	1,090	1,090
4	116	184	1,090	1,090	1,090	1,090	1,090	1,090	1,090	1,090	1,090	1,090	1,090